FEDERAL UNIVERSITY OF SÃO CARLOS
EXACT SCIENCE AND TECHNOLOGY CENTRE
DEPARTMENT OF CHEMISTRY
POSTGRADUATE PROGRAM IN CHEMISTRY

DOCTORAL THESIS

EXTREMOPHILES IN ASTROBIOLOGY: CONTRIBUTIONS TO THE UNDERSTANDING OF BIOSIGNATURES PRODUCTION AND SURVIVAL MOLECULAR STRATEGIES

Alef dos Santos*

A thesis submitted in fulfilment of the requirements for the degree of Doctor of Science in Organic Chemistry

Supervisor: Prof. Dr. Edson Rodrigues Filho
Supervisor: Prof. Dr. Alexandre Soares Rosado
Co-supervisor: Prof. Dr. Eduardo Jorge Pilau

***Scholarship CAPES (**n. 88887.598052/ 2021–00 and 88881.682425/2022–01**)**

São Carlos – SP
2024

UNIVERSIDADE FEDERAL DE SÃO CARLOS

Centro de Ciências Exatas e de Tecnologia
Programa de Pós-Graduação em Química

Folha de Aprovação

Defesa de Tese de Doutorado do candidato Alef dos Santos, realizada em 06/12/2024.

Comissão Julgadora:

Prof. Dr. Edson Rodrigues Filho (UFSCar)

Prof. Dr. Mauro Sergio Ferreira Santos (JPL-NASA)

Prof. Dr. Ian Castro Gamboa (UNESP)

Prof. Dr. Fernando Cassas Salles Machado (UFSCar)

Profa. Dra. Carla Porto da Silva (MS Bioscience)

O Relatório de Defesa assinado pelos membros da Comissão Julgadora encontra-se arquivado junto ao Programa de Pós-Graduação em Química.

The Earth is the cradle of humanity, but no one can live in the cradle forever!
Земля – колыбель человечества, но нельзя вечно пребывать в колыбели.

Konstantin Tsiolkovsky

LIST OF PUBLICATIONS

1. ***dos Santos A**., Schultz J., Dal'Rio I., Trapp A. M., Molodon F., Tenório B. G., Stajich E. J., Marcus de Melo Teixeira M. M., Pilau J. E., Rosado S. A., Rodrigues-Filho E., (2025) "Black yeast as a Model Eukaryotic Organism for Astrobiological Studies on Microbial Interactions with Martian Regolith Analogs". *JACS Au* 5, (5), 1, 187–203. https://doi.org/10.1021/jacsau.4c00869

2. ***dos Santos A**., Schultz J., Souza O. F., Rodrigues R. F., Braga V. T., Pilau J. E., Rosado S. A., Rodrigues-Filho E., (2024) "Survival Strategies of Rhinocladiella similis in Perchlorate Rich Mars Like Environments". (*npj Microgravity*, under review)

3. ***dos Santos A**., Schultz J, Trapp A. M., Molodon F., Romaneko A., Jaiswal K. A., Rodrigues-Filho E Rosado S. A. (2024) "Investigating Polyextremophilic Bacteria in Al Wahbah Crater, Saudi Arabia: A Terrestrial Model for Life on Saturn's Moon Enceladus". *Astrobiology* 24 (8), 824-838 (**Issue Cover**). https://doi.org/10.1089/ast.2024.0017

4. **dos Santos A**., Birolli, W. G., Souza, F. O., Giovanella, P., Cabral, L., de Farias, G. S., Pilau, E. J., Sette, L. D., & Rodrigues-Filho, E. (2025). Leveraging Antarctic psychrotolerant fungi for PAH biodegradation, unveiling key factors influencing the process. *Chemosphere*, 373, 144138. https://doi.org/10.1016/j.chemosphere.2025.144138

5. Gimenez J., Bonatti S., Basaglia M., Bettini S., Garcia R., Azevedo E., **dos Santos A**., Samara M., Helal E., Demarquette N., Homem M., Cruz S. A. (2024). "UV-C induced photodegradation of polypropylene." (*Polymer Degradation and Stability* under review).

6. Penteado P. S., Di-Medeiros Leal M. C. B., Carosio M. G. A., **dos Santos A**., Segatto M. L., Pavarini D. P., Silva D. F. da, Amaral J. C., da Silva M. F. das G. F., Zeidler V. G. Z., Ferreira A. G., "Green Extraction and NMR Analysis of Bioactives from Orange Juice Waste" (*Foods* under review)

7. Alves M. A. P. M., dos **Santos A.,** *et al.* (2024) "Antioxidant Polyene Steroids from the Copper-Mine Soil Derived Fungus Talaromyces Fuscoviridis" (preprint) https://doi.org/1010.2139/ssrn.4999187

8. Schultz J., **dos Santos A**., Patel N., Rosado A.S. (2023) "Life on the Edge: Bioprospecting Extremophiles for Astrobiology," Journal of the Indian Institute of Science 103 (3), 721- 737. https://doi.org/10.1007/s41745-023-00382-9

9. Bonatti E., dos Santos A., Birolli W.G., Rodrigues-Filho E. (2023) "Endophytic, Extremophilic and Entomophilic Fungi Strains Biodegrade Anthracene Showing Potential for Bioremediation" World Journal of Microbiology and Biotechnology 39 (6), 152. https://doi.org/10.1007/s11274-023-03590-8

10. **dos Santos, A.,** Rodrigues-Filho E., Homem M.G.P. (2021) "Analysis of Microbial Lipids Deposited on Mars Global Simulant (MGS-1) by Geomatrix-assisted Laser Desorption/Ionization-mass Spectrometry," International Journal of Astrobiology 20 (3), 234-240. https://doi.org/10.1017/S1473550421000100

11. Birolli, W. G., **dos Santos A.,** Pilau, J. E., & Rodrigues-Filho, E. (2021). New Role for a Commercially Available Bioinsecticide: Bacillus thuringiensis Berliner Biodegrades the Pyrethroid Cypermethrin. ACS Environmental science & technology, 55(8), 4792–4803. https://doi.org/10.1021/acs.est.0c06907

12. **dos Santos A.,** Rodrigues-Filho E. (2019) "New Delta 8-9 Pregnenes Steroids Isolated from the Extremophile Fungus Exophiala oligosperma," Natural Product Research 35 (15), 2598-2601. https://doi.org/10.1080/14786419.2019.1684277

13. Din, Z. U., **dos Santos, A**., Trapp, M. A., Lazarin-Bidóia, D., Garcia, F. P., Peron, F., ... & Rodrigues-Filho, E. (2016). Curcumin inspired synthesis of unsymmetrical diarylpentanoids with highly potent anti-parasitic activities: in silico studies and DFT-based stereochemical calculation. MedChemComm, 7(5), 820-831.https://doi.org/10.1039/C5MD00599J

* articles comprising this thesis

Book Chapter

1. Schultz J.,Correa S. S., **dos Santos A.,** Rosado S. A., "3.3 - Disentangling the Autotrophic Thermophiles: Concepts, Diversity, and Emerging Trends" Microbial Diversity in the Genomic Era, 281-300.

AWARDS AND GRANTS

2023 Visiting PhD scholarship – ELAP grant (Government of Canada)

2022 Best Poster Award – Extremophile2022

2022 Travel Award – Extremophile2022

2022 Visiting PhD scholarship – National Council for the Improvement of Higher Education scholarship (CAPES – Brazil).

2021 PhD's scholarship – National Council for the Improvement of Higher Education scholarship (CAPES – Brazil)

2016 Undergraduate Research Program – National Council for Scientific and Technological Developments scholarship (CNPq – Brazil)

ACKNOWLEDGEMENTS

I would like to express my sincere gratitude, especially to my parents, Cibele and Adriano, who have always motivated and believed in me, even during difficult times.

I am thankful to Professor Edson Rodrigues Filho for his 11 years of friendship and guidance. He has been and will continue to be a great mentor in my scientific journey, always encouraging me, supporting my ideas, and fostering a critical perspective on science. Thank you very much, Professor Edinho.

I also extend my appreciation to Professor Eduardo Jorge Pilau for agreeing to co-supervise my work and for opening the doors of his laboratory during part of my doctoral studies.

A special acknowledgment goes to Professor Dr. Alexandre Rosado, my supervisor during my time as a visiting student at KAUST. I am deeply grateful for his willingness to involve me in his research group and support my project.

I also extend my gratitude to Professor Kurt Konhauser for welcoming me to his laboratory during part of my doctorate in Canada.

I am grateful to Dr. Junia for teaching me all I know about molecular biology and genomics, and for encouraging me to embrace challenges despite my fears.

My thanks to Dr. Marília for her insightful discussions and guidance on metabolomics and mass spectrometry.

I thank Dr. Flvuio, Isabella Dal'Rio and Professor Marcus Teixeira for carrying out the bioinformatics analysis and teaching me how to analyze this type of data.

I am grateful to Professor Giba, Professor Tiago, and Professor Manoel for their valuable discussions and teachings.

I must also recognize the contributions of all the professors and technicians in the chemistry department who have supported me over the past 11 years.

I appreciate all the members of LaBioMMi, LabMass, MEGB Lab, and the NMR lab for their support throughout my journey.

I would like to express my gratitude to the Brazilian funding agencies CAPES, CNPq, and FAPESP for their financial support of my research.

Finally, I would like to thank my friends from both my undergraduate and postgraduate studies, as well as my family and my wife, Dafne, for their unwavering support and understanding during my academic journey.

TABLE LIST

FIGURE LIST

ABSTRACT

“EXTREMOPHILES IN ASTROBIOLOGY: CONTRIBUTIONS TO THE UNDERSTANDING OF BIOSIGNATURES PRODUCTION AND SURVIVAL MOLECULAR STRATEGIES”. The origin, evolution, and survival of life in extraterrestrial environments are fundamental questions that drive scientists to search for evidence of life beyond Earth. The science dedicated to investigating these questions is astrobiology, a relatively new field that integrates various areas of the natural sciences, such as astronomy, geology, chemistry, and biology. In this context, the search for habitable environments is essential to explore the possibility of extraterrestrial life. Currently, it is known that some celestial bodies in our solar system, such as Mars and the icy moons Enceladus and Europa, exhibit or have exhibited potentially habitable conditions. However, Earth remains the only known planet that harbors life, serving as the primary guide in this search for answers. This thesis investigates the use of extremophilic microorganisms, such as a black yeast and alkaliphilic bacteria, as models to understand the molecular mechanisms of survival and the production of biosignatures when exposed to conditions that simulate the geochemistry of Mars and the oceans of Enceladus. First, the potential of the black yeast strain *Rhinocladiella similis* as a eukaryotic model in astrobiological studies was explored. Genomic and proteomic analyses revealed that when exposed to synthetic regolith simulating Martian soil and perchlorate salts, the yeast significantly altered its metabolism, producing various proteins and enzymes to cope with oxidative stress, in addition to activating chemical detoxification processes and increasing melanin production. The yeast also produced unique molecules under these conditions, such as osmolytes, oxylipins, and siderophores. Moreover, the study investigated the potential of a volcanic crater in Saudi Arabia as a promising environment for the discovery of polyextremophilic bacteria that could serve as models in astrobiology. Several halophilic bacteria were isolated and characterized by 16S sequencing, and two of them, from the genus *Halalkalibacterium halodurans*, were subjected to genomic and metabolomic analyses to investigate their survival capabilities under conditions that simulate the oceans of Enceladus. Their chemical signatures were analyzed using a molecular network approach via mass spectrometry, aiming to identify potential biosignature targets. In summary, this study demonstrated that through multi-omic tools such as genomics, proteomics, and metabolomics, it was possible to deepen the understanding of the molecular strategies employed by these extremophilic microorganisms under astrobiologically relevant conditions, showing that these microorganisms are valuable models for understanding potential life beyond Earth.

Keywords: extremophile; multi-omics; space exploration; microrganism; Mars; icy moons

RESUMO

“EXTREMÓFILOS EM ASTROBIOLOGIA: CONTRIBUIÇÕES PARA A COMPREENSÃO DA PRODUÇÃO DE BIOASSINATURAS E DAS ESTRATÉGIAS MOLECULARES DE SOBREVIVÊNCIA”. A origem, evolução e sobrevivência da vida em ambientes extraterrestres são questões fundamentais que impulsionam os cientistas a buscar evidências de vida além da Terra. A ciência que se dedica a investigar essas questões é a astrobiologia, um campo relativamente novo que integra diversas áreas das ciências naturais, como astronomia, geologia, química e biologia. Nesse contexto, a busca por ambientes habitáveis é essencial para explorar a possibilidade de vida extraterrestre. Atualmente, sabe-se que alguns corpos celestes em nosso sistema solar, como Marte e as luas geladas Encélado e Europa, apresentam ou já apresentaram condições potencialmente habitáveis. No entanto, a Terra continua sendo o único planeta conhecido que abriga vida, servindo como principal guia nessa busca por respostas. Esta tese investiga o uso de microrganismos extremófilos, como uma levedura negra e bactérias alcalifílicas, como modelos para compreender os mecanismos moleculares de sobrevivência e a produção de bioassinaturas quando expostos a condições que simulam a geoquímica de Marte e dos oceanos de Encélado. Primeiramente, foi explorado o potencial da cepa de levedura negra *Rhinocladiella similis* como modelo eucariótico em estudos astrobiológicos. Análises genômicas, proteômicas e metabolomicas revelaram que, ao ser exposta a regolito sintético que simula o solo de Marte e a sais de perclorato, a levedura alterou significativamente seu metabolismo, passando a produzir diversas proteínas e enzimas para lidar com o estresse oxidativo, além de ativar processos de desintoxicação química e aumentar a produção de melanina. A levedura também produziu moléculas únicas nessas condições, como osmólitos, oxilipinas e sideróforos. Além disso, o estudo investigou o potencial de uma cratera vulcânica na Arábia Saudita como um ambiente promissor para a descoberta de bactérias poliextremófilas que poderiam servir como modelos em astrobiologia. Diversas bactérias halofílicas foram isoladas e caracterizadas por sequenciamento de 16S, e duas delas, do gênero *Halalkalibacterium halodurans*, foram submetidas a análises genômicas e metabolômicas para investigar sua capacidade de sobrevivência em condições que simulam os oceanos de Encélado. Suas assinaturas químicas foram analisadas utilizando uma abordagem de rede molecular via espectrometria de massas, visando identificar possíveis alvos de bioassinaturas.Em suma, este estudo demonstrou que, por meio de ferramentas multiômicas como genômica, proteômica e metabolômica, foi possível aprofundar a compreensão das estratégias moleculares empregadas por esses microrganismos extremófilos em condições de interesse astrobiológico, mostrando que esses microrganismos são bons modelos para entender a possível vida além da Terra.

Palavras-chave: extremófilo; multiômica; exploração espacial; microrganismo; Marte; luas geladas

SUMMARY

CHAPTER 1 - BACKGROUND AND MOTIVATION

The first chapter presents the general aspects of astrobiology and how extremophiles can be used for understand the possible microbial extraterrestrial life.

1.1 - ASTROBIOLOGY: LIFE IN THE UNIVERSE

Astrobiology is an interdisciplinary scientific field that aims to understand the origin, evolution, distribution, and future of life in the universe. It addresses fundamental questions regarding the possible existence of life beyond Earth and the methods to detect it (SCHAIBLE *et al.*, 2024). Although the term "astrobiology" has gained relevance in recent decades, the central issues of this discipline trace back millennia, when ancient civilizations speculated about the possibility of life on other worlds (NASCIMENTO-DIAS & MARTINEZ-FRIAS, 2023). However, it was only in the twentieth century, with advances in molecular biology, organic chemistry, and space exploration, that astrobiology began to consolidate as a formal scientific field (SCHAIBLE *et al.*, 2024).

Space exploration, initiated in the 1950s and driven by the space race between the United States and the Soviet Union, revealed the necessity to investigate the habitability of other celestial bodies (NASCIMENTO-DIAS & MARTINEZ-FRIAS, 2023). Discoveries of organic molecules in space, along with the Apollo missions and lander sent to Mars, raised questions about the viability of life beyond Earth (DICK, 2009). The term "exobiology", coined in the 1960s, initially described this search for extraterrestrial life, focusing on possible organisms and their forms of existence. During this period, space agencies, such as National Aeronautics and Space Administration (NASA) and Soviet space program, also expressed concerns regarding planetary contamination, both through the introduction of terrestrial microorganisms to other planets (direct contamination) and the risk of astronauts and cosmonauts bringing potential extraterrestrial organisms back to Earth (reverse contamination) (DICK, 2009; KUZICHEVA & GONTAREVA, 2003).

In the absence of concrete discoveries of extraterrestrial life, the field expanded to the study of the chemical precursors of life and the environments that could support it on other planets. The transition from "exobiology" to "astrobiology" reflects this broadening of scope, recognizing that science requires concrete subjects of study, and that, to date, there is no direct evidence of life beyond Earth (NASCIMENTO-DIAS & MARTINEZ-FRIAS, 2023; DICK, 2009). As scientific knowledge advanced, astrobiology incorporated the study of the origin, evolution, and distribution of life in the universe, including Earth in a cosmological context. The term "astrobiology" was adopted to reflect a more comprehensive approach, integrating disciplines such as biology, chemistry, geology, and astronomy, with the goal of understanding the phenomenon of life in the universe. Currently, this approach encompasses studies of the conditions that enabled the emergence of life, investigated through prebiotic

chemistry experiments, as well as an understanding of the evolution of living organisms on Earth, exploring their physiological limits and the vast diversity of life forms (SCHAIBLE *et al.*, 2024).

Astrobiology also investigates the habitability of other planets and moons, aiming to identify conditions suitable for sustaining life. Crucial factors, such as the presence of liquid water, energy sources, and the availability of organic molecules, are analyzed to determine the viability of extraterrestrial environments harboring life. Mars, for instance, is a recurring target of studies due to evidence suggesting that liquid water once existed on its surface and the discovery of organic molecules in recent samples (CLARK *et al.*, 2021; BEECH & COMTE, 2021). In addition to Mars, moons such as Europa and Enceladus, which possess subsurface oceans beneath their icy crusts, are considered promising locations for the existence of microbial life (CHATTERJEE, 2023). In this context, the search for biosignatures – evidence of biological processes, such as fossils, complex organic molecules, and chemical species – is central to the efforts of this field. This opens up the possibility for the chemical sciences to contribute significantly to the advancement of astrobiology (CHAN *et al.*, 2019).

The future prospects of astrobiology are quite promising. With advancements in molecular biology, analytical technologies, and the proliferation of omics sciences, laboratory experiments are becoming increasingly robust, providing insights and fundamental targets for understanding life in the universe, as demonstrated throughout the chapters of this work. In the field of space exploration, missions such as Mars Sample Return, which aims to bring Martian soil samples to Earth (CHEN *et al.*, 2023), and future exploration missions to moons like Europa, Titan and Enceladus, have the potential to provide the first direct evidence of biosignatures beyond Earth (WEBER *et al.*, 2023; DACHWALD *et al.*, 2020). Furthermore, the continuous development of exoplanet observation technologies will allow for more detailed characterization of their atmospheres, significantly increasing the chances of detecting biosignatures on planets beyond the Solar System.

1.2 - EXTREMOPHILES: A GENERAL OVERVIEW

The discovery of extremophilic microorganisms has challenged classical conceptions about the limits of life on Earth. Until the early 20th century, it was widely believed that life was only possible in environments with moderate conditions of temperature, pH, pressure, and salinity. However, the identification of microorganisms inhabiting extreme environments – such as hydrothermal vents, hypersaline lakes, and arid deserts – has not only redefined our understanding of the requirements for life but has also opened new frontiers for exploring biology under extreme conditions.

The term "extremophile" is derived from the Latin extremus, meaning "*extreme*", and *philos,* meaning "lover", referring to organisms that thrive under adverse conditions. A significant milestone in modern microbiology occurred in the 1960s when Thomas Brock discovered microorganisms capable of surviving at high temperatures in the hydrothermal springs of Yellowstone (BROCK & FREEZE, 1969). Since then, extremophiles have been identified in a variety of hostile environments, including hypersaline habitats, areas with high radiation, and highly acidic or alkaline conditions (such as in Rio Tinto and Lake Natron), the icy deserts of Antarctica, or even on the surfaces of artifacts exposed to space, each exhibiting remarkable biological adaptations (ALAZARD *et al.*, 2003; BAKER & BANFIELD, 2003; AISLABIE & MCLEOD, 2006; BAKER-AUSTIN & DOPSON, 2007; PULSCHEN *et al.*, 2015; ALTAIR *et al.*, 2018; MERINO *et al.*, 2019).

These microorganisms are classified based on the conditions in which they thrive. Among them are thermophiles and hyperthermophiles (organisms that grow at high and very high temperatures, respectively), psychrophiles (which thrive at low temperatures), acidophiles and alkaliphiles (adapted to acidic or basic pH levels), barophiles (which prefer high pressure), halophiles (which require salt to grow), and oligotrophs (which thrive in environments with low nutrient content). Additionally, many of these organisms are polyextremophiles, adapted to survive in habitats where multiple physicochemical parameters reach extreme values. A notable example is certain archaea found in thermal springs, which not only survive at elevated temperatures but also thrive in acidic conditions rich in metal cations (MERINO *et al.*, 2019).

Due to the lack of evidence of life beyond Earth, extremophiles emerge as the best models for understanding whether life could exist on other planets. Thus, extremophiles generate particular interest in astrobiology because of their ability to survive and thrive under conditions analogous to those of other celestial bodies. Mars, for example, presents

environments with extreme temperatures, high radiation, and elevated concentrations of perchlorate salts. These factors, combined with the discovery of liquid water in the Martian subsurface, suggest that halophilic and radiotolerant microorganisms could potentially survive on that planet (WADSWORTH & COCKELL, 2017). Similarly, the icy moons of the solar system, such as Europa and Enceladus, which possess subsurface oceans covered by thick ice crusts, are promising targets in the search for extraterrestrial life. Psychrophiles and high-pressure-adapted organisms, like those found in Earth's deep oceans, could serve as analogs for these potential alien ecosystems (PATHANIA *et al.*, 2022).

Motivated by this fascinating world of extremophiles, the following chapters will explore the use of these microorganisms – specifically a strain of black fungus and polyextremophilic bacteria from Saudi Arabia – as models to understand life beyond our planet, using multi-omics approaches.

CHAPTER 2 - BLACK FUNGUS *RHINOCLADIELLA SIMILIS* AS A EUKARYOTIC MODEL TO UNDERSTAND LIFE ON MARS

2.1 - *RHINOCLADIELLA SIMILIS*: A MODEL EUKARYOTIC ORGANISM FOR ASTROBIOLOGICAL STUDIES ON MICROBIAL INTERACTIONS WITH MARTIAN SOIL ANALOGS[1]

2.1.1 - Introduction

As space exploration advances, the search for signs of previous or existing life on other celestial bodies has become a major challenge (MOL, 2023). In astrobiology, the quest for extraterrestrial life faces significant technical limitations in onsite analysis because of the difficulty of sending human resources. Currently, the most viable approach to determining extraterrestrial life is biosignature detection using analytical techniques (e.g., Raman spectroscopy, Fourier-transform infrared spectroscopy, and mass spectrometry [MS]) coupled with rovers and landers. These biosignatures range from small molecules, such as O_2, to complex organic compounds, such as amino acid derivatives, DNA fragments, membrane fatty acids, and secondary metabolites (HUIDOBRO *et al.*, 2022; BAPAT & RAJAMANI, 2023; ANSARI, 2023).

In our solar system, Mars is the most promising candidate for hosting microbial life. Because the physical and chemical conditions of certain regions on Mars are similar to those on Earth, these locations may potentially harbor extremophilic microbes, making them focal points for future robotic and human exploration (ABRAHAMSSON & KANIK, 2022). Compared with the icy moons of the outer solar system, Mars' proximity to Earth makes it the most accessible destination for space exploration. Consequently, it has been the target of major missions, such as Mars 2020 and ExoMars 2022, aimed at detecting previous or existing life (ANSARI, 2023; VAGO & WESTALL, 2017). Although the surface conditions on Mars are harsh, its subsurface is a potential habitat because it is shielded from ionizing radiation and contains stable deposits of briny liquid water (ANSARI, 2023; OROSEI *ET AL.*, 2018).

Earth is the only planet confirmed to sustain life. Thus, investigations of biological molecules produced by terrestrial microorganisms under conditions simulating those on celestial bodies of interest, such as Mars, are crucial (SCHULTZ *et al.*, 2023).

[1] This section is an adapted version of the paper:

dos Santos A., Schultz J., Dal'Rio I., Trapp A. M., Molodon F., Tenório B. G., Stajich E. J., Marcus de Melo Teixeira M. M., Pilau J. E., Rosado S. A., Rodrigues-Filho E., (2025) "Black yeast as a Model Eukaryotic Organism for Astrobiological Studies on Microbial Interactions with Martian Regolith Analogs". JACS Au 5, (5), 1, 187–203. https://doi.org/10.1021/jacsau.4c00869

Extremophiles are of particular interest because they have evolved to thrive under hostile environmental conditions (MERINO *et al.*, 2019). On Earth, these microorganisms have been isolated from extreme environments that resemble Martian conditions, including the Atacama Desert, Antarctic Dry Valleys, and Death Valley, and artificial environments like chemically contaminated areas and space station modules (BIJLANI *et al.*, 2022; SCHULTZ *et al.*, 2023; SIMPSON *et al.*, 2023). Extremophilic bacteria and archaea isolates from these environments have been used as models for understanding potential extraterrestrial life forms (CARRÉ *et al.*, 2023; NOIRUNGSEE *et al.*, 2024). However, because of their complexity and later evolutionary emergence, fungi have only recently been used as models for studying extraterrestrial life forms (SIMÕES *et al.*, 2023).

Fungi play crucial roles in extreme environments, particularly in nutrient recycling and soil microorganism modulation (COLEINE *et al.*, 2022). Characterization of novel extremophilic fungi and analysis of their activities under Martian-like conditions (atmosphere, geochemistry, and temperature) provide insights into potential life on Mars. Black yeasts are of particular interest for studies on eukaryotic survival under Martian conditions because their high melanin pigmentation levels and diverse nature indicate significant astrobiological potential (CASSARO *et al.*, 2022; GEVI *et al.*, 2022). However, investigations of the genetic and metabolic mechanisms responsible for their adaptability and potential biosignatures under Martian conditions are scarce.

In this context, metabolomics and genomics are powerful tools for understanding the survival mechanisms of black fungi on Mars and detecting biosignatures indicative of life. Thus, an omics approach will expand our knowledge of these microorganisms' survival strategies and interactions with the Martian environment, thereby enabling the identification of potential biomarkers on other planets (SEYLER *et al.*, 2020), particularly regarding molecular aspects. Using metabolomics and MS techniques, we can analyze metabolites to identify specific biosignatures that can be targeted for the search for life on Mars.

In this study, we characterized a polyextremophilic black yeast using a multiomics approach to elucidate the molecular mechanisms of survival when cultured in media containing high-fidelity synthetic Martian regolith (MGS-1), thereby simulating microorganism–soil interactions to investigate the resulting biosignatures. Using a combination of genomics, metabolomics, and MS, we identified siderophores, oxylipins, and indole-related compounds as potential biosignatures for astrobiological purposes.

2.1.2 - Material and Methods

2.1.2.1 - Black Yeast Collection, Isolation, and Culture Conditions

Fungal isolation was initially reported by SANTOS and RODRIGUES-FILHO (2019). The black yeast strain analyzed in this study was discovered in an amber flask containing an aqueous HCl solution (pH 1.5) that had been stored in our laboratory (Laboratório de Bioquímica Micromolecular de Microorganismos [LaBioMMi], São Carlos, Brazil). An aliquot (100 µL) of this HCl solution was transferred into Petri dishes containing Czapek Dox medium and incubated at 25 °C for 5 days. Subsequently, viable colonies were isolated on semisolid potato dextrose agar (PDA). Pure colonies were preserved in a 15% glycerol/H_2O solution and were stored in our local collection under the designated code LaBioMMi 1217 (SANTOS *et al.*, 2021).

2.1.2.2 - Morphological Analysis

To phenotypically and morphologically identify the fungus strain LaBioMMi 1217, we inoculated it on two distinct culture media, PDA and Mycosel, to promote growth and incubated the cultures at 25 °C for 15 days. The colony diameter (mm), structure, pigmentation, and other morphological characteristics were recorded, and colonies were photographed using a smartphone camera.

Next, the colonies were microcultivated (PRASKAH *et al.*, 2016). Briefly, a small block (1 cm x 1 cm) of PDA was placed in the center of a sterile slide. All four sides of the agar were inoculated with the isolate, and a sterile coverslip was gently placed over the agar block. Slide culture was maintained in a moist Petri dish lined with filter paper soaked in sterile water at 25 °C. After 15 days, the fungus had grown onto the coverslip and the slide. The coverslip was then gently removed using sterile forceps and placed on a clean slide for the observation of colony morphology and features using a DMi8 inverted optical microscope (Leica).

2.1.2.3 - Whole Genome Sequencing

We meticulously isolated total genomic DNA from a monosporic colony of black fungus strain LaBioMMi 1217 to conduct a thorough analysis, including precise

taxonomic characterization, phylogenetic assessment, diversity profiling, and ecological implications. Briefly, approximately 1 g of wet cells was collected via centrifugation (16,000×*g*) and lysed by ultrasound at 70 Hz for 30 min. Subsequently, the genomic DNA was extracted using a Wizard Genomic DNA Purification Kit (Promega, USA). DNA was quantified using a Qubit 4.0 Fluorometer with a Qubit dsDNA HS Assay Kit (Invitrogen, USA), and the quality was assessed by 1% agarose gel electrophoresis stained with SYBR Safe DNA Gel Stain (Invitrogen) and visualized using a iBright Imaging Systems (Thermo Fisher Scientific). The extracted genomic DNA was sent to Macrogen Inc. (Seoul, South Korea) for whole genome sequencing (WGS) using an Illumina platform.

A TruSeq Nano DNA Kit (Illumina) was used to construct paired-end sequencing libraries (2 × 150 bp) with 350-bp insertions. The input material was 110 μg/μL of DNA, according to the manufacturer's instructions. The quality of the final libraries was assessed using an Agilent 2100 Bioanalyzer (Agilent Technologies). WGS was performed on a NovaSeq 6000 System (Illumina) following the manufacturer's instructions, achieving a minimum data output of 10 Gb per sample. The raw reads were deposited in the Sequence Read Archive (SRA) repository (accession no. SRR28554191, BioProject PRJNA1005689). The WGS data for the analyzed fungal strain (*Rhinocladiella similis* LaBioMMi 1217) was deposited in GenBank (accession no. JAZDCV000000000, BioProject PRJNA1068593).

The raw reads were filtered using NGS QC Toolkit v2.3 (PATEL & JAIN, 2012) to obtain high-quality (HQ) vectors and adaptor-free reads for genome assembly (HQ cutoff read length, 80%; cutoff quality score, 20). The HQ reads were then used for genome assembly using the Automatic Assembly For The Fungi v0.3.3 pipeline (STAJICH & PALMER, 2019). First, the Illumina sequencing reads were trimmed using the BBDuk tool of BBMap v38.95 software (https://sourceforge.net/projects/bbmap/). Second, BBMap was used to eliminate contaminant reads. Third, resultant HQ reads were assembled using SPAdes v3.15.4 (BANKEVICH *et al.*, 2012). Fourth, contaminant contigs were identified and removed using the National Center for Biotechnology (NCBI) tool FCS-GX (ASTASHYN *et al.*, 2023). Fifth, duplicated contigs were purged using minimap2 (LI, 2018), and the final assemblies were polished using Pilon v1.24 software (WALKER *et al.*, 2014). Finally, the scaffolds were sorted by length, and the fasta headers were renamed for further annotation. The assembly quality was verified using QUAST v5.1.0 (GUREVICH *et al.*, 2013) and completeness by BUSCO using the chaetothyriales_odb10 database (SEPPEY *et al.*, 2019).

2.1.2.4 - Multilocus Sequence Analyses (MLSAs)

First, we identified the sequence of the *ITS1-2* locus of strain LaBioMMi 1217 from the assembled genome using BLASTn analysis and compared it against the BLASTnr database. The initial assessment of the genetic background of the LaBioMMi 1217 strain indicated that it belonged to either *R. similis* or *Exophiala spinifera*. Therefore, we performed MLSA to obtain robust phylogenic data based on the *ITS*, *LSU*, *tef1*, *rpb1*, and ß-tubulin loci (CHANDER *et al.*, 2022). The available sequences of the aforementioned loci belonging to Clade 1 contained members of Herpotrichiellaceae and were retrieved from the NCBI database. The *ITS*, *LSU*, *tef1*, *rpb1*, and ß-tubulin sequences were identified and retrieved from the LaBioMMi 1217 genome sequence using BLASTn. The individual gene sequences for the five datasets were aligned separately using the PASTA software (MIRARAB *et al.*, 2015).

Next, alignment positions were purged using ClipKIT v1.3 with the smart-gap function. The individual alignments were then concatenated for phylogenetic analysis using IQ-TREE v2.1.1 software (MINH *et al.*, 2020). ModelFinder was used to evaluate the best DNA substitution model (KALYAANAMOORTHY *et al.*, 2017). Ultrafast bootstraps and the Shimodaira–Hasegawa-like approximate likelihood ratio test (SH-aLRT) were used for branch support (ANISIMOVA & GASCUEL, 2006). Finally, the tree topologies were visualized using the FigTree software (http://tree.bio.ed.ac.uk/software/figtree/).

2.1.2.5 - Genome Annotation and Comparative Genomic Analysis

The assembled LaBioMMi 1217 sequence was annotated using the funannotate v1.8 pipeline (PALMER & STAJICH, 2020). TANTAN (FRITH, 2011) was used to identify and mask repetitive DNA content using the funannotate mask command.

For gene prediction, we used mRNA molecules isolated from LaBioMMi 1217. Briefly, approximately 500 mg of mycelia cultured on PDA was harvested for total RNA extraction. Mycelial cells were lysed for 30 min using Buffer RLT (Qiagen) and glass beads. Then, we used an RNeasy Kit to extract total RNA according to the manufacturer's instructions. Approximately 1 µg of total RNA was used as the input material for constructing sequencing libraries using a TruSeq Stranded mRNA Library Prep Kit (Illumina). The quality of the final libraries was assessed using an Agilent 2100 Bioanalyzer. The libraries were sequenced on the NovaSeq 6000 System (2 × 150 bp) according to the manufacturer's

instructions, achieving a minimum data output of 2 Gb per sample. The raw mRNA reads were deposited in the SRA database (accession no. SRR28554245).

Gene models were predicted using evidence-based and ab initio (i.e., structure-based) software. Aiming to find conserved gene models, we used mRNA reads assembled via Trinity and PASA (GRABHERR *et al.*, 2011) for training the ab initio predictors Augustus (SEPPEY *et al.*, 2019), GlimmerHMM (DELCHER *et al.*, 1999), SNAP (KORF, 2004), and CodingQuarry (TESTA *et al.*, 2015). The self-training GeneMark-ES algorithm was also used with the option for fungal genomes (LOMSADZE, 2005). The weighted consensus gene structure was obtained via EVidenceModeler (HAAS *et al.*, 2008) using the following weights: PASA = 6, Augustus HiQ = 2, and CodingQuarry = 2. The remaining predictors were set to 1. Genes <50 amino acids and those identified as transposable elements were excluded from the dataset. tRNAscan-SE was used to predict tRNAs (CHAN & LOWE, 2019).

In addition, the funannotate annotate function was used to annotate genes using eggNOG (HUERTA-CEPAS *et al.*, 2019), Pfam (MISTRY *et al.*, 2021), InterPro (BLUM *et al.*, 2021), Gene Ontology (GO) terms (Gene Ontology Consortium, 2004), MEROPS (RAWLINGS *et al.*, 2018), and the Fungal Secretome Database (CHOI *et al.*, 2010). FungiSMASH, the fungal-genome-specific version of antiSMASH 6.0 (BLIN *et al.*, 2021) was used to predict biosynthetic gene clusters.

We also employed a phylogenomic approach using the PHYling v2 pipeline (https://github.com/emmadebayos/PHYling_unified/) with sets of universal single-copy fungal markers available from the BUSCO database (SIMÃO *et al.*, 2015). We then used hidden Markov models to search for each biomarker in the fungi_odb10 database using the hmmalign tool. Subsequently, individual alignments were trimmed using ClipKIT v1.3 (STEENWYK *et al.*, 2020) with the smart-gap function to remove spurious positions. Next, individual alignments were concatenated to reconstruct the maximum-likelihood species tree using IQ-TREE v2 software (MINH *et al.*, 2020). ModelFinder was used to evaluate each marker's best protein substitution model (KALYAANAMOORTHY *et al.*, 2017). Branch support was assessed using ultrafast bootstraps (MINH *et al.*, 2013) and SH-aLRT (ANISIMOVA & GASCUEL, 2006). The tree topology was visualized using FigTree software. Finally, we used the funannotate compare function to perform comparative genomic analyses of *Rhinocladiella* fungi. We counted various genomic features, including Pfam, carbohydrate-active enzymes (CAZymes), MEROPS, transmembrane proteins, secreted proteins, clusters of orthologous groups (COGs), secondary metabolites, and fungal

transcription factor domains, plotting each category with a standard deviation >1 in a heat map.

We performed data mining using the functional tables generated by Pfam, InterPro, and NCBI COG. Manual categorization was used to search for genes and metabolites of interest for astrobiology applications, such as genes for ultraviolet (UV) radiation resistance, cold tolerance, osmotic stress tolerance, oligotrophic metabolism, and Fe metabolism. To gain a comprehensive understanding of the similarities and differences between the studied strains (our strain and the five closely related strains belonging to the *Rhinocladiella* and *Exophiala* genera) regarding protein prediction with a focus on astrobiological aspects, we generated a pangenome using anvi'o (EREN *et al.*, 2021) and the annotated genomes (.gbk files), as previously described. The proteins of each metabolism of interest were counted in a dereplicated manner, plotting the presence and absence of the proteins in each analyzed genome.

2.1.2.6. - LaBioMMi 1217 Culture on Synthetic Martian Regolith Substrate

After culturing LaBioMMi 1217 for 15 days at a controlled temperature of 25 °C on PDA, we used a sterile inoculation loop to transfer a pure colony to a Falcon tube containing 10 mL of 0.9% NaCl. Then, the cell suspension was sequentially diluted to an optical density of 0.7–0.9 at 595 nm (final concentration: 10^7–10^8 cells/mL). This cell suspension was used as the inoculum for an experiment to culture LaBioMMi 1217 in a synthetic Martian regolith (CANNON *et al.*, 2019). Briefly, 100 µL of the prepared cell suspension was inoculated into 50-mL Erlenmeyer flasks containing 20 mL of potato dextrose broth (PDB; Sigma-Aldrich) and 5 g of synthetic Martian regolith (MGS-1; ratio 1:4 [v/w]) with 1.5% (w/w) magnesium perchlorate.

The experimental control comprised 20-mL PDB inoculated with LaBioMMi 1217. To eliminate molecules originating from the culture medium and MGS-1 during data processing, experimental blanks were used (no inoculum suspension). Subsequently, the flasks were subjected to orbital agitation (150 rpm) and cultured for 10 days at a constant temperature of 25 °C. The experiments were conducted in five replicates.

2.1.2.7 - Scanning Electron Microscopy (SEM) Analysis

Samples were prepared for SEM by transferring 10 µL of each treatment (LaBioMMi 1217 in the presence and absence of MGS-1) to a silicon glass support, followed by fixation in 3% glutaraldehyde for 3 h. The fixed samples were dehydrated in a graded series of isopropanol (35%, 50%, 75%, 90%, and 100%), underwent critical point drying for 5 h, and finally coated with metallic iridium particles. Images were captured using field emission SEM (Merlin Gemini, Zeiss).

2.1.2.8 - Microbial Metabolite Extraction

To investigate the production of secondary fungal metabolites, PDB cultures were transferred from Erlenmeyer flasks to 50-mL Falcon tubes. We added 5 g of MGS-1 to the control experiments. To perform metabolomic analysis without interference from the matrix during extraction, no MGS-1 was added to the blank experiments. The samples were frozen at −80 °C for 24 h and then lyophilized. The metabolites and lipids were extracted using liquid–liquid separation method. Briefly, 20 mL of lysis solution containing MTBE:MeOH (4:1, v/v) was added to each tube, and the cells were lysed by placing the tubes on a vertical shaker for 60 min. Then, 15 mL of H_2O:MeOH (4:1, v/v) was added, and the tubes were placed in an ultrasonic bath at approximately 20–30 kHz for 20 min. Next, 1 mL of the hydroalcoholic phase from each extract was transferred to an Eppendorf tube and completely dried under a fast vacuum. The dried extracts were reconstituted in 250 µL of acetonitrile (ACN; purity ≥99.9%, Sigma-Aldrich) for liquid chromatography–high-resolution tandem mass spectrometry (LC–HRMS/MS) analysis.

2.1.2.9 - LC – HRMS/MS Analysis

The hydroalcoholic crude extracts underwent untargeted screening and metabolomic analysis using a Vanquish Ultra-High-Performance Liquid Chromatography (UHPLC) system coupled with an ID-X Tribrid mass spectrometer (Thermo Fisher Scientific) equipped with a heated electrospray ionization (ESI) source. Chromatographic separation was performed using an 2.1 × 50 mm × 1.7 µm Acquity UHPLC BEH C18 column (Waters Corp.) maintained at 40 °C. The injection volume of each sample was 10 µL. The flow rate was set at 0.5 mL min^{-1}, and a 15-min gradient was applied for separation using mobile phases A (H_2O with 0.1% formic acid) and B (ACN with formic acid 0.1%) under the following conditions: 0–1 min, 5% B; 1–3 min, 5% B to 15% B; and 3–15 min, 15% B to 100% B. Washing was

performed using 100% B and equilibrated with 5% A. The MS results were calibrated using an Pierce™ FlexMix™ Calibration Solution (Thermo Fisher Scientific) according to the manufacturer's instructions. Positive-ion mode ESI was applied to the compounds of interest using the following MS parameters: sheath gas flow rate, 40; auxiliary gas flow rate, 20; spray voltage, 4.0 kV; capillary temperature, 350 °C; auxiliary gas heater, 250 °C; S-lens RF level, 50; and resolution, 60,000. We used normalized collision energies of 15, 25, 35, and 45 eV for the MS/MS measurements. Pooled injected samples were used for quality control (QC).

2.1.2.10 - MS Data Processing

The processing workflow was performed using Compound Discoverer (CD) v3.3 software. First, spectra were selected from the raw data, followed by retention time (RT) alignment with a tolerance of 0.5 min and mass accuracy of 5 ppm. Then, unknown compounds with an RT tolerance of 0.7 min and mass deviation of 5 ppm were detected and grouped. In the second step, a feature table was created and statistical analyses were performed. Confidence with which a compound is named (i.e., annotated) followed the Metabolomics Standards Initiative guidelines (SUMNER *et al.*, 2007), where the annotation is classified according to four levels: unknown compounds (Level 4, low), putatively characterized compounds (Level 3, medium), putatively annotated compounds (Level 2, high), and identified metabolites (Level 1, highest). Annotation was based on precise mass analysis (error range: 0–2 ppm) and the MS/MS fragmentation profiles from the mzCloud and mzVault databases. Analytical standards were injected to confirm oxylipin detection. The CD workflow included the creation of a molecular network, where the MS/MS spectra of the biomarkers of interest were analyzed and grouped using a coverage of 60, a score of 50, and a fragment match of 25. The images generated by the molecular network were colored manually using InkScape v1.3.2 software.

2.1.2.11 - Effect of MGS-1 on Metabolite Extraction and Experimental Control Design

It is crucial to meticulously design the entire workflow when conducting metabolomics analysis to identify biomarkers. In particular, the extraction process must be considered to prevent biased data interpretation. In the experiment aimed at observing variations in metabolism, the fungus was cultured in the presence of a particulate material (i.e., the synthetic Martian regolith MGS-1). However, the presence of MGS-1 may have

facilitated cell lysis during extraction, enhancing the retrieval of metabolites. Therefore, we assessed the influence of MGS-1 on the extraction process to explore its effect on the induction of the molecules. This preliminary assessment guided our selection of the most suitable control experiment for statistical comparison. To this end, crude extracts from all samples were evaluated by ultra-high-performance (UHPLC–MS/MS), and an unsupervised analysis (principal component analysis, PCA) was performed.

2.1.2.12 - Laser Desorption Ionization Mass Spectrometry (LDI-MS) Analysis of Microbial Extract-Doped MGS-1

We adapted the method of SANTOS *et al.* (2021) for the LDI-MS analysis of microbial extract-doped MGS-1. Briefly, we added 5 mg of the dried hydroalcoholic extract of the fungus cultured in the previous experiment to 1 mL of LC–MS grade MeOH, transferred the solution to a microtube containing 500 mg of MGS-1, and vortexed at 70 Hz for 5 min. Then, we used a micropipette to transfer 1 µL of each prepared suspension to different points of the sample holder and dried them for 15 min at room temperature.

Measurements were performed using an Autoflex Speed mass spectrometer (Bruker Daltonics, Bremen, Germany). A 355nm Nd:YAG laser source operating at a frequency of 10 Hz and 70% of the nominal power focused on a point approximately 5 µm in diameter was used to induce ionization/desorption processes. Positive-ion mass spectra were acquired after time-of-flight separation in reflectron mode with an acceleration voltage of 20 kV. All spectra were collected from an average of 100 laser shots. A standard mixture for low masses was used for mass calibration. MTP 384 polished steel target plate and MGS-1 mineral origin matrices were used. The operating pressure of the spectrometer was approximately 10^{-7} mbar.

2.1.3 - Results

2.1.3.1 - Morphological and Molecular Characterization of LaBioMMi 1217

The morphological characteristics of the fungal strain LaBioMMi 1217 were assessed after 20 and 15 days of culture on PDA (Figure 2.1A) and Mycosel medium (Figure 2.1B), respectively. Irregular-shaped brown colonies with a rough texture were observed on PDA, and the periphery had dark greenish-gray pigmentation (Figure 2.1A).

Optical microscopy of the fungus in filamentous form revealed thick-walled, dematiaceous, and septated hyphae containing lateral and apical conidiophores with elongated to ovoid conidia (Figure 2.1D). In contrast, yeast-like microcolonies, approximately 2 mm in diameter, were observed on Mycosel medium. The colonies had dark brown pigmentation that appeared gelatinous in the center and slightly lighter at the periphery (Figure 2.1B). Optical microscopy revealed several yeast-like cells, some of which were budding, and pseudohyphae (Figure 2.1C). These morphological characteristics were consistent with those of the *Rhinocladiella* and *Exophiala* genera.

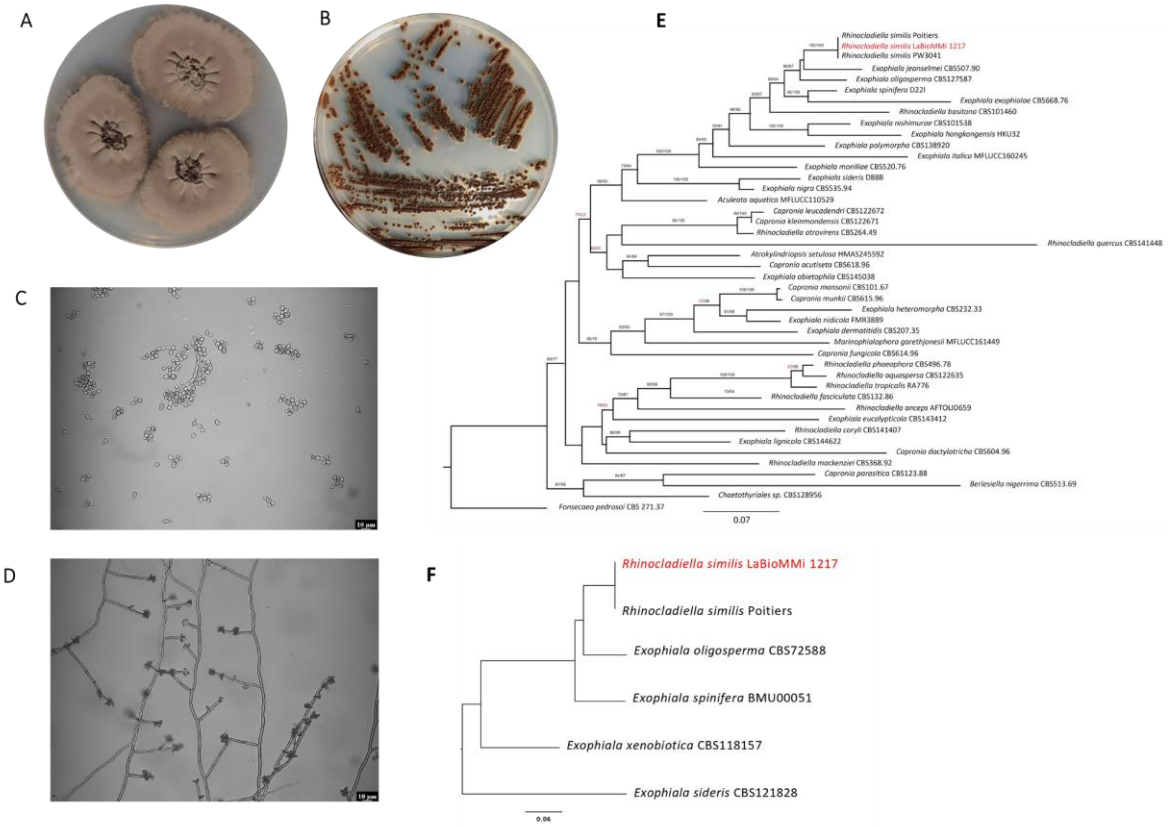

FIGURE 2.1 – Morphological and molecular characterization of fungal strain LaBioMMi 1217.

Macroscopic structure of the fungus cultured on (A) potato dextrose agar for 20 days and (B) Mycosel medium for 15 days. Microscopic structure of the fungus cultured on (C) Mycosel medium for 15 days and (D) potato dextrose agar for 20 days. (E) Concatenated multilocus sequence analysis (MLSA) tree based on five conserved marker genes (*ITS*, *LSU*, *tef1*, *rpb1*, and ß-tubulin) extracted from whole genome sequencing (WGS) data from LaBioMMi 1217 or available genes in databases. The MLSA tree was rooted in *Fonsecaea pedrosoi*. (F) WGS-based phylogenomic analysis of *R. similis* using midpoint rooting. We constructed a phylogenomic tree for *Rhinocladiella* and *Exophiala* strains using available genomic sequences.

The molecular typing results for LaBioMMi 1217 indicated that it belonged to *R. similis* based on three criteria. First, the BLAST analysis of the sequenced ITS fragments showed 100% identity with the type strain CBS 111763 (accession no. NR_166008.1). Second, MLSA using five different nuclear markers commonly employed to distinguish species within the order Chaetothyriales revealed that LaBioMMi 1217 formed a monophyletic cluster with other *R. similis* strains and was closely related to other extremotolerant fungi, such as *E. jeanselmei*, *E. oligosperma*, and *E. spinifera* (Figure 2.1E). Third, phylogenomic analysis (Figure 2.1F) confirmed the MLSA results, with the *R. similis* strains LaBioMMi 1217 and Poitiers forming a strong dyad that was closely related to the aforementioned *Exophiala* strains.

2.1.3.2 - Genomic Features of R. Similis LaBioMMi 1217 and Closely Related Strains

The genomic sequence of *R. similis* LaBioMMi 1217 was deposited in GenBank (accession no. JBBMOB000000000, BioProject PRJNA1005689). The *R. similis* LaBioMMi 1217 genome was assembled into 80 scaffolds (total size = 34,715,284 bp), with an average scaffold size of 433,941 bp (N50 = 1,238,920 bp, L50 = 10) and a GC content of 50.98%. Genome annotation revealed 12,908 genes comprising 12,857 protein-coding genes and 51 tRNAs (Table 2.1).

TABLE 2.1 – Genome characterization and assembly statistics of *Rhinocladiella similis* LaBioMMi 1217 and its closely related strains in the *Exophiala* genus.

Feature	***R. similis* LaBioMMi 1217**	***R. similis* Poitiers**	***E. xenobiotica* CBS118157**	***E. spinifera* BMU00051**	***E. sideris* CBS121828**	***E. oligosperma* CBS72588**
Total length (bp)	34715284	34259553	31405760	32380025	29505589	38224514
No. of contigs	80	12	15	7	5	143
No. of contigs >100 kb	43	9	7	7	4	22
L50	10	4	3	3	2	5
L90	29	8	7	7	4	17
N50	1238920	4787646	5039080	4872376	7897194	3385568
N90	310628	2323203	3649802	3759476	4504137	346205
Unique proteins	175	146	1,158	968	1,294	1,611
Pfam domains	16,078	16,132	13,573	13,598	13,853	16,048

GO terms (molecular function)	2,401	2,402	2,429	2,451	2,516	2,384
GO terms (biological process)	1,794	1,898	1,977	1,994	1,973	1,83
GO terms (cellular component)	1,507	1,644	1,736	1,765	1,754	1,584

Comparison of the two *R. similis* genomes with the closely related strains belonging to the *Exophiala* genus revealed several distinctive characteristics. There was a strong positive correlation between genome size and the number of genes ($R = 0.9319$, $p < 0.01$). The species with the largest genome size and gene content was *E. oligosperma*, followed by *R. similis* species. Both were phylogenetically related, indicating that gene expansion occurred in both species (Table 2.1), as reflected by a prominent expansion of Pfam domains. Overall, this pattern was also observed in secreted proteins (Figure 2.2A), secondary metabolite clusters (Figure 2.2B), and proteases (MEROPS, Figure 2.2C) but not in carbohydrate-degrading enzymes (CAZymes), particularly when compared with the pectin lyase genes of *E. spinifera* and *E. xenobiotica* (Figure 2.2D). Notably, the MEROPS subfamilies A1A, S33, S12, S09X, M20D, and C69 were expanded in the *R. similis/E. oligosperma* dyad relative to other *Exophiala* species (Figure 2.2C). Similarly, we also observed an expansion of secondary metabolite clusters related to the production of isocyanide nonribosomal peptide (NRP) and other NRPs in those species (Figure 2.2B). Regarding the CAZyme families, we observed an expansion of glycoside hydrolases (GHs) GH3, GH32, and GH130 and auxiliary activities (AAs) AA1, AA7, and AA8 (Figure 2.2D). Finally, the transcription factor classes fungal Zn(2)-Cys(6) binuclear domain (IPR001138) and KilA-N domain (IPR018004) were expanded in the *R. similis/E. oligosperma* dyad, whereas the helix-loop-helix DNA-binding domain (IPR011598) and STE-like transcription factor (IPR003120) were contracted (Figure S1.1). These genomic differences might impact the species' ecology. Besides these differences, we observed a negative correlation between the number of proteins and the GO terms related to biological processes ($R = -0.9003$, $p < 0.05$) and cellular components ($R = -0.8617$, $p < 0.05$), indicating that species with fewer protein-coding genes had a more diversified metabolism compared with species with a higher number of protein-coding genes.

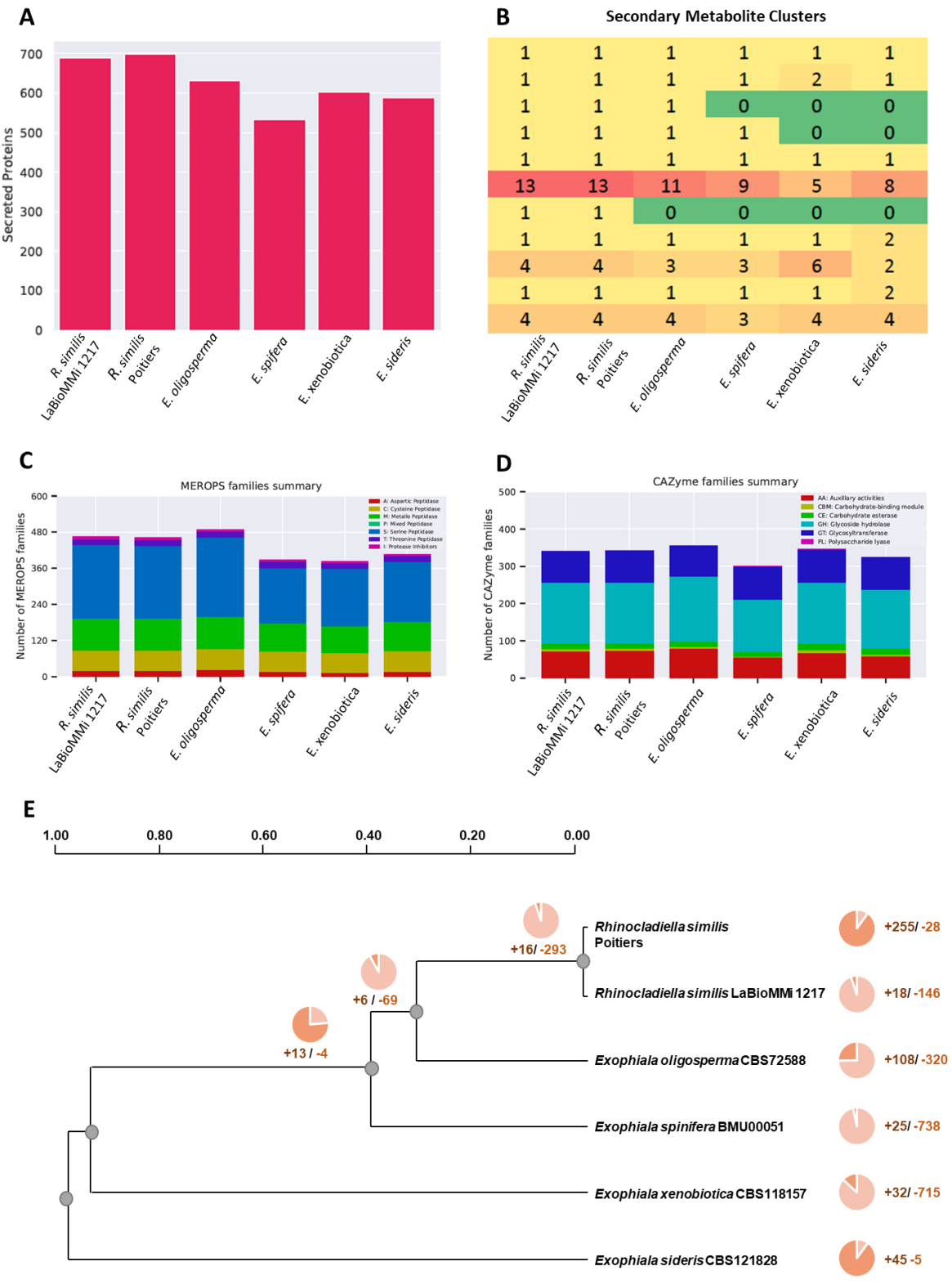

FIGURE 2.2 – Comparative genomic analysis of Rhinocladiella similis LaBioMMi 1217 and its closely related strains.

(A) Relative predicted amount of secreted proteins. (B) Predicted biosynthetic gene clusters. (C) Relative distribution of the predicted protease (MEROPS) groups. (D) Bar plot of the CAZyme family domains of *Rhinocladiella* and *Exophiala* species. (E) Phylogenetic tree showing gain and loss of InterPro domains among six genomes (*R. similis*, n = 2; *Exophiala* spp., n = 4).

We used the CAFE5 tool to test the distribution of such gene families using the birth–death model. *Rhinocladiella similis* LaBioMMi 1217 exhibited an expansion of 18 and a reduction of 146 InterPro domains ($p < 0.05$; Figure 2.2E). The GO term conversion of the acquired InterPro domains revealed that they were related to metabolic processes associated with aromatic and nitrogenous compounds and organic acid transport. In contrast, the contracted GO terms were related to the regulation of transmembrane transport, DNA-templated transcription, catalytic processes, protein transport, and transcription regulation from RNA polymerase II promoter. These findings indicated that *R. similis* LaBioMMi 1217 lost domains related to transcription control as well as protein degradation, folding, and transport.

We observed similarities and differences between the studied strains in the pangenome generated from the annotated genomes. We identified 117 unique predicted proteins and 972 core proteins in the *R. similis* LaBioMMi 1217 genome. Additionally, compared with the other analyzed strains, *R. similis* LaBioMMi 1217 genes related to proteins potentially useful in astrobiologically relevant conditions were more evident. Therefore, we investigated the metabolic adaptations of *Exophiala* and *Rhinocladiella* that might facilitate their viability under challenging environmental conditions similar to those on Mars by analyzing Pfam and InterPro terms associated with dehydration, desiccation, rehydration, heat shock, chemical detoxification, osmotic stress, UV resistance, and Fe metabolism (Figure 2.3A). The comparative analysis also revealed that *R. similis* LaBioMMi 1217 had higher number of proteins related to Fe metabolism (n = 6), heat shock (n = 29), and chemical detoxification (n = 46). Notably, *R. similis* LaBioMMi 1217 also had higher number of proteins related to UV tolerance (n = 4), salt stress (n = 5), and osmotic stress (n = 11) but lower number of proteins related to desiccation (n = 1), dehydration (n = 1), and water stress (n = 5) compared with the other strains.

Table S1.2 lists the proteins associated with each function screened in the genomes of the analyzed strains. Of these, 23 were selected for further investigation (Figure 2.3B), revealing notable differences between the Pfam and InterPro terms among the analyzed species. Proteins associated with dehydration and omostic stress, such as those in the catalase domain (IPR011614), and those associated with osmotic stress response, extracellular FtsH production, and chitin synthesis regulation (PF11785, and PF12273, respectively) were observed in all analyzed strains. When filtered for terms related to saline stress, stress responsive alpha-beta barrel protein (IPR013097) was present in all strains, except for *E. spinifera*. Additionally, *R. similis* LaBioMMi 1217 possessed multiple genes related to the

synthesis of proteins involved in heavy metal detoxification (IPR045181, and IPR017969), siderophore production siderophore and transport (IPR007037, IPR013113, and IPR039374).

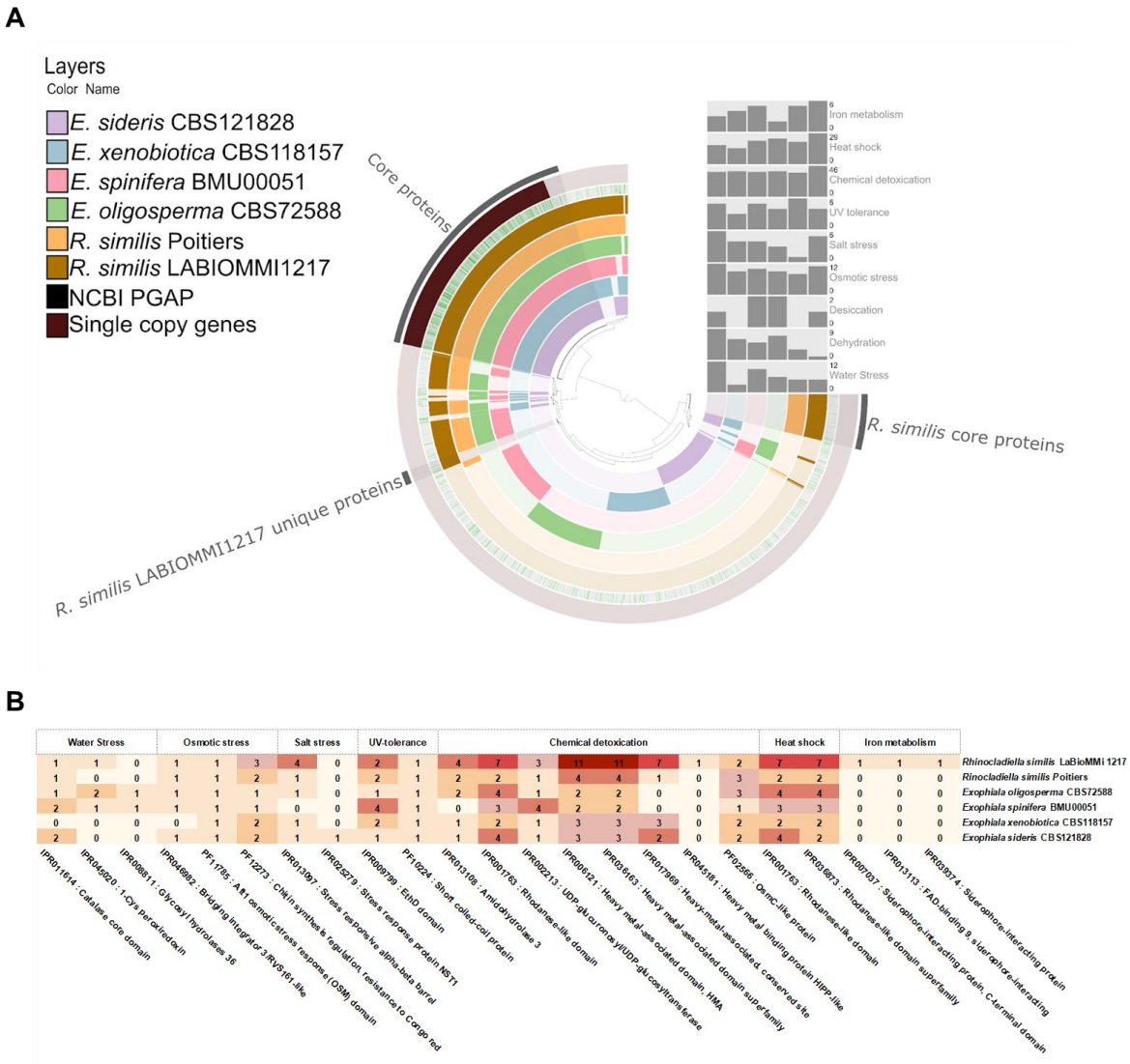

FIGURE 2.3 – (A) Comparative analysis of the *Rhinocladiella* and *Exophiala* genomes illustrating the shared and unique proteins. The gray bars indicate the annotated protein counts associated with specific functions. (B) Relative distribution of predicted protein terms in the Pfam and InterPro databases filtered according to dehydration, desiccation, rehydration, chemical stress, UV resistance, and iron metabolism.

2.1.3.3 - Effect of MGS-1 on *R. Similis* LaBioMMi 1217 Morphology

LaBioMMi 1217 was cultured in the presence and absence of synthetic Martian regolith MGS-1, and morphological changes were examined using SEM. Fungal pseudohyphae were observed in the absence of MGS-1 (Figure 2.4A), indicating a transition

between unicellular (yeast-like) and multicellular (filamentous) phases characteristic of dimorphic fungal species. These structures are formed by yeast-like cells that remain attached after cell division and form tube-like chains, but they do not possess the same degree of cohesion and cytoplasmic continuity as genuine hyphae. In the experiment containing MGS-1, the yeast-like form of the fungus, characterized by a unicellular spherical or oval shape, was dispersed among the minerals present in the regolith (Figure 2.4B).

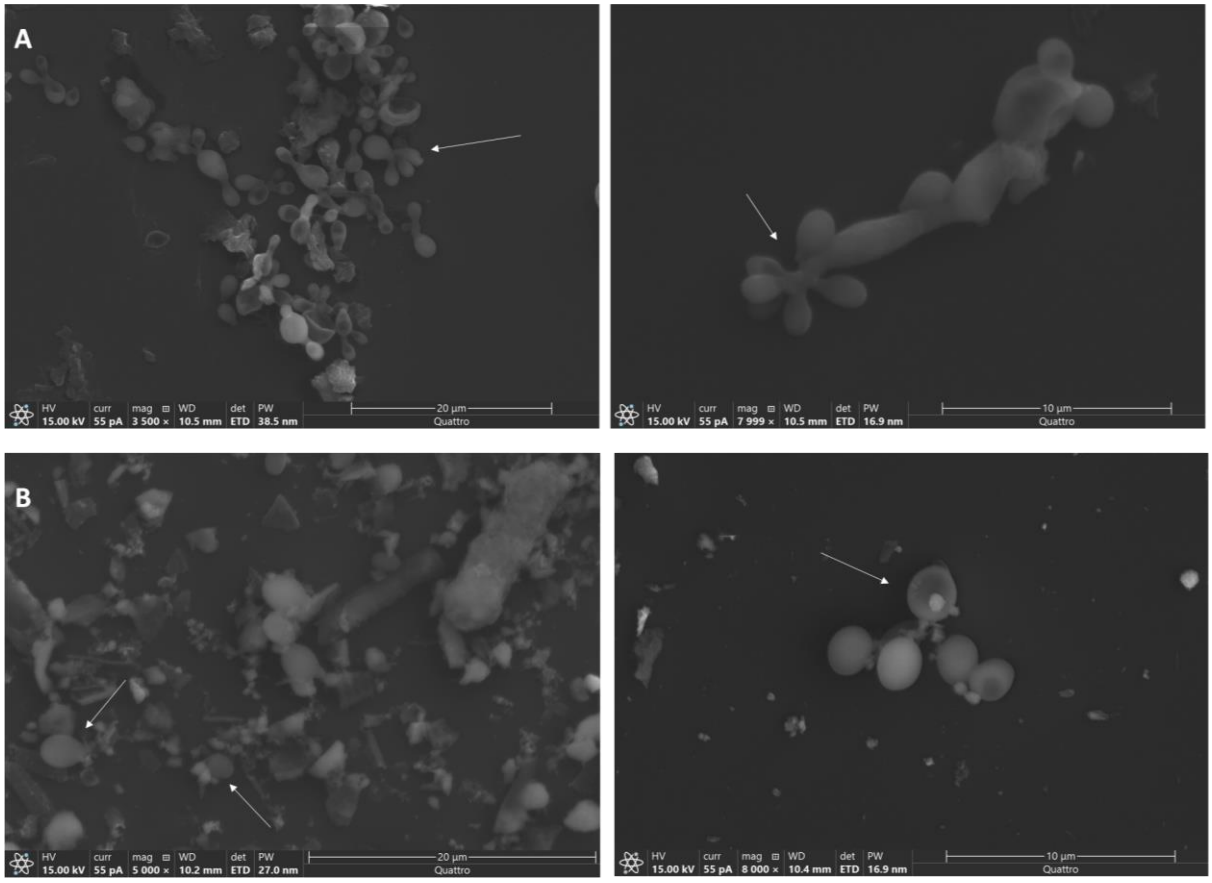

FIGURE 2.4 – Scanning electron microscopy images of *R. similis* LaBioMMi 1227.

Rhinocladiella similis LaBioMMi 1227 cultured in (A) potato dextrose broth (PDB) and (B) PDB supplemented with MGS-1 at a ratio of 1:4 (v/w). White arrows indicate cellular structures (pseudohyphae and yeast forms).

2.1.3.4 - Effect of MGS-1 on Metabolite Extraction and Experimental Control Design

To determine the most suitable control experiment for statistical comparison, the crude extracts obtained from all samples were subjected to UHPLC–MS/MS, and the results were evaluated using unsupervised analysis (PCA). Figure S1.2A presents the discrepancies among all groups in the unsupervised analysis, revealing distinctions between

blanks and adjusted or unadjusted samples. The box plot in Figure S1.2B exemplifies the comparison of feature areas *m/z* 237.0756 and RT 4.985 min for adjusted and unadjusted controls. The increased area in the adjusted control feature (with MGS-1 incorporation during extraction) compared with the unadjusted control indicated that MGS-1 optimized the extraction process. Thus, we chose to proceed with our investigation of the microorganism's metabolism by comparing the adjusted control samples with those containing fungus with regolith.

2.1.3.5 - Metabolomic Differentiation in *R. Similis* LaBioMMi 1217 Cultured with MGS-1

To investigate the effect of the synthetic Martian regolith MGS-1 on *R. similis* metabolism, we used UHPLC–MS/MS to evaluate the crude extracts of the fungus in the presence of the control regolith and its respective blanks. PCA was conducted to provide an overview of the data. The PCA score plot (Figure 2.5) revealed that the first two principal components accounted for 48.8% (29.1% and 19.7% for PC1 for PC2, respectively) of the overall data variance, showing a separation trend between the fungus in the presence of regolith (fungus with regolith) and the fungus cultured solely in PDB (adjusted control). The control group samples were distributed throughout the third quadrant, and the distribution of the samples of the fungus with regolith varied in the first quadrant. Because the separation between the groups was evident using the unsupervised method, a supervised analysis was unnecessary. The reproducibility of the instrumental system (i.e., both the chromatographic and mass spectrometric components) was assessed by jointly analyzing the QC samples, which were tightly clustered in the center of the PCA score plot, indicating stable performance (Figure 2.5).

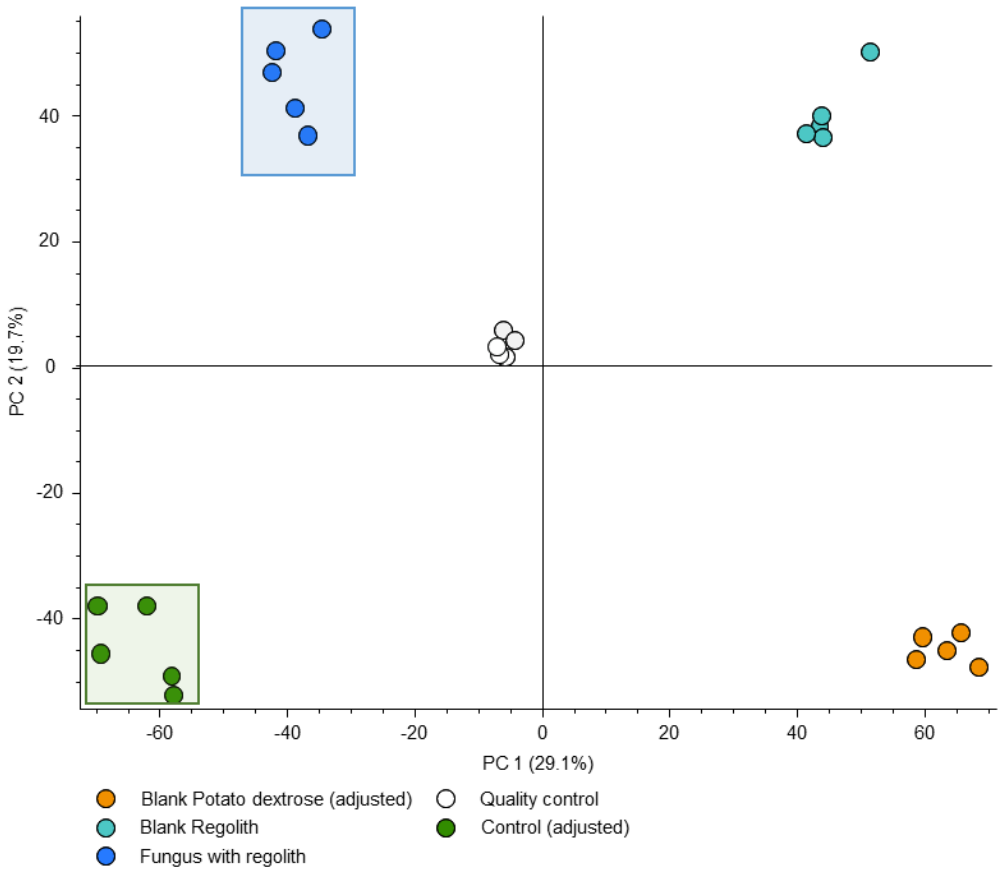

FIGURE 2.5 – Statistical analysis of UHPLC–MS/MS data of *R. similis* LaBioMMi 1217 in MGS-1 regolith medium and under control conditions.

Principal component analysis plot showing variances in metabolite production between control and regolith medium experiments and clustering among replicate samples.

We considered a $\log_2$ fold change ≥ 2 as an indicator of metabolites upregulated in the presence of MGS-1. Such screening yielded 244 features with a significant increase in their area in the presence of MGS-1, indicating that the metabolites were potentially induced by the mineralogical components of MGS-1. Of them, 211 were statistically significant (*t*-test, p-value ≤ 0.05). Six metabolites were annotated based on precise mass analysis (error range: 0–2 ppm) and MS/MS fragmentation. The annotated compounds were identified as 3-(2-hydroxyethyl)-indol-5-ol (*m/z* 178.0862, p-value = 1.13×10^{-4}), methyl indole-3-acetic acid (*m/z* 190.0862, p-value = 3.07×10^{-3}), indole-3-lactic acid (*m/z* 206.0811, p-value = 2.61×10^{-4}), iso-12-oxo-phytodienoic acid (iso-13-EPI-12-OXO-PDA; *m/z* 293.2111, p-value = 1.05×10^{-3}), cis-12-oxo-phytodienoic acid (*cis*-13-EPI-12-OXO-PDA; *m/z* 293.2111, p-value = 8.59×10^{-4}), and 9-oxo-10,12-octadecadienoic acid (9-KODE; *m/z* 295.22681, p-value = 2.22×10^{-2}). 9-KODE was classified as a Level 1

annotation because its MS/MS spectrum and RT were comparable with an analytical standard. Figure 2.6 shows the MS/MS spectra and box plots of the areas of putatively annotated metabolites.

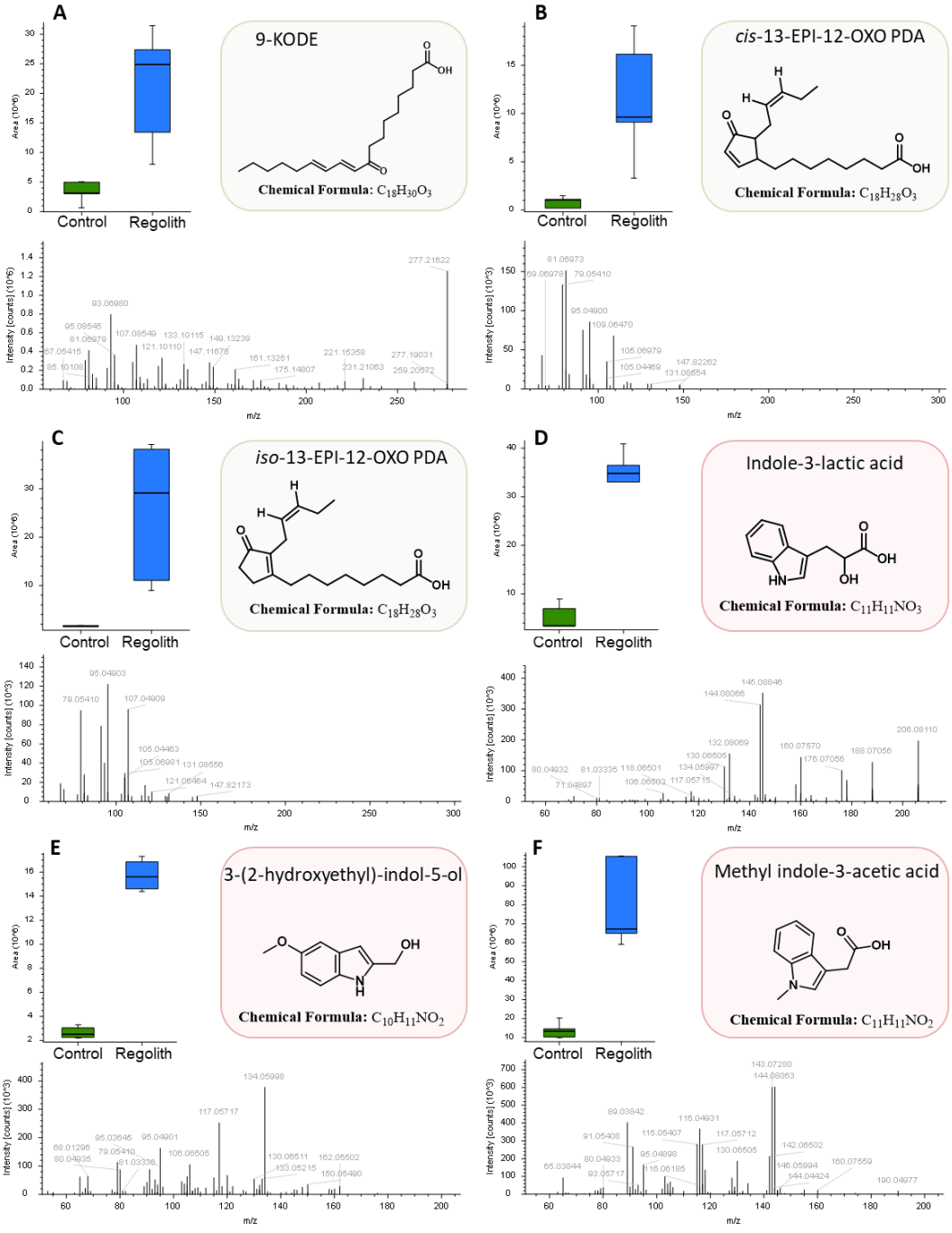

FIGURE 2.6 – MS/MS spectra of the annotated molecules accompanied by a box plot illustrating the average ion intensity of molecules upregulated by the fungus when cultured in the presence of MGS-1.

These include the oxidized fatty acids: (A) 9-KODE, (B) cis-13-EPI-12-OXO-PDA, and (C) iso-13-EPI-12-OXO-PDA. Additionally, the indolic derivatives: (D) indole-3-lactic acid, (E) 3-(2-hydroxyethyl)-indol-5-ol, and (F) methyl indole-3-acetic acid.

The MS/MS spectra of oxidized fatty acids, such as iso-13-EPI-12-OXO-PDA (*m/z* 293.2111), *cis*-13-EPI-12-OXO-PDA (*m/z* 293.2111), and 9-KODE (*m/z* 295.2268), exhibited fragmentation profiles in positive-ion mode that appeared to act as a unique signature for each molecule. As illustrated in the spectra presented in Figures 2.6A-C, although there were similarities in fragment ions, the relative intensities differed significantly. Confidence in the annotations indicated by databases was strengthened by the consistency observed for 9-KODE when compared with its known analytical standard (Figure S1.8) because it presented the same MS/MS spectrum and similar RT.

We delved deeper into the spectral peculiarities of indolic acid derivatives. The MS/MS spectrum (Figure 2.6D) of indole-3-lactic acid with $[M + H]^+$ at *m/z* 206.0811 highlighted a base peak at *m/z* 145.0884. This fragmentation was characteristic of the indole core after losing an acid group, forming a stabilized cation. A high-intensity peak was also observed at *m/z* 144.0806, which was interpreted as the additional loss of an H atom from the ion at *m/z* 145.0884. The ion at *m/z* 188.0705, representing a mass difference of 18 Da relative to the molecular ion, indicated the loss of H_2O. The peak at *m/z* 160.0757 indicated the loss of the carboxyl group [-COOH]. Peaks at *m/z* 132.0806 and *m/z* 130.0650 indicated subsequent fragmentations of the indole structure, representing alternative decomposition pathways during fragmentation.

The MS/MS spectrum (Figure 2.6E) of 3-(2-hydroxyethyl)-indole-5-ol with $[M + H]^+$ at *m/z* 178.0862 displayed main fragments at *m/z* 134.0559, *m/z* 117.0517, *m/z* 106.0605, and *m/z* 95.0491, indicating indole ring fragmentation and subsequent loss of functional groups. A base peak was also observed at *m/z* 134.0559, indicating a neutral loss of the hydroxyethyl group $[M + H - C_2H_4O]^+$, representing the most stable fragment formed during ionization.

The MS/MS spectrum (Figure 2.6F) of methyl indole-3-acetic acid with $[M + H]^+$ at *m/z* 190.0862 showed a base peak at *m/z* 144.0806, characteristic of indole nucleus fragmentation after losing the methoxy group [-OCH_3]. Another high-intensity peak was observed at *m/z* 143.0728, indicating the simultaneous fragmentation of the indole core and the loss of an H atom. Additional fragment ions included *m/z* 160.0756, possibly related to the loss of the carboxyl group [-COOH]; *m/z* 116.0493 and *m/z* 117.0512, which may represent subsequent indole nucleus fragmentations; and peaks at *m/z* 95.0498 and *m/z* 89.0384, representing more extensive structural fragmentations.

To determine whether other features induced by MGS-1 were related and to potentially propagate annotation to other ions, we performed molecular network analysis

using the spectral comparison-based tool CD v3.3 with the MS/MS data of all 211 statistically significant features. The spectra were grouped based on coverage, the number of matching fragments, and similarity scores, resulting in clustering into four spectral families (Figure 2.7), indicating that MGS-1 increased molecule production and induced entire molecular families.

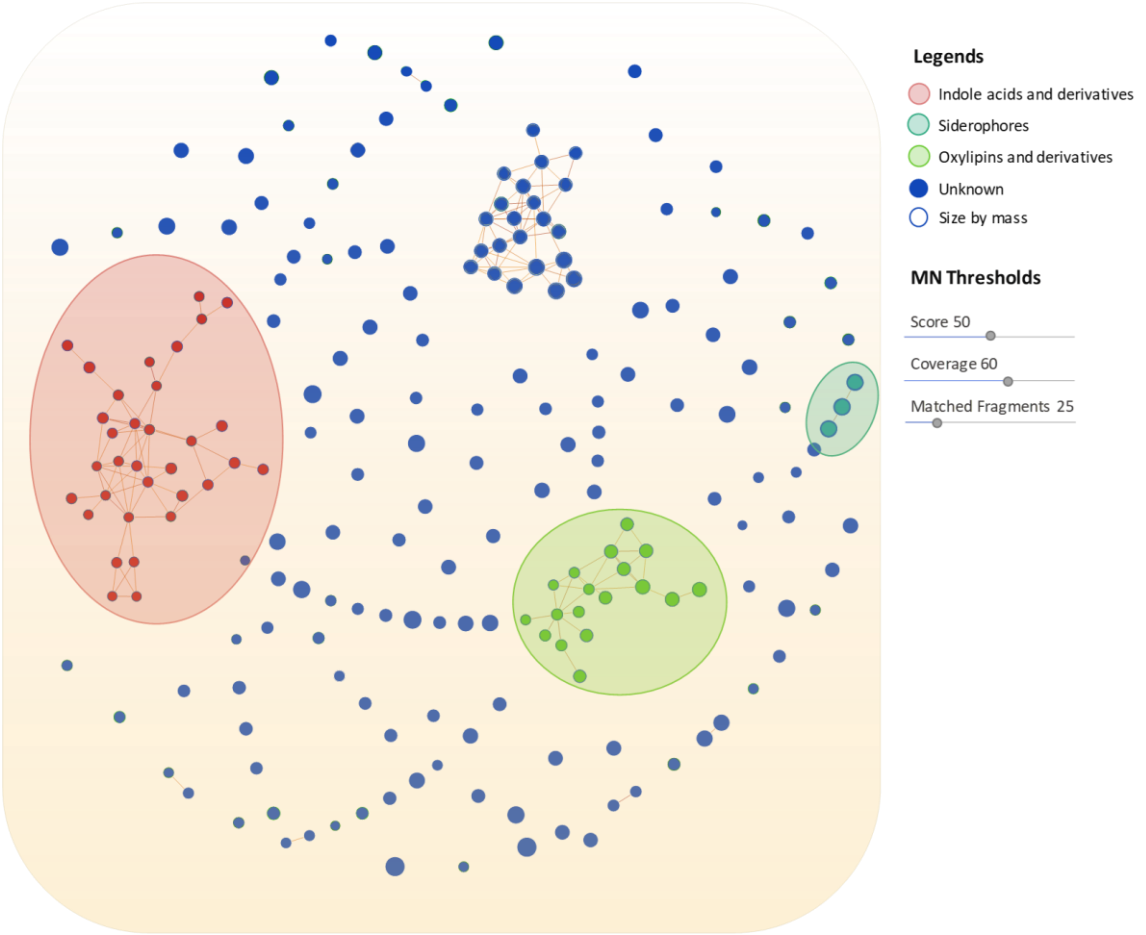

FIGURE 2.7 – Molecular network generated using Compound Discover v3.3 software.

Here, each node represents a feature with high-resolution mass and retention time. The software also grouped metabolites according to their structural functions. Molecular families, including indole derivatives, oxylipins, and siderophores, were classified based on the annotated nodes.

The previously annotated compounds were distributed into two molecular families: indolic acid derivatives and oxylipin derivatives (Figure 2.8A).

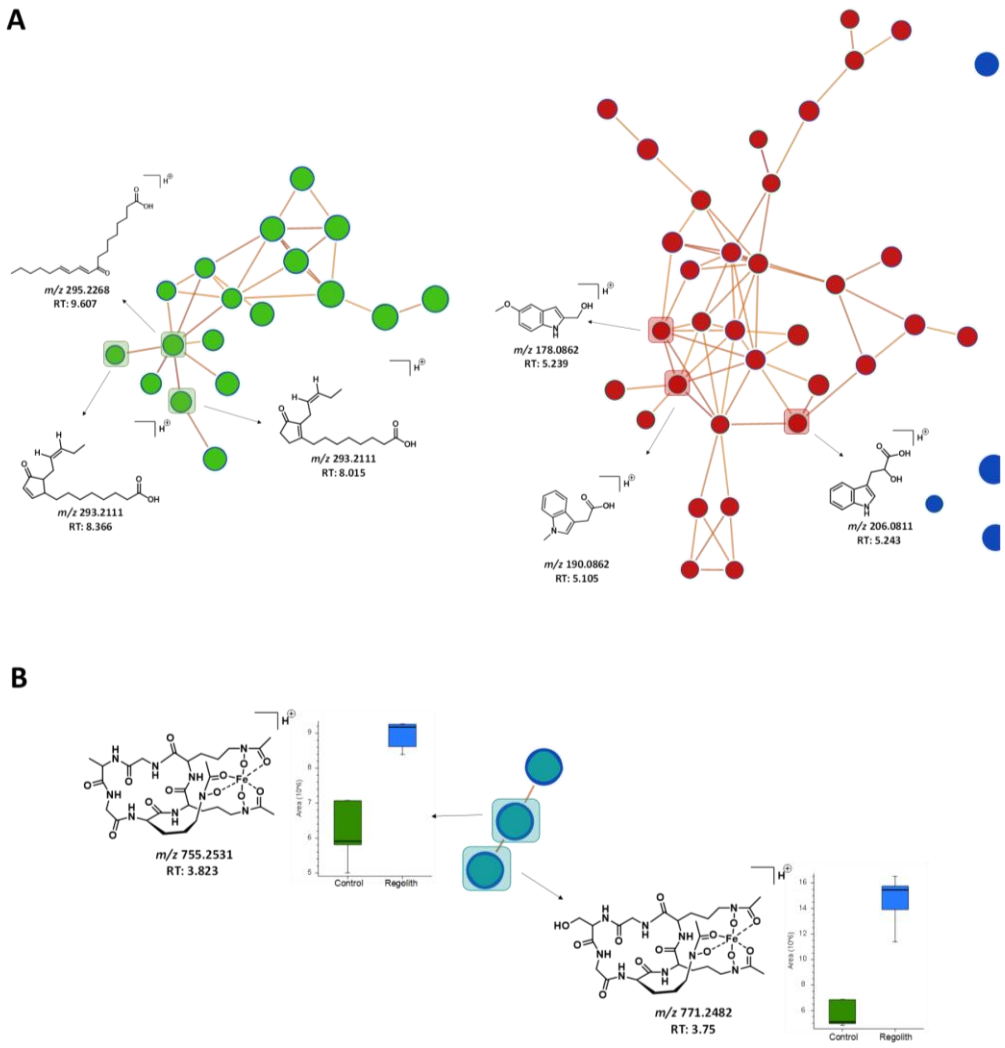

FIGURE 2.8 – Expansion of molecular clusters according to the structure of their respective ions.

(A) Molecular network (MN) of the two annotated families, as obtained by MS/MS spectrum comparison. Green, indolic acid and its derivatives; red, oxylipins and derivatives. (B**)** MN of the siderophore molecular family. Box plots of areas with increased production in the MGS-1 regolith experiment.

Based on manual observation of the MS/MS spectra, a molecular family comprising only three nodes was annotated. This was prompted by an initial observation of a difference of 18 Da between the ion at *m/z* 755.2531 and the ion at *m/z* 771.2482, indicating a difference in hydroxylation. We also observed an atypical isotopic pattern of the precursor ions (Figure S1.11), indicating the presence of an Fe atom. Using fragmentation mechanisms, these two features were manually annotated as siderophores and were supported by the literature (MAWJI *et al.*, 2008). Supplementary Figures S1.9 and S1.10 present proposed fragmentation mechanisms for these molecules. Thus, the ions at *m/z* 755.2531 (*p*-value = 5.13×10^{-3}) and *m/z* 771.2482 (p-value = 3.91×10^{-2}) were putatively annotated (Level 2) as

ferrichrome C and ferricrocin, respectively. Figure 2.8B presents the molecular family of siderophores, and the box plots of the areas show the increased production of these two molecules in the presence of synthetic Martian regolith MGS-1.

2.1.3.6 - Detectability of Biosignatures Produced by R. Similis LaBioMMi 1217 in Synthetic Martian Regolith Matrices Using LDI-MS

To investigate the capability of LDI-MS to detect biosignatures on Mars, the extract containing the metabolites identified as biomarkers of the fungus–mineral interaction in the untargeted metabolomics experiment underwent a simulation of detection by LDI-MS. Measurements in the range of *m/z* 200–600 were performed for samples containing the extract of *R. similis* LaBioMMi 1217 cultured in the presence of MGS-1 and dispersed in the same regolith. Despite the roughness of the MGS-1 matrix, it was we obtained spectra with sufficient mass resolution to identify the target compound. We observed a variety of high-intensity ions in the *m/z* 200–250 range and other ions with lower intensity in the *m/z* 300–350 range. Some ions were also observed *m/z* 510–550 range, indicating the presence of organic molecules with lipid-like characteristics. No ions were detected in the mass region of siderophores. Figure 2.9 presents the expanded spectrum in the *m/z* 200– 600 range.

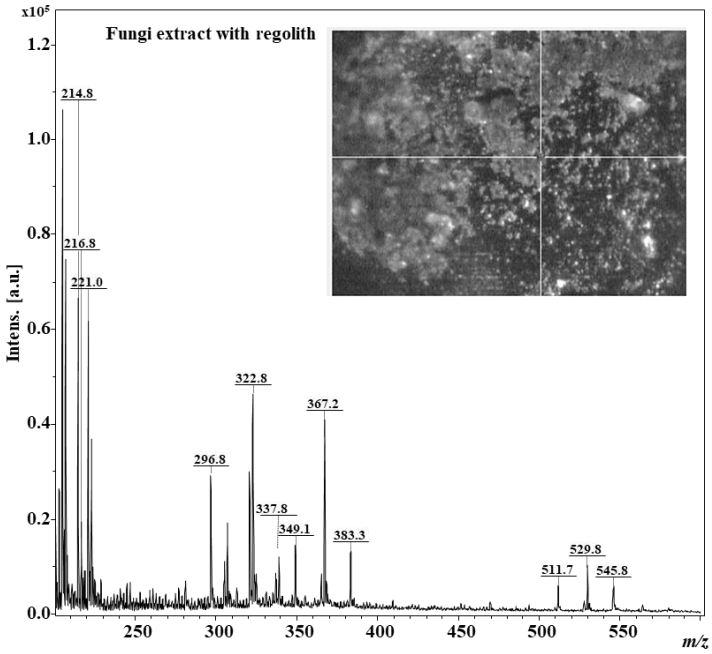

FIGURE 2.9 – Laser desorption ionization mass spectrometry spectrum obtained in the *m/z* 200–600 range for *Rhinocladiella similis* LaBioMMi 1217 extract-doped MGS-1.

2.1.4 - Discussion

The search for eukaryotic models, such as fungi, in the field of astrobiology, is gaining attention due to their significant contributions in extreme environments on Earth, indicating that they are capable of potential contributions on other planets (SIMÕES *et al.*, 2023). The fungus *Cryomyces antarcticus*, a black yeast isolated from the McMurdo dry valleys in Antarctica, is recognized as the most stress-resistant fungal microorganism found on Earth and in simulated space environments, and it has been used as a model for life on Mars (ONOFRI *et al.*, 2020). Our results indicated that in addition to the genus *Cryomyces*, representatives of the family *Herpotrichiellaceae* also show potential astrobiological applications because some are polyextremophiles, capable of surviving under a wide range of stressors. Thus, they may be capable of withstanding the extreme conditions of extraterrestrial environments (PULSCHEN *et al.*, 2018; TESEI, 2022; THITLA *et al.*, 2023). Our phylogenomic and metabolomic findings contribute to understanding these microorganisms as candidate models of astrobiological life, with a primary focus on their biosignature production and interaction with the geochemical aspects of Mars. To our knowledge, this is the first report to explore *R. similis* as an astrobiological model and focus on its extremophilic genomic traits and biosynthesized metabolites.

The genetic characterization of isolate LaBioMMi 1217 revealed that in addition to being a strain of the species *R. similis*, it was closely related to yeasts of the genus *Exophiala*, such as *E. oligosperma.* Some members of the genus *Exophiala* have been studied for astrobiological purposes. For example, *Exophiala* sp. strain 15LV1, isolated from the Atacama Desert, survived high levels of UV radiation (exposure to 1 kJ/m^2 of UVC) and stratospheric balloon flight experiments (PULSCHEN *et al.*, 2018).

Our genomic analysis revealed that species of *Rhinocladiella* and *Exophiala* produced predicted proteins (Pfam and InterPro terms) associated with dehydration and desiccation stress responses. Genetic characteristics associated with desiccation and oligotrophy were observed in *R. similis* LaBioMMi 1217 and *E. oligosperma* CBS72588, which might promote their adaptation to conditions with low nutrient levels and limited organic matter, making them good candidates for experiments simulating the chemical conditions of Martian soil (PRICE *et al.*, 2022). All analyzed strains produced proteins predicted as related to UV resistance. Because of their highly pigmented nature, the presence of laccases might be associated with melanin biosynthesis (GAO *et al.*, 2022).

Regarding geochemistry, Martian regoliths are as rich in ferric minerals (i.e., hematite) and perchlorate salts. Thus, by filtering for proteins associated with chemical detoxification and Fe metabolism, we found that when compared with the other analyzed strains, *R. similis* LaBioMMi 1217 produced a considerable number of proteins that could be used as mechanisms to assess environmental stress, such as the 74 proteins associated with the cytochrome P450 superfamily. Studies on the bacterial genus *Rhodococcus* have demonstrated significant overexpression of these proteins when cultured in the presence of perchlorate (YADAV *et al.*, 2022). Additionally, our strain (*R. similis* LaBioMMi 1217) was the only one to produce proteins associated with siderophore transport, indicating its capability to survive in environments rich in perchlorate, such as Martian brines. We also observed that *R. similis* LaBioMMi 1217 was the only strain to produce proteins associated with the production and transport of siderophore molecules. Considering the conditions on Mars, these proteins may play a role in the mechanism of Fe acquisition from the oxides present on Mars (BARTON *et al.*, 2012; HUANG *et al.*, 2022).

The surface of Mars is an extremely hostile environment for all forms of life, mainly due to the combination of UV radiation and perchlorates in the regolith. Hence, the subsurface has emerged as an interesting niche to investigate how astrobiological models cope in these environments. To better understand the microorganism–regolith interactions from a Martian perspective, and considering the capabilities of *R. similis*, we investigated its morphology and metabolism using experiments simulating Martian geochemistry. Our investigation of morphological changes in *R. similis* LaBioMMi 1217 when interacting with simulated Martian soil revealed that it used its dimorphic capacity to survive in these harsh conditions. This same type of adaptation was also observed when the same yeast was cultured in perchlorate brines (SANTOS *et al.*, in press), indicating that this morphological change may be related to the presence of saline and oxidative stress in the simulated soil medium. In the presence of environmental stress, this same plasticity has been reported for several other melanized fungi (SEYEDMOUSAVI *et al.*, 2014). Given the high complexity of the synthetic regolith used in our experiments and the addition of perchlorate, it is difficult to ascertain which factor is truly responsible for this change in plasticity because the presence of regolith alone plays an oxidizing role due to its high hematite content (CANNON *et al.*, 2019; RAMALHO *et al.*, 2022).

Molecules were also induced by the Martian geochemistry. These interesting molecular classes revealed insights into how *R. similis* LaBioMMi 1217 metabolism might change under Martian conditions. The observation of oxylipins, which are metabolites derived

from polyunsaturated fatty acids, such as arachidonic acid, as a biomarker of the fungus–Martian geochemical interaction is quite remarkable. In complex organisms, oxylipins act as signaling molecules that regulate developmental processes and mediate responses to biotic and abiotic stressors (BRODHUN & FEUSSNER, 2011). Although the function of this class of molecules in fungi remains poorly understood, experiments with filamentous fungi of the *Aspergillus* genus have demonstrated that oxylipins are crucial mediators of the stress response to aid growth, reproduction, and sporulation (LIU *et al.*, 2023). Oxylipin production in yeasts, such as *Candida albicans*, is associated with biofilm formation, which enhances substrate adhesion (NIU *et al.*, 2020). Considering the increased production of these metabolites by the fungus *R. similis* and the predominance of yeast-like cells in the presence of medium containing synthetic Martian regolith, we assume that oxylipins are associated with the change from the filamentous to the yeast-like stage or with biofilm formation to improve contact with regolith particles.

In our experiment, we also observed an increased production of molecules containing the indole group, such as indole lactic acid, which is a key intermediate in melanin biosynthesis in organisms, including black yeasts (CARR *et al.*, 2023; LIU *et al.*, 2021). Melanin production plays crucial roles in different biological systems, including protection against environmental stressors, such as UV and ionizing radiation, oxidative agents, thermal extremes, and osmotic pressure. For example, experiments with gamma radiation led to a significant increase in melanin production by *E. dermatitidis* ATCC 34100 (YUZON *et al.*, 2023), and the yeast strain *Hortaea werneckii* EXF 225 began to produce melanin to cope with a high salt content (KEJŽAR *et al.*, 2013). Because perchlorate was present in the Martian soil mimic used in our experiments, we inferred that increased melanin biosynthesis may be a coping mechanism for osmotic stress. As observed in a study with the same strain under conditions of perchlorate brine, *R. similis* LaBioMMi 1217 showed modulated pigmentation in the presence of perchlorate brines (SANTOS *et al.*, in press).

Siderophores are secondary metabolites that capture Fe from the environment and are produced by various microorganisms, including fungi (PECORARO *et al.*, 2021). Fe is an essential micronutrient for most life forms, and the ability to acquire Fe^{3+} from environments where this form is scarce or unavailable is a crucial survival strategy. Among the siderophores, ferricrocin and ferrichrome production by several fungus species, particularly black yeasts, are the most well-known mechanisms of virulence (SAV *et al.*, 2016). The discovery that the fungus *R. similis* LaBioMMi 1217 is capable of increasing ferricrocin production, especially in an Fe-rich environment, represents an intriguing and

potentially relevant discovery for astrobiology. The ability to produce ferricrocin derivatives may enable the fungus to access Fe from the regolith that may not be readily available in a form that the fungus can use, such as iron oxide. Additionally, this discovery could have implications for the detection of life on Mars. Because this compound class has a specific chemical complexity and is only produced by living organisms, it may be a potential biosignature.

Regarding the detectability of biosignatures on Mars, the Rosalind Frankin rover, which is being sent on the ExoMars mission by the European Space Agency to search for traces of life, will carry an LDI-MS-type spectrometer. To simulate the molecules induced by Martian regolith, we analyzed the crude extract containing MGS-1-induced molecules using LDI-MS, with the regolith itself serving as the matrix. The LDI-MS spectrum showed a grouping of ions in the *m/z* 300 region, which, in previous studies on the same fungal strain using this technique, was associated with the presence of lipids, such as the *m/z* 337.8 ion, a possible Fe^{2+} adduct of oleic acid (SANTOS *et al.*, 2021). Taking into account the high concentrations of Fe in the minerals found in Martian soil (CANNON *et al.*, 2019), the *m/z* 349.1 ions warrant attention, considering the same chelation mechanism with Fe, likely corresponding to the Fe adduct of the oxylipin 9-KODE, with a theoretical molecular formula of $C_{18}H_{29}O_3$, calc. as $[M - H + {}^{56}Fe^{2+}]^+$ at *m/z* 349.1, and *m/z* 367.2, probably corresponding to the Fe adduct of some oxidized fatty acid, with a theoretical molecular formula of $C_{18}H_{31}O_4$, calc. as $[M - H + {}^{56}Fe^{2+}]^+$ at *m/z* 367.2.

In terms of astrobiology, the potential for fungi to produce oxylipins in response to regolith interaction means that they can be valuable biosignatures. Furthermore, owing to their lipidic nature, they would be preserved in the Martian environment (WILHELM *et al.*, 2017) for potential detection by LDI-MS in situ in the near future.

2.1.5 - Conclusion

Our research highlights the relevance of R. *similis* LaBioMMi 1217 and other closely related black fungi as robust models for astrobiology due to their adaptations and resilience to extreme environments analogous to those on Mars, particularly those related to Martian geochemistry. Genomic analysis revealed that *Exophiala* spp. and *Rhinocladiella* spp. harbored several stress resistance genes relevant to Martian conditions, including those associated with UV radiation resistance and/or tolerance, cold temperatures, high salinity, and enhanced nutrient uptake in oligotrophic environments. The black fungi model *R. similis*

LaBioMMi 1217 exhibited notable morphological plasticity and the ability to produce molecules, such as oxylipins, melanin precursors, and melanin itself, in response to simulated Martian geochemistry. The increased production of oxidized fatty acids, indole derivatives, and siderophores indicates a potential survival strategy under conditions of Martian geochemistry, including the metabolization of Fe from regolith minerals.

The detection of these molecules, particularly those of a lipid nature, such as oxidized fatty acids, indicates their potential as biosignatures of life on Mars. Furthermore, these molecules were detected in simulations using LDI-MS, reinforcing their viability as indicators of life.

2.2 - SURVIVING MARS: *RHINOCLADIELLA SIMILIS* AND LIFE IN PERCHLORATE-RICH ENVIRONMENTS

2.2.1 - Introduction

The quest to understand habitability on extraterrestrial planets, particularly Mars, is an intriguing journey that expands the frontiers of our knowledge. The discovery of perchlorates in Martian soil, confirmed by several NASA missions, such as the Phoenix lander, Mars Reconnaissance Orbiter, and the rover Curiosity, highlights the significance of exploring the interaction between terrestrial microorganisms and these extreme salt conditions (BILLI *et al.*, 2021; CASSARO *et al.*, 2022; HECHT *et al.*, 2009). Perchlorates, particularly magnesium perchlorate ($Mg(ClO_4)_2$), have been identified as predominant compounds in Martian soil, with concentrations ranging between 0.4 and 0.6 wt% (KOUNAVES *et al.*, 2014). The propensity of these salts to form brines by absorbing atmospheric water vapor, and subsequent deliquescence proposes a hypothetical medium for the existence of liquid water at sub-zero temperatures, creating potential niches for microbial life (HEINZ *et al.*, 2020; MARTÍNEZ & RENNO, 2013; OROSEI *et al.*, 2018).

Discovering terrestrial microorganisms that can tolerate perchlorates has been a challenge. Perchlorate is a potent oxidant, and the search for perchlorate resistance and tolerance metabolisms in microorganisms is an emerging field. Research has shown that some archaea (i.e., *Haloferax mediterranei* and *Halorubrum lacusprofundi*), bacteria (i.e., *Halomonas venusta* and *Planococcus halocryophilus)*, and fungi (i.e., *Purpureocillium lilacinumcan, Debaryomyces hansenii*, and *Cryomyces antarcticus*) resist extremely high concentrations of perchlorates (BEBLO-VRANESEVIC *et al.*, 2017; BILLI *et al.*, 2021; HEINZ *et al.*, 2019; KISH *et al.*, 2009). These can provide insights for future research to develop more effective and useful biological systems on Mars to understand better how life could have been established on the Red Planet and for *in situ* resource utilization. The tolerance of eukaryotic organisms, such as yeasts and other fungi, to magnesium perchlorate remains largely unexplored, especially at high concentrations (more than 0.15 M). Since sodium ions have an osmotic effect at high concentrations and are not chaotropic similar to magnesium, sodium perchlorate is only useful for certain studies, such as understanding the

[2] This section is an adapted version of the paper:

dos Santos A., Schultz J., Souza O. F., Rodrigues R. F., Braga V. T., Pilau J. E., Rosado S. A., Rodrigues-Filho E., (2024) “Survival Strategies of Rhinocladiella similis in Perchlorate Rich Mars Like Environments”. (npj Microgravity, under review)

effect of the perchlorate anion (HEINZ *et al.*, 2019); therefore, they may not fully reflect the challenges posed by Martian soil, which predominantly contains magnesium perchlorate. Hence, investigating the effects of magnesium perchlorate is crucial, as it provides a more accurate simulation of Martian soil conditions. Another poorly explored factor is the survival of microorganisms under combined exposure to ultraviolet (UV)-C radiation and perchlorate salts. This combination is commonly found on the Martian surface, given Mars' extremely rarefied atmosphere, which allows UV-C to reach the surface and perchlorate brines. This coexistence of environmental stressors has shown significant bioactivity for bacteria (WADSWORTH & COCKELL, 2017); however, further investigation is needed for extremophilic eukaryotic microorganisms.

The black yeast *R. similis*, belonging to a class of fungi known for their robustness in extreme terrestrial environments, has emerged as an intriguing model to investigate microbial resistance and adaptability in simulated Martian conditions, given that this class of microorganisms has previously been used as an astrobiological model (TESEI, 2022). Faced with the aforementioned challenges, it is essential to report unique microbial-origin chemical entities (i.e., molecules and biominerals) produced in the presence of perchlorate. Such molecules may serve as indicators of biological activity, assisting in distinguishing between abiotic and biotic processes. Determining how extremophilic microorganisms could survive under these conditions at the molecular level is crucial for understanding potential life forms on Mars. Additionally, understanding the chemical signatures and molecules produced by microbial life in perchlorate-rich environments can significantly contribute to ongoing efforts in astrobiology, assisting in the formulation of life detection strategies for future missions to Mars (LOPEZ *et al.*, 2019; SANTOS *et al.*, 2021; HEINZ *et al.*, 2022).

This study examines the tolerance of *Rhinocladiella similis* to magnesium perchlorate and its survival under UV-C radiation, a harsh condition on Mars. By analyzing the metabolic and proteomic responses of *R. similis* to high concentrations of magnesium perchlorate, we seek to uncover this organism's molecular profile and survival mechanisms in extreme environments. Understanding these molecular aspects will enhance our knowledge of potential life forms in Martian saline settings and inform the design of future Mars rovers for biosignature detection, indicating which molecules they might find on the Martian surface.

2.2.2 - Material and Methods

2.2.2.1 - Microbial Material

The fungi strains used in this study include two species of black yeasts isolated from distinct environments. *Rhinocladiella similis* strain LaBioMMi 1217 was identified as a contaminant in a hydrochloric acid solution with a pH of 1.5 (SANTOS & RODRIGUES-FILHO, 2019). The *Exophiala* sp. strain 15Lv1 was isolated from the desertic soil of the Atacama Desert by PULSCHEN *et al.* (2015) to use as a comparative control in the conducted experiments due to its promising application for astrobiology research. Both strains were characterized and taxonomically identified using molecular biology approaches (PULSCHEN *et al.*, 2015; SANTOS & RODRIGUES-FILHO, 2019; SANTOS *et al.*, in press).

2.2.2.2 - Resistance to UV-C Radiation in a Perchlorate Magnesium Condition

Following a 78-hour incubation at 25 °C in potato dextrose broth (PDB), the fungi cells of both cultured strains were rinsed twice with 1 mL of a 0.9% w/w NaCl and $Mg(ClO_4)_2$ solution, facilitated by centrifugation. The resultant pellet was resuspended in 5 mL of sterile NaCl and $Mg(ClO_4)_2$ solutions, and the concentration was adjusted to 10^6–10^7 cells L-1 using a spectrophotometer.

This cell suspension was then transferred to a sterile 10 cm diameter glass Petri dish and subjected to UV-C irradiation (Model G30T8 from LightTech Lamp Technology, Hungary) within a biosafety cabinet, emitting at a wavelength of 254 nm. The irradiation process was meticulously monitored throughout the experiment via a radiometer (model VLX-3W) equipped with a UV photocell (model CX254). The precise distance between the UV-C lamp and the sample was adjusted to ensure accurate UV-C flux. The Petri dish, housing the cell suspension in saline solution, was exposed to escalating doses of UV-C radiation, starting with zero (serving as control), followed by doses of 100, 200, 300, and 400 J m^2 s^{-1}. From the control, a 100 µL aliquot of the cell solution was carefully removed from the Petri dish, and a serial ten-fold dilution (10^{-2} to 10^{-6}) was performed. Subsequently, 10 µL from each dilution was inoculated onto square Petri dishes laden with potato dextrose agar. The aforementioned process was replicated for other radiation doses, with the Petri dish containing the cell suspension positioned within the UV-C radiation field.

Following irradiation, the plates were incubated for 72 hours, and the colony-forming units (CFUs) were assessed by counting the colonies in the dilution range of 30 to 300 CFUs. The acquired data were plotted to generate survival curves (N/N_0), illustrating the

resilience and survivability of the cells under varying levels of UV-C radiation in conjunction with magnesium perchlorate exposure.

The *Exophiala* sp. 15Lv1 strain was chosen as a comparative model based on the understanding of the responses induced against UV radiation in previous studies, where it demonstrated strong resistance to UV-C radiation, establishing this yeast as an astrobiological model for understanding how eukaryotic microorganisms survive in Martian surface conditions (PULSCHEN *et al.*, 2015). Given these observations, we expanded our studies to the *Rhinocladiella similis* strain LaBioMMi 1217, another black yeast from the same Herpotrichiellaceae family.

2.2.2.3 - Screening of Survival under Different Magnesium Perchlorate Concentrations

Both strains of black yeast were cultured in triplicate in PDB, under agitation at 150 rpm, at 26 °C for 72 hours. An aliquot from each triplicate was removed and diluted with PDB medium to achieve an OD_{600} of 0.125 for the cell suspension, corresponding to a final OD_{600} of approximately 0.05 in each well of the 96-well plate. The experiment was conducted using a SpectraMax Paradigm Multi-Mode Microplate Reader (Molecular Devices), with the absorbance measured at 600 nm. In each well, 80 µL of the fungal suspension (OD_{600} of 0.125) and 120 µL of growth medium with varying concentrations of magnesium perchlorate were added, resulting in a final volume of 200 µL in each well. The magnesium perchlorate concentrations evaluated included 31.25 mmol L^{-1}, 62.5 mmol L^{-1}, 125 mmol L^{-1}, 250 mmol L^{-1}, 500 mmol L^{-1}, 750 mmol L^{-1}, and 1000 mmol L^{-1}. Absorbance spectra were obtained every 6 hours over 4 days.

2.2.2.4 - Cultivation of Rhinocladiella similis Strain LaBioMMi 1217 on a Magnesium Perchlorate Substrate for Microscopy, Proteomics, and Metabolomics

The *R. similis* strain was cultivated in 50 mL Erlenmeyer flasks containing 20 mL of PDB (Sigma Aldrich) with 0.5 mol L^{-1} of magnesium perchlorate. The fungus was also grown in a pure PDB medium for use as the biological control. Both treatments had their respective negative controls (culture medium without microbial cells) and were conducted in five replicates. The microorganism was grown in an orbital shaker at 25 °C and 150 rpm for 20 days. After the cultivation period, the content was transferred to Falcon tubes, and

centrifugation was performed to separate the broth from the fungal biomass. Biomasses were washed using saline solution, and the broth was frozen at -80 °C before being lyophilized.

2.2.2.4.1 - Scanning Electron Microscopy (SEM) Analysis

For SEM samples, 10 μL of each treatment (fungus in the presence and absence of magnesium perchlorate) were transferred to a silicon glass support, followed by fixation in a 3% glutaraldehyde solution for 3 hours. The fixed samples were dehydrated in a series of isopropanol gradients (35%, 50%, 75%, 90%, and 100%), subjected to critical point drying for 5 hours, and finally coated with metallic iridium particles. Images were captured using a Zeiss Merlin Gemini field emission SEM instrument.

2.2.2.4.2 - Sample Preparation for Proteomics

Proteins from the strain LaBioMMi 1217 were extracted to analyze the proteome. After washing and lyophilizing, fungal cell lysis was performed using the mechanical lysis method through maceration with liquid nitrogen. The triturated material was resuspended in phosphate-buffered saline (PBS) and centrifuged at 5000 ×g to remove cellular residues. In the protein extract, precipitation was carried out with cold acetonitrile (ACN), followed by pelleting of the proteins through centrifugation at 16,000 ×g for 15 minutes. This process was repeated three times to ensure the protein material was adequately cleaned. The proteins in the pellet were resuspended in a digestion buffer (50 mmol L^{-1} ammonium bicarbonate), and protein concentrations were determined using the Bradford protein assay. Using 200 μg of the sample, the stages of denaturation and reduction/alkylation (8 M urea, 50 mM DTT, 250 mM iodoacetamide) were performed, incubating the samples at 95 °C for 5 minutes. Then, modified trypsin (Promega) was added in an enzyme-to-protein ratio of 1:50, and the samples were incubated at 37 °C for 16 hours. The solution containing the digested proteins was centrifuged at 5000 × g for 2 minutes. The peptides were desalted using OASIS® HLB (Waters) desalting columns, according to the manufacturer's protocol. The desalted samples were dried in a vacuum concentrator. Dried peptides were dissolved in 0.1% (v/v) formic acid and quantified by measuring absorbance at 280 nm using a NanoDrop-type spectrophotometer.

2.2.2.4.3 - Mass Spectrometry (LC–MS/MS) Proteomics Analysis

The resuspended samples containing 330 ng of digested peptides were analyzed using the Ultimate 3000 nano-RSLC system coupled to an Orbitrap Fusion Lumos mass spectrometer (both from Thermo Scientific). A 100 µm × 2 cm C18 trapping column was used for the preconcentration of peptides for 10 min using 0.1% TFA (v/v) with a flow rate of 20 µL/min followed by separation on a 75 µm × 50 cm C18 analytical column (both PepMap RSLC, Thermo Scientific) with a 90 min LC gradient ranging from 3% to 35% of buffer B: 84% ACN, 0.1% formic acid at a flow rate of 250 uL/min. The Orbitrap Fusion Lumos MS was operated in the data-dependent acquisition (DDA) mode, and MS survey scans were acquired from *m/z* 300 to 1500 at a resolution of 120,000 using the polysiloxane ion at *m/z* 445.12002 as lock mass. The quadrupole isolated the precursor ions with a window of 0.4 *m/z*. The acquisition was performed in the top speed mode, selecting the most intense signals within a cycle time of 3 s between survey scans and subjecting them to higher energy collisional dissociation (HCD) with a normalized collision energy of 32%. Fragment ions were analyzed in the orbitrap using a resolution of 15.000 (MS/MS). Selected parent ions were included in a dynamic exclusion for 15 s. Automatic gain control (AGC) target values were set to 2 × 105 for MS and 5 × 104 for MS/MS, for which the maximum injection times were 120 and 250 ms, respectively. Precursor ions with charge states of +1, > +7, and unassigned were excluded from the MS/MS analysis, and monoisotopic peak determination was set to ‘peptide’.

2.2.2.4.4 - Proteomics Data Analysis

The raw spectra (.raw) were deconvoluted using the MaxQuant software (version 1.6.17.0). Spectra were matched against the FASTA file with all CDS of *Rhinocladiella similis* derived from genome sequencing (13,921 entries). The search parameters included a tolerance of 20 ppm for the first search and the main search with a tolerance of 4.5 ppm. Trypsin was chosen as the enzyme, allowing a maximum of two missed cleavage sites. The carbamidomethyl (Cys) modification was selected as a fixed modification, and oxidation (Met) and acetylation (protein N-terminal) were set as variable modifications. For peptide identification, a minimum of 1 unique peptide was used. A reverse decoy database determined that the false discovery rate (FDR) was < 1%.

The data statistical analysis was performed in the R environment using the packages “tidyverse”, “dplyr”, “missForest”, and “genefilter”. Briefly, the potential

contaminants and reverse IDs were filtered, the intensity values were transformed to Log_2, and the proteins containing more than 50% of the missing values were removed. The random forest (RF) method was used for data imputation (JIN *et al.*, 2021). Following, the values were normalized by the column median (protein intensities for each experimental data) and submitted to the student t-test. Upregulated proteins were defined using a p-value < 0.05 and log_2-transformed fold change (FC) > 1. Downregulated proteins were defined using a p-value < 0.05 and log_2-transformed FC < 1. The enrichment of biological processes with up- and downregulated proteins was performed using the ShinyGO 0.80 platform (http://bioinformatics.sdstate.edu/go/). The PCA, volcano plot, and enrichment graphs were generated using the online platform (https://www.bioinformatics.com.cn/en).

2.2.2.4.5 - Extraction of Extracellular Microbial Metabolites

After 20 days of cultivation, 20 mL of fermentation broth was collected and centrifuged in 50 mL Falcon tubes. The same amount of magnesium perchlorate was added to all control samples to standardize the procedure. Subsequently, the samples were frozen at -80 °C for 24 hours. After complete freezing, samples were lyophilized until the total sublimation of the fermentation broths. The resulting dry extracts were rehydrated with 5 mL of ultra-pure water. These aqueous extracts were then subjected to a clean-up process using Shop Sep-Pak® C18 Cartridges, 500 mg (Waters Corporation), to remove excess magnesium perchlorate. The elution of metabolites was conducted with ACN, and the eluted fractions were concentrated and transferred to vial bottles for subsequent analysis by LC–MS.

2.2.2.4.6 - UHPLC-MS/MS Analysis and Processing of Metabolomic Data from Metabolic Extracts

The fungi extracts were characterized by UHPLC (Shimadzu, Nexera X2, Japan) equipped with a Bruker BRHSC18022050 column. All solvents were HPLC grade (> 99%, J.T. Baker, Phillipsburg, USA, or Sigma-Aldrich, St. Louis, USA). The separation gradient comprised solutions A (0.1% v:v formic acid) and B (ACN with 0.1% v:v formic acid). The gradient was set using 5% B (0–1 min), 70% B (1–10 min), 98% B (12–20 min), and 5% B (20–25 min). Temperature and flow rate were set at 40 °C and 0.250 mL min^{-1}, respectively.

The eluted compounds were analyzed by a quadrupole/time of flight (QQTOF) high-resolution mass spectrometer (MS, Impact II, Bruker Daltonics Corporation, Germany) equipped with an electrospray ionization source (ESI) in positive mode. MS parameters were as follows: capillary voltage of 4500 V (potential plate end of −500 V), gas flow of 8 L min^{-1} at 180 °C, nebulization gas pressure of 4 bar. Data acquisition was monitored at mass/charge (*m/z*) ranges between 50 and 1300 at 5 Hz. The five most intense ions were selected for automatic tandem mass spectrometry (Auto MS/MS). Data acquisition and the feature table process were performed using Hystar Application software version 3.2 and MetaboScape®. The multivariate and univariate statistical analyses, including principal component analysis (PCA), were carried out using the MetaboAnalyst 4.0 platform by removing features with at least 50% missing values and estimating the remaining missing values using the KNN algorithm. Additionally, feature filtering with RSD (relative standard deviation) > 30% in the QC samples, normalization by the median, and data scaling by the auto-scaling method were performed. To screen out significant differential metabolites, it was considered variable importance in the projection Log_2 (FC) ≥ 2.0 and *p*-value < 0.05 using the t-test.

A molecular network of the metabolites of interest was created using the online workflow (https://ccms-ucsd.github.io/GNPSDocumentation/) on the Global Natural Products Social Molecular Networking (GNPS) website (http://gnps.ucsd.edu). The data were filtered by removing all MS/MS fragment ions within +/- 17 Da of the precursor *m/z*. MS/MS spectra were window-filtered by choosing only the top 6 fragment ions in the +/- 50 Da window throughout the spectrum. The precursor ion mass tolerance was set to 0.02 Da, and an MS/MS fragment ion tolerance of 0.02 Da. Then, a network was created where edges were filtered to have a cosine score above 0.60 and more than 4 matched peaks. Further, edges between two nodes were kept in the network if, and only if, each node appeared in each other's respective top 10 most similar nodes. Finally, the maximum size of a molecular family was set to 20, and the lowest-scoring edges were removed from molecular families until the molecular family size was below this threshold. The spectra in the network were then searched against GNPS' spectral libraries. The library spectra were filtered in the same manner as the input data. All matches kept between network spectra and library spectra were required to have a score above 0.55 and at least 4 matched peaks (WANG *et al.*, 2016). The annotation process conforms to Level 2 identification standards outlined by the Metabolomics Standards Initiative (MSI) (SUMNER *et al.*, 2007).

2.2.2.4.7 - Data Availability

The WGS, genome annotation and raw data of the analyzed fungal strain (*Rhinocladiella similis* LaBioMMi 1217) have been deposited in GenBank under BioProject PRJNA1005689 and accession number JBBMOB000000000. For metabolomic data acquired using the ESI+ MS technique, interested parties can access them through the GNPS using the identifier ID=31f75023299848cbb0c7539b1fed5b58. Proteomics mass spectra and associated data have been uploaded into PRIDE (ProteomeXchange Consortium) under the dataset identifier PXD050600.

2.2.3 - Results

2.2.3.1 - Resistance to UV-C Radiation in Magnesium Perchlorate Conditions

Aiming to understand the resistance of black yeasts to environmental stresses (UV-C and magnesium perchlorate), we conducted a study comparing the survival of *Rhinocladiella similis* strain LaBioMMi 1217 and *Exophiala* sp. 15Lv1 to UV-C (256 nm) only, and UV-C combined with magnesium perchlorate (0.9 wt% $Mg(ClO_4)_2$). Thus, the results from this study would enhance our understanding of how the survival of these black yeast would occur in perchlorate brines, simulating those found on Mars.

We observed that the isolated *Rhinocladiella similis* strain LaBioMMi 1217 showed significant resistance to high doses of UV radiation in a perchlorate matrix compared to the standard strain of *Exophiala* sp. 15Lv1 (Figure 2.10). In the absence of magnesium perchlorate, the eukaryotic model *Exophiala* sp. 15Lv1 displays a higher survival rate at all tested doses of UV-C radiation. However, this dynamic changes in the presence of magnesium perchlorate, where the *R. similis* strain shows a higher survival rate to the oxidative stress induced by the combination of UV-C and magnesium perchlorate; the cell viability was reduced only once. These results suggest that combining UV radiation with perchlorate salts can be particularly harmful, even for microorganisms well-known to resist UV-C irradiation; however, *R. similis* can cope well with such a harsh environment.

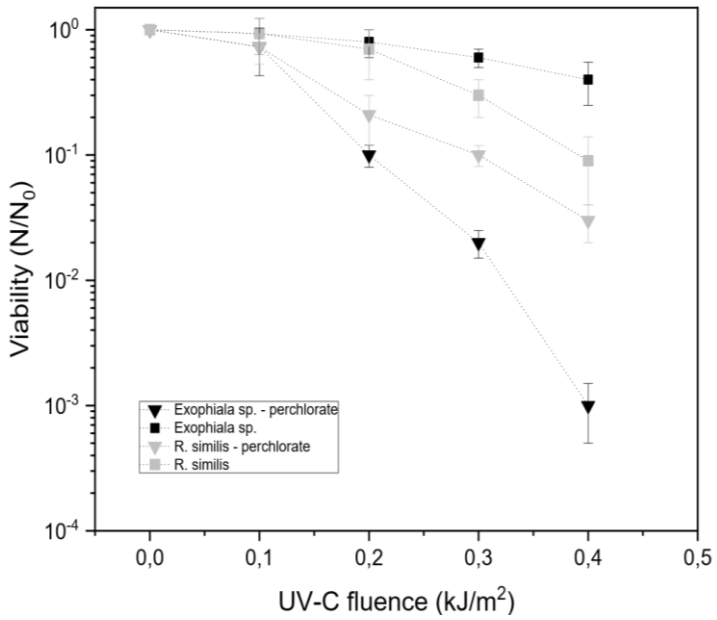

FIGURE 2.10 – Effects of UV-C-irradiated $Mg(ClO_4)_2$ on two different species of black fungus.

■ = control experiment (only UV-C), black yeast UV-C with 0.9 wt% NaCl. ▼= black yeast with perchlorate 0.9 wt% $Mg(ClO_4)_2$.

2.2.3.2 - Survival under Different Magnesium Perchlorate Concentrations

Considering the significance of perchlorate brines on Mars as promising locations for the existence of liquid water and potential extraterrestrial life, this study focused on monitoring the growth of two species of black yeasts from the *Herpotrichiellaceae* family. These species have demonstrated notable adaptability to Martian-like conditions. Experiments were conducted across a gradient of magnesium perchlorate concentrations, ranging from 31.25 mmol L^{-1} to 1 mol L^{-1}. The choice of this specific salt was strategic, considering the lack of data on the effects of magnesium perchlorate salts on microorganisms, coupled with its higher toxicity compared to sodium perchlorate and its prevalence on the Martian surface.

Overall, a common trend in fungal growth was detected: A decrease when the perchlorate concentration increased. The growth curve analyses (Figure 2.11) revealed that both tested strains of black yeast sustained great growth at magnesium perchlorate concentrations of 250 mmol L^{-1}, indicating substantial tolerance to this electrolyte. However, increasing the concentration to 500 mmol L^{-1} resulted in a significant delay in the growth of *Exophiala* sp. (Figure 2.11A) compared to *R. similis* (Figure 2.11B). This contrast becomes even more pronounced at a concentration of 750 mmol L^{-1}, where *Exophiala* sp. failed to exhibit an effective growth profile, while *R. similis*, despite the growth rate reducing and the

decrease in cell density, still managed to increase. These findings indicate the differential resilience of these species to high concentrations of perchlorate, a critical aspect for understanding the viability of life on Mars brines.

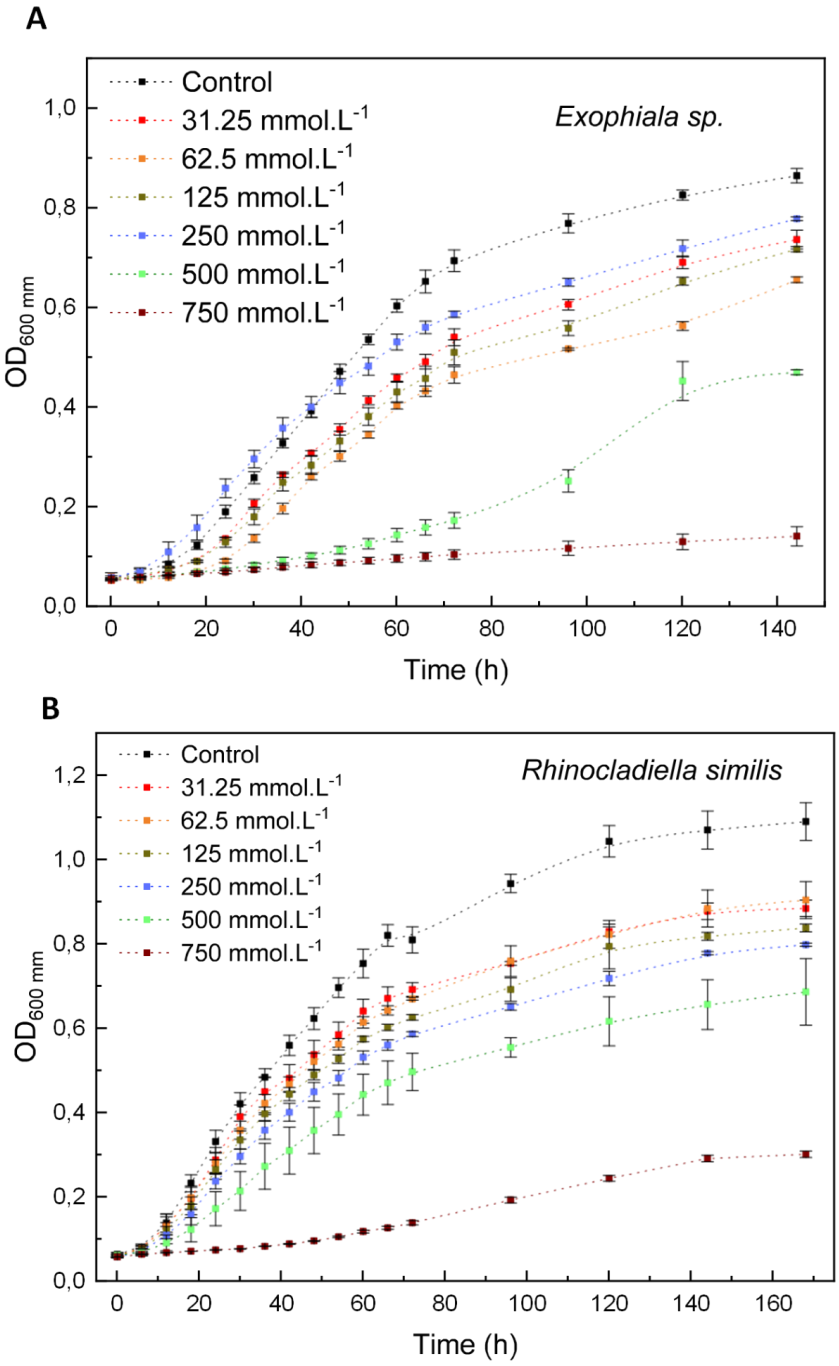

FIGURE 2.11 – Growth curves of *Exophiala* sp. (A) and *Rhinocladiela similis* (B) under different $Mg(ClO_4)_2$ concentrations and control (medium perchlorate-free).

Cultures were grown in PDB in a 96-well plate at 25 °C with the indicated $Mg(ClO_4)_2$ concentrations. The initial inoculum, with freshly harvested overnight PDB cells, was adjusted to 0.125 OD_{600}. No growth was observed in 1 M perchlorate concentration.

2.2.3.3 - Morphology Analysis of Rhinocladiella similis Strain LaBioMMi 1217 in Perchlorate Brines

Given the notable resistance of *R. similis* to magnesium perchlorate, additional experiments were conducted to investigate its morphological changes. It was observed that *R. similis* exhibited predominantly filamentous growth under perchlorate-free conditions (Figure 2.12A), suggesting that the absence of magnesium perchlorate favors the phenotypical change in the yeast cell morphology. In addition, it was noted that the fermentation broth acquired a greenish-brown coloration after cultivation. In contrast, in the presence of magnesium perchlorate (Figure 2.12B), yeast-like cells predominated, indicating that the dimorphism of *R. similis* can be influenced by the magnesium perchlorate. Furthermore, the fermentation broth appeared darker under this condition, suggesting an increase in melanin production by the fungus in response to the osmotic stress caused by the perchlorate.

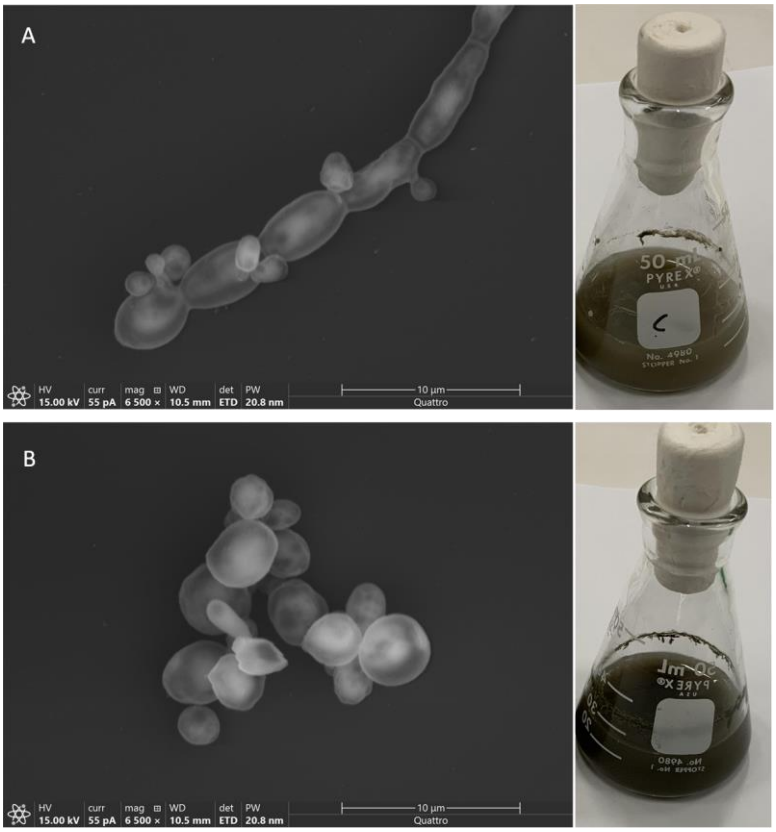

FIGURE 2.12 – Microscopic (SEM) and macroscopic responses to magnesium perchlorate conditions.

(A) Left: magnification of cells in PDB culture medium, showing pseudohypha behavior. Right: cells dispersed in PDB culture medium with a gray coloration; (B) left: magnification of the fungus cells in PDB culture medium at a $Mg(ClO_4)_2$ concentration, highlighting the yeast form. Right: cells are dispersed in a PDB culture medium with a darker color due to the intensified melanin production through the formation of darker cells.

2.2.3.4 - Proteomic Analysis of the Fungus R. similis at a High Concentration of Magnesium Perchlorate

To discern the response to magnesium perchlorate-induced stress in the *R. similis* strain at the protein level, the proteome of cell cultures containing $Mg(ClO_4)_2$ and no additional salt in the growth medium were analyzed. The microorganism was cultivated under the same concentrations used for morphological analyses (500 mmol L^{-1} of $Mg(ClO_4)_2$). To ensure greater reliability in the data, all samples were prepared as biological quintuplicates (n = 5), and the cells were harvested in the late phase to obtain a profile closely representing what would be found on Martian brines.

In total, 1321 proteins were quantified in the proteomic assays, whereby it was observed that 169 upregulated proteins and 227 were downregulated, considering the *p*-value ≤0.05 + $\log_2$(FC)±1 (Table S1.5). The PCA graph (Figure 2.13A) shows two principal components, accounting for 53% of the total data variance (37% for PC1 and 16% for PC2), revealing a separation trend between the two groups: The fungus in the presence of magnesium perchlorate (Perchlorate) and the fungus grown in the absence of magnesium perchlorate (Control). This indicates that magnesium perchlorate played a significant role in changing the *R. similis* proteome. Differentially regulated proteins can be observed in the volcano plot analysis (Figure 2.13B). These analyses demonstrate that magnesium perchlorate significantly impacts the proteome of *R. similis*.

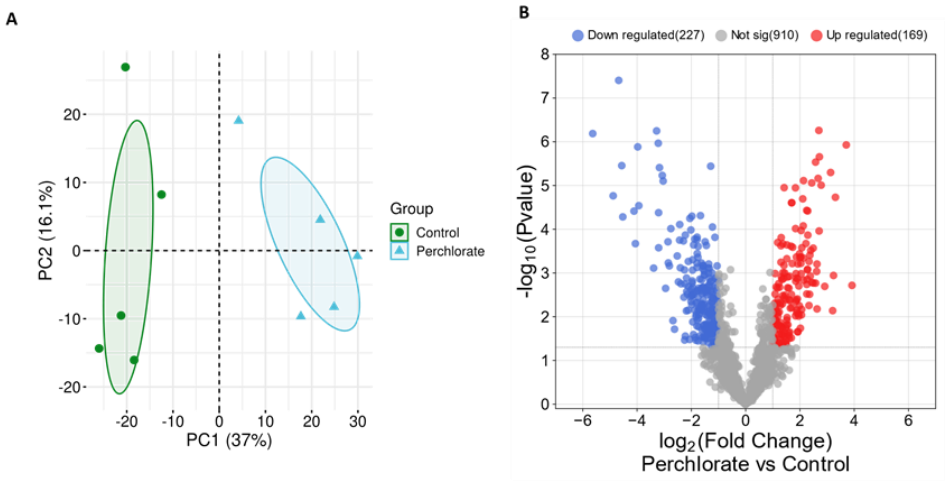

FIGURE 2.13 – (A) Principal component analysis (PCA) depicting data variance and clustering among the proteomics samples: Perchlorate (500 mmol L^{-1} $Mg(ClO_4)_2$) and Control (culture medium only). (B) Volcano plot showing the differentiation between up- and downregulated proteins (perchlorate *vs.* control log-ratio). Only features with $\log_2$(FC) ± 1 and *p*-value < 0.05 were considered significantly regulated. Blue dots represent the downregulated proteins, and the red dots are upregulated in the perchlorate-treated group.

Gene Ontology (GO) analysis was used to investigate the biological processes altered in the fungus due to the high perchlorate concentrations. The downregulated proteins were highly related to the “carboxylic acid metabolic process”, “nucleobase-containing small molecule metabolic process”, “nucleotide metabolic process”, “cellular respiration”, “aerobic respiration”, “tricarboxylic acid cycle”, and “ATP metabolic process” (Figure 2.14A). Interestingly, the fungus seems to switch its metabolism to a lower survival rate in stressful conditions with high perchlorate content. The enriched biological processes associated with the upregulated proteins were “cellular response to chemical stimulus”, “organic substance catabolic process”, “regulation of protein phosphorylation activity”, “small molecule metabolic process”, “organic hydroxy compound metabolic process”, “lactate metabolic process”, “response to toxic substance”, “dephosphorylation”, “cellular response to toxic substance”, and “cellular detoxification” (Figure 2.14B). The increase in proteins responsible for responding to chemical stress and cellular detoxification suggests a cellular adaptation to neutralize the adverse condition generated by perchlorate. In addition, the increase in those proteins could explain the survival of *R. similis* even in such stressful conditions. Altogether, the results reveal the molecular effects in *R. similis* following exposure to high perchlorate concentrations.

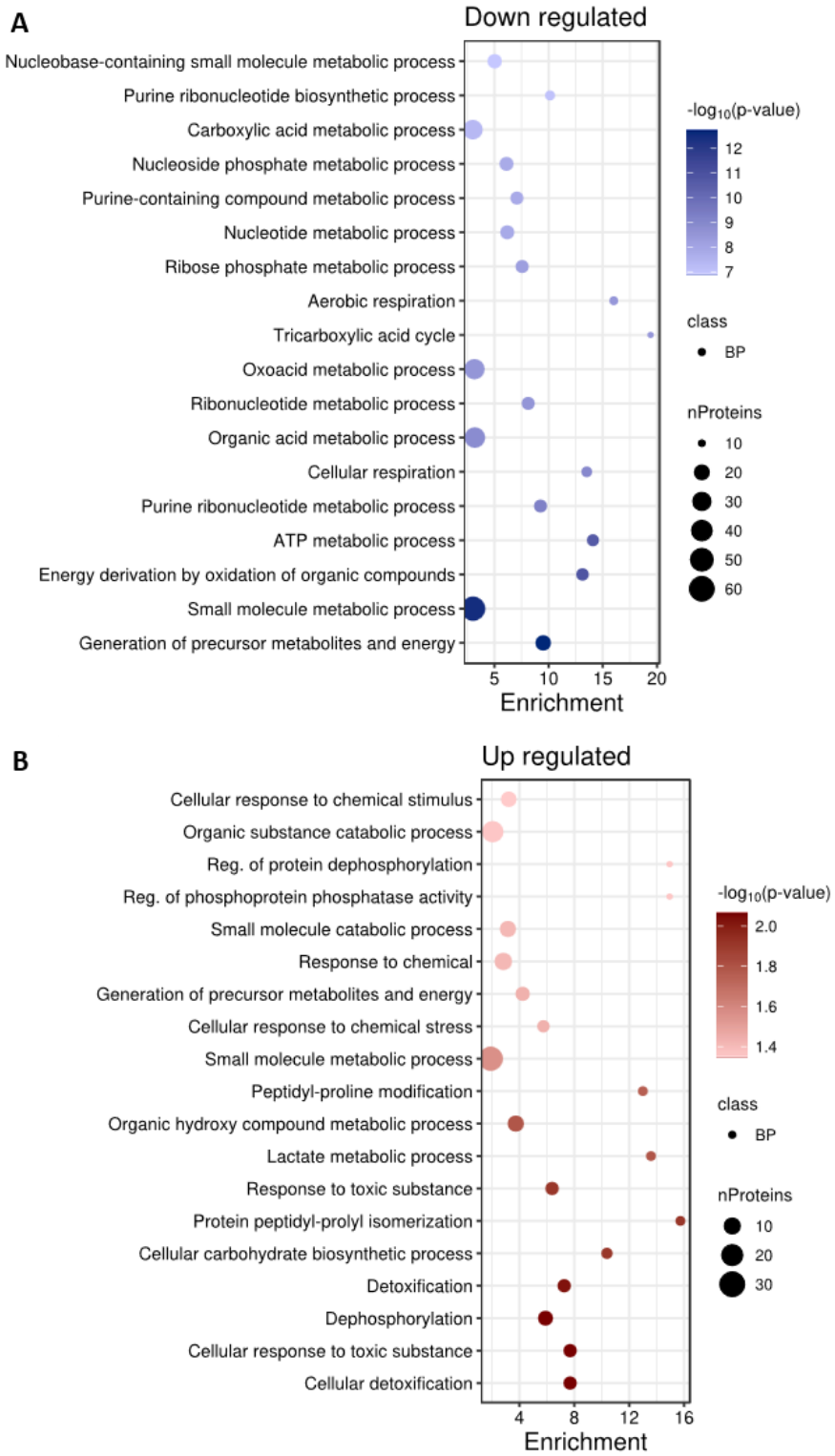

FIGURE 2.14 – Assessing the Gene Ontology biological processes associated with up- and downregulated proteins.

(A) Enriched biological processes related to downregulated proteins. Data indicate the processes that are potentially reduced in the presence of perchlorate. Each node represents a different biological process; darker blue means more significant statistics (lower *p*-value). (B) Enriched biological processes associated with upregulated proteins. Each node represents a different biological process; darker red means more significant statistics (lower *p*-value). Data indicate the processes that are potentially increased in the presence of magnesium perchlorate salt.

A broader analysis assessing the enriched biological processes, in the case of the upregulated proteins, suggests that most expressed proteins are associated with combating stress induced by chemical species. Among the most expressed biological processes, seven are related to defense or chemical detoxification, indicating that this perchlorate-rich environment is not the most suitable for *R. similis* cells to inhabit, even though they proliferate and manage to survive, demonstrating their tolerant rather than extremophilic nature. One negatively regulated biological process stands out among the analyses. Proteins associated with aerobic respiration exhibited decreased expressions. This indicates that cells prefer to undergo fermentation rather than cellular respiration under high perchlorate concentration conditions. This finding is consistent with the morphology of the fungus under these conditions, which appears predominantly as yeast, considering that it has dimorphic characteristics and can choose between the filamentous and yeast forms depending on the condition in which it is inserted. Additionally, several processes related to cell division and multiplication were downregulated, indicating a stagnation in population growth.

2.2.3.5 - Molecular Biosignature Production in High Concentrations of Magnesium Perchlorate

To investigate the effect of magnesium perchlorate on the production of extracellular biomolecules (i.e., metabolites) of the black yeast *R. similis*, crude extracts of the fungus in the presence of the salt were evaluated by UHPLC-MS/MS. A principal component analysis was conducted to provide an overview of the data (Figure S.14).

The first two principal components, accounting for 60.6% of the overall data variance (36.4% for PC1 and 24.2% for PC2), showed a separation trend between the two groups: The fungus in the presence of perchlorate salt (Perchlorate group) and the fungus grown solely in the PD culture medium (Control group), both highlighted in the PCA plot (Figure S.14). The separation between the groups was much clearer through the unsupervised method, making a supervised analysis unnecessary. The reproducibility of the instrumental system, both chromatographic and mass spectrometry parts, was assessed by jointly analyzing the QC samples. The tight clustering of the QCs in the center of the PCA score plot demonstrated the instrument's stable performance. The statistical treatment result table from MetaboAnalyst 4.0 can be found in Table S1.5.

To discover the chemical identity of features that exhibited an increase in production, features were selected with $\log_2(FC) > -2$ and *p*-values < 0.05 for a precise mass

analysis (with error margins ranging from 0 to 2 ppm) and tandem mass spectrometry (MS/MS) fragmentation profiles, summing 324 features of interest, which were submitted to the GNPS and Sirius platforms for their annotation.

The molecular network generated by the GNPS platform is depicted in Figure S.15. Using this approach, it was possible to annotate four compounds (Figure 2.15), along with the plots illustrating the increase in production. In the molecular network analysis, various molecular clusters are observed, totaling 12 clusters, each with more than three nodes. This suggests that magnesium perchlorate may play a role in activating previously silenced genes belonging to different molecular families. Among these clusters, one had a chemical entity identified, while another exhibited four nodes ranked among the top 10 most upregulated.

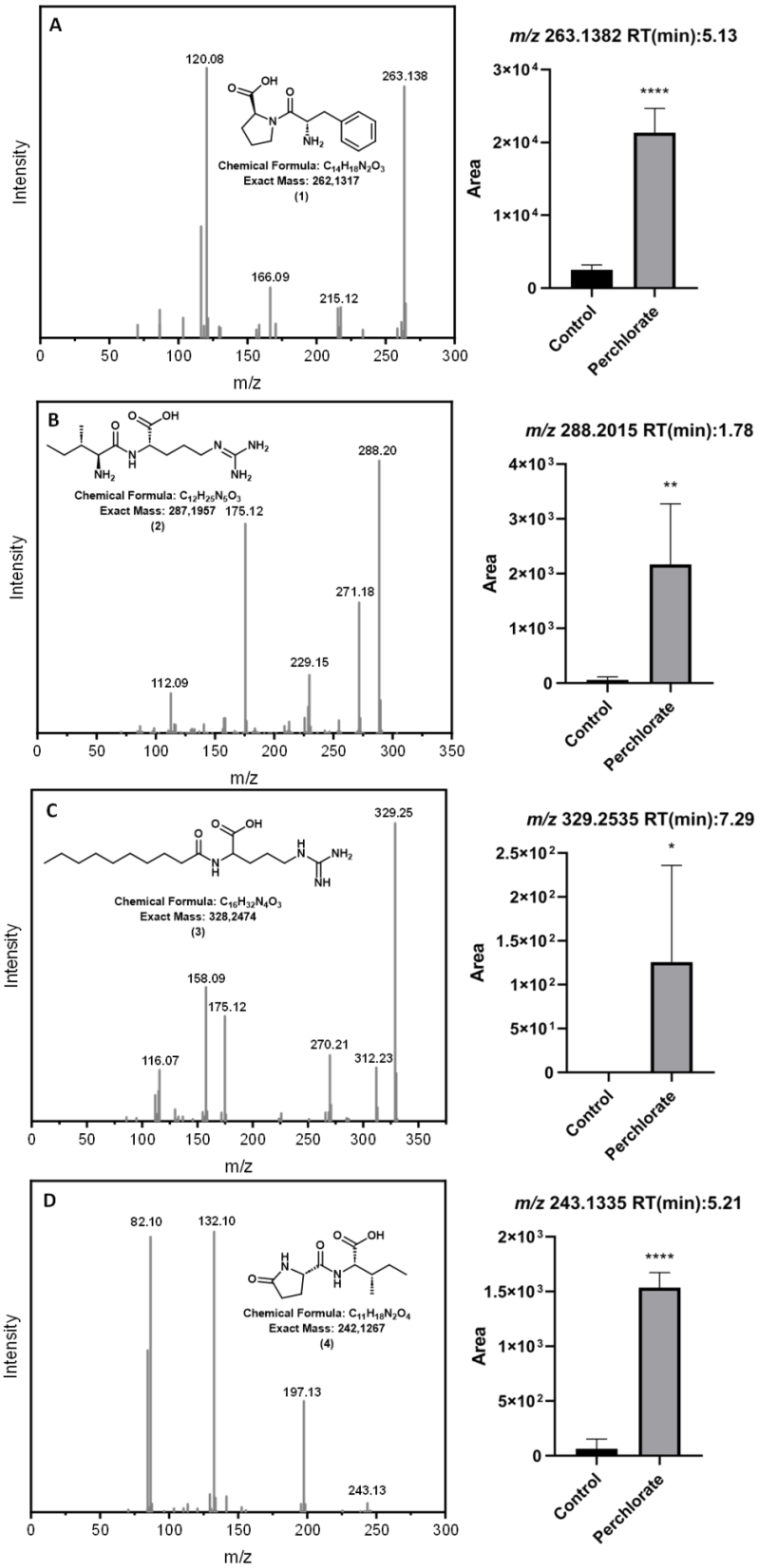

FIGURE 2.15 – Selected differential metabolites between the control experiment and the magnesium perchlorate experiment were annotated using the library of the GNPS platform.

The '*' symbol indicates the summary of the statistical significance level (*p*-value).

The molecules annotated based on their fragmentation profiles belong to the class of peptides. Among these are decanoylarginine (1), with $[M+H]^+$ at *m/z* 236.1852; *L*-phenylalanyl-*L*-proline (2), with $[M+H]^+$ at *m/z* 288.2015; *N,N*-dimethylarginine (3), with $[M+H]^+$ at *m/z* 329.2535; 5-oxopyrrolidine-2-carbonyl-*L*-isoleucine (4), with $[M + H]^+$ at *m/z* 243.1335. The error variation in parts per million (ppm) for the annotated molecules was less than 2. All the ions highlighted in the molecular network are listed in Table 2.2, along with their *m/z*, RT, log2(FC), and *p*-values.

TABLE 2.2 – Relationship of the Highlighted Ions in the Molecular Network with $\log_2$ (FC) Information and *p*-value.

Entry	**Name**	**Precursor ion (*m/z*)**	**RT (min)**	**$\log_2$ (FC)**	***p*-value**
1	Decanoylarginine	263.1382	5.13	2.307	5.37E-06
2	L-phenylalanyl-L-proline	288.2015	1.78	4.3232	3.11E-03
3	N,N-dimethylarginine	329.2535	7.92	2.0753	1.34E-03
4	5-oxopyrrolidine-2-carbonyl-L-isoleucine	243.1335	5.21	3.2194	2.18E-06
5	unknown peptide	978.9351	5.88	8.409	2.00E-03
6	unknown peptide	947.4641	6.25	9.3673	6.03E-04
7	unknown peptide	929.9464	6.2	9.041	5.34E-05
8	unknown peptide	939.452	6.89	7.1738	2.52E-03
9	unknown peptide	938.9517	6.26	12.064	1.10E-03
10	unknown	838.442	7.7	8.267	7.42E-07
11	unknown	736.4276	6.4	7.0625	1.31E-07
12	unknown	1019.977	6.18	7.4388	4.39E-03
13	unknown	375.121	5.76	8.0418	4.04E-06
14	unknown	739.3218	3.72	7.2852	7.67E-07

Due to the scarcity of specialized libraries on extremophilic fungi, none of the features among the top 10 areas of increased ions had a spectral match in the databases; however, based on the fragmentation profile, the cluster that concentrates the ion features **5**, **6**, **7**, **8**, and **9** could be a peptide. The mass spectra (Figure 2.16) revealed that this molecule is doubly charged due to *m/z* values being greater than the chosen precursor ion for fragmentation. This indicates that the mass of these molecules is greater than 1000 Da. The charge state for the respective peptides could be verified by the mass difference of 0.5 units in the isotopic envelope, corresponding to 2 charges $[M+2H]^{2+}$ for the analytes in question. The fragmentation profile also displays typical peptide fragments, as shown in Figure 2.16. For the precursor ion *m/z* 978.939 (peptide 5), it is possible to observe the fragment ions *(m/z* 838.427; 709.387; 610.318 and 497.235) formed from characteristic peptide cleavages in its MS/MS spectrum; generating fragments of the type *y*- and *b*- series ions based on the difference in mass between these fragments (Δ *m/z*), it is possible to infer which amino acids are connected to the same peptide backbone.

The peptides detected by mass spectrometry in the experiment with magnesium perchlorate are in the same cluster of the molecular network generated by the GNPS platform due to their similar fragmentation pattern, suggesting that they are part of the same chemical class or even that they are structurally very similar. All these ions relating to peptides (5, 6, 7, 8, and 9), when subjected to fragmentation by CID (collision-induced dissociation), generated a fragment ion of the immonium type *m/z* 86.096, which is diagnostic of the presence of the amino acid residues I/L (SOLE-DOMENECH *et al.*, 2010). By utilizing the difference between the fragmented ions, many amino acids could be identified by *de novo* sequencing, for example, in Figure 2.16. However, other spectroscopic techniques are required to elucidate the peptide completely.

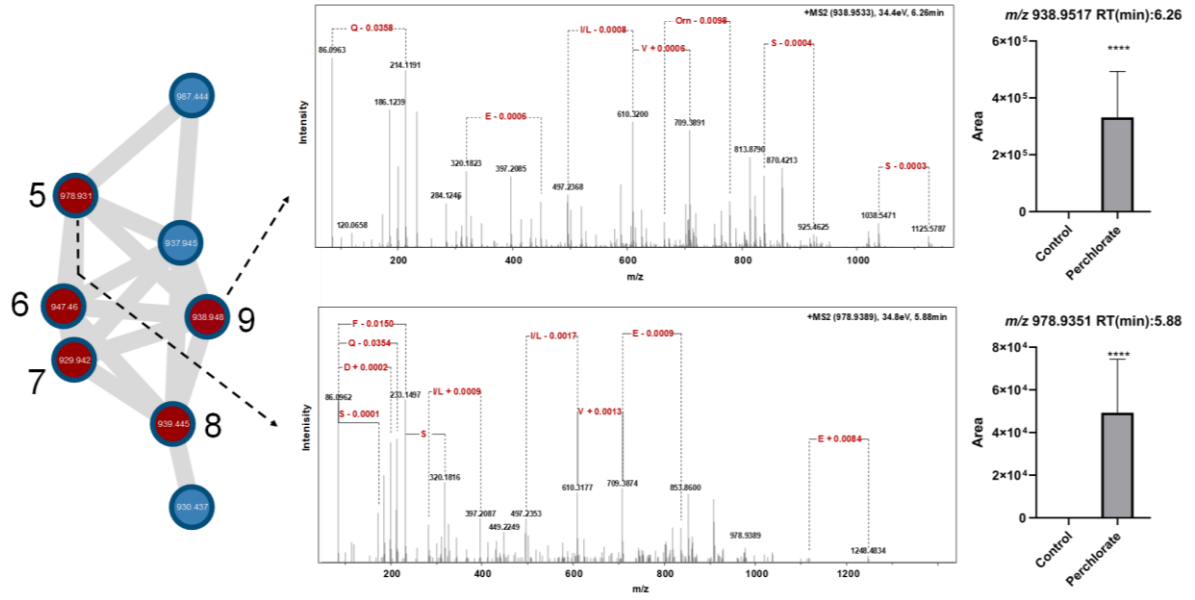

FIGURE 2.16 – Molecular clusters exhibiting five nodes among the most upregulated, along with the MS/MS spectra of ions with *m/z* 938.9517 and *m/z* 978.9351, illustrate the similarity in the fragmentation profile and the typical cleavage pattern of peptides.

2.2.4 - Discussion

2.2.4.1 - Survival Ability in Magnesium Perchlorate Condition

Perchlorates have been found on the surface soil of Mars, and due to their characteristics of absorbing water from the thin Martian atmosphere, stable brines can (temporarily) exist and provide water for the potential existing life (HECHT *et al.*, 2009; GLAVIN *et al.*, 2013). Thus, it is necessary to test, under laboratory conditions, the ability of the microorganisms to adapt and survive in perchlorate brines, as they could be a habitat for putative life on Mars (BEBLO-VRANESEVIC *et al.*, 2020). However, perchlorate is a highly oxidizing compound that damages the main functions of terrestrial organisms, interrupting a series of metabolic processes and causing cell and internal damage. Moreover, combined with ionizing radiation, the negative effects of perchlorate are potentialized.

WADSWORTH and COCKELL (2017) observed a severe bactericidal effect of UV light under short-wave UV-C radiation (up to 60 seconds) on *Bacillus subtilis* cells growing in magnesium perchlorate medium. In contrast, the data reported here showed that black yeast has greater cell viability under the tested UV-C radiation dose and influence of magnesium perchlorate, especially the *R. similis* LaBioMMi 1217. Black yeast specializes in

extremotolerance and is among the most stress-resistant eukaryotes on Earth. This melanized group has been shown as a good candidate for astrobiology studies through ground-based facilities and space missions. For example, ONOFRI *et al.* (2012) tested the ability of *Cryomyces antarcticus* and *C. minteri* to survive long-term space travel. After 1.5 years of exposure at the International Space Station (ISS), remarkably, the cells remained viable. In terms of tolerance, several microorganisms have been reported as tolerant to perchlorates, including halotolerant archaeal and bacterial strains, yeast *Debaryomyces hansenii* (HEINZ *et al.*, 2020), and fungi, such as *Purpureocillium lilacinum* and *Cryomyces antarcticus* (HEINZ *et al.*, 2020; CASSARO *et al.*, 2022); however, most can grow in conditions up to 0.4 mol L^{-1} of perchlorate concentration. Currently, the most tolerant microorganism reported is the halotolerant yeast *Debaryomyces hansenii*, being able to grow in a liquid medium containing 2.4 M $NaClO_4$ (HEINZ *et al.*, 2020), more than twice the record of the prior microbe, the bacterium *Planococcus halocryophilus* (HEINZ *et al.*, 2019). Our fungal strain *R. similis* showed surprising tolerance and grew in magnesium perchlorate conditions up to 0.75 M during the 7 days of cultivation. Furthermore, resistance to the toxic effects of the irradiated perchlorate was observed. Follow-up studies to reveal the mechanisms of resistance of the black fungus *R. similis* to the deleterious properties of these combined factors would constitute interesting lines of inquiry for astrobiological implications (i.e., extraterrestrial life, planetary protection, and Bioregenerative Life Support Systems based on *in situ* resource utilization). Changes at a structural level were detected using SEM, in addition to macroscopic observations, highlighting the stress responses to perchlorates, whereas we observed that the *R. similis* changed from a multicellular filamentous growth form to unicellular yeast. The morphogenic shift is a common strategy among fungi to adapt to the new prevailing conditions (NADAL *et al.*, 2008). Melanin production, as we observed, was useful for the growth of the black yeast *Hortaea werneckii* in NaCl concentrations (KOGEJ *et al.*, 2007) and magnesium perchlorate in *Cryomyces antarcticus* (CASSARO *et al.*, 2022). Different studies report that the accumulation of pigments is a strategy used to mitigate oxidative stress when exposed to perchlorate salt (RZYMSKI *et al.*, 2022).

2.2.4.2 - Molecular Adaptations for Endurance in Magnesium Perchlorate Saline Environments

The investigation of the protein machinery to understand the effects of perchlorate stress on fungi is in its early stages, with only one study identified so far. HEINZ

et al. (2020) developed a study using proteomics to investigate the fungus *Debaryomyces hansenii* in high concentrations of sodium perchlorate and observed that salt stress-resistant yeasts undergo significant changes when cultured in this salt. Currently, no studies have been conducted on the change in the proteomic profile of the yeast class known as black yeast under conditions of high concentrations of magnesium perchlorate. Thus, this work presents some initial insights into how black fungus cells cope with stress caused by magnesium perchlorate.

In filamentous fungi and yeasts, environmental stress situations often trigger communication from the cell envelope to the nucleus through specific signaling pathways, such as those related to mitogen-activated protein kinase, accompanied by changes in cytoskeletal matrices. It has been observed that several proteins participating in these signaling pathways are positively activated in response to perchlorate treatment (HEINZ *et al.*, 2022). For example, the serine-threonine phosphatase proteins (RBB50_004446) and histidine phosphatase (RBB50_005453), when positively activated, regulate the expression of glycerol biosynthesis (JOSHUA & HÖFKEN, 2019). This can result in a more efficient reduction in intracellular water activity than other compatible solutes (ALVES *et al.*, 2015).

Osmotic stress generally induces some form of oxidative stress, for example, by producing reactive oxygen species (ROS) in mitochondria (ZOROV, 2013). Therefore, proteins involved in responses to oxidative stress are also expected to be regulated under saline stress conditions. Indeed, we found that the antioxidant activity and metabolic processes of glutathione are positively regulated in $Mg(ClO_4)_2$ stressed samples, including the enzymes catalase (RBB50_004981) and superoxide dismutase (RBB50_012728), allowing cellular protection against oxidative stress. The increased abundance of these proteins was also found in the fungus *Debaryomyces hansenii* under conditions of high perchlorate anion concentration, indicating that different species of fungi have the same response to this stress (HEINZ *et al.*, 2020).

We also observed that a family of enzymes had its expression increased in the presence of high concentrations of magnesium perchlorate, where three peptidyl-prolyl cis-trans isomerases (RBB50_004565; RBB50_003292; RBB50_007691; RBB50_011626) were positively regulated. These enzymes have been previously investigated in halotolerant strains of *P. oxalicum*, with reported increased expression under salt stress conditions attributed to their role in protein folding. Peptidyl-prolyl cis-trans isomerases (PPIases) facilitate the proper folding of proteins by catalyzing the cis-trans isomerization of prolyl peptide bonds, a process crucial for maintaining proper protein structure and function (SINGH *et al.*, 2021).

Both the magnesium cation and the perchlorate anion are chaotropic ions, which destabilize biomacromolecules in the cell wall (WILLIAMS & HALLSWORTH, 2009). Black yeast, which was used in this study, contains melanin in the cell wall in addition to the classical biomolecules chitin and glucan (NOSANCHUK *et al.*, 2015). Thus, the darkening of the fungus biomass in the presence of perchlorate salt correlates. The expression of the enzyme laccase (RBB50_005731), belonging to melanin biosynthesis, was increased, indicating that melanin production is indeed occurring in the cell as a way to make the cell wall more resistant to the chaotropic effects of magnesium perchlorate. Additionally, the enrichment of the biological process organic hydroxy compound metabolic process indicates that hydroxylated molecules, such as fungal melanin, are being produced. Melanin production is extremely interesting in this context because it protects against chaotic and oxidative effects generated by chemical species or UV-C radiation, situations also found on Mars.

An enzyme that has drawn considerable attention due to its increased abundance is the haloacid dehalogenase-like hydrolase enzyme (RBB50_003417). In marine environments with high pollution from halogenated compounds, this enzyme serves as a mechanism to dehalogenate these compounds and make the environment safer (WANG *et al.*, 2021). Considering the surface of Mars, this mechanism could be very useful for microbial life since perchlorate derivatives (i.e., hyperchlorites) are excellent halogenates of organic molecules. Thus, the explanation for the increase is that perchlorate is halogenating molecules and making the environment even more toxic. The fungus produces this enzyme to cope with this toxic stress as a defense mechanism.

2.2.4.3 - Production of Molecular Biosignature and their Impacts on the Detection of Life on Mars

The search for life beyond Earth, especially on celestial bodies within our solar system, remains a significant challenge due to limitations in human resources for collecting samples and conducting microbiological analyses. However, various space agencies have been investing in technologies for detecting molecules *in situ*, known as bio-signatures (ABRAHAMSSON & KANIK, 2022). Advances in mass spectrometry applied to space exploration actively contribute to the development of more robust equipment in terms of sensitivity, resolution, and the ability to analyze molecules of different sizes, making the use of complex organic molecules as bio-signatures a powerful tool for detecting evidence of extraterrestrial life. (CHOU *et al.*, 2021). The search for complex molecules as evidence of

life beyond Earth turns out to be a very promising approach, as many of these molecules are produced exclusively by biotic processes, such as long-chain unsaturated lipids, polypeptides, and other molecules resulting from secondary metabolism (ABRAHAMSSON & KANIK, 2022). In this sense, it becomes necessary to understand which molecules could be produced in astrobiologically relevant environments.

The molecules produced by the fungus *R. similis* in our simulated magnesium perchlorate brine experiment provide extremely interesting insights into what microorganisms could produce under these conditions. The presence of various molecules with a proline group, such as L-phenylalanyl-L-proline (2) and 5-oxopyrrolidine-2-carbonyl-L-isoleucine (4), observed in the directed annotated metabolomics experiment, provides indications that the fungus under study used molecules as osmolytes to mitigate the saline stress it was being subjected to. This type of molecule production has already been observed in studies with halophilic bacteria (DIEHL *et al.*, 2013). Proline and derivatives are crucial in maintaining cellular osmotic balance and ensuring proper function under saline stress conditions (CHUN *et al.*, 2018). Furthermore, proline is vital in determining protein and membrane structures and eliminating ROS in complex organisms during water stress (CHUN *et al.*, 2018). Identifying these molecules on Mars could indicate which microorganisms utilize these molecular functions to cope with environmental stress.

Decanoylarginine (1) and *N*,*N*-dimethylarginine (3) were also observed and are two molecules derived from arginine, also considered polyamines. These molecules may result from the degradation of proteins related to the signaling process from stress caused by perchlorate. The methylation of arginine post-translationally is a method for some cells to signal the stress caused by an oxidative agent (XU *et al.*, 2021). The presence of these metabolites may be associated with the degradation of proteins that undergo this post-translational modification (XU *et al.*, 2021), given that in this experiment, the expression of peptidases increased in the presence of perchlorate. Another possibility is that polyamines are important in response to stress and that their metabolic pathway has been conserved in all living organisms, suggesting that the main role of polyamines is to promote the restoration of cellular homeostasis, allowing survival under stressful conditions. In *S. cerevisiae*, the expression of the main permease for high-affinity polyamine import coincided with the osmotic stress imposed by high concentrations of NaCl, KCl, or sorbitol (LEE *et al.*, 2002; AOUIDA *et al.*, 2005), thus generating an increase in the production of these molecules.

Indeed, the production of peptides with molecular masses between 1800–2000 Da was significantly increased in the presence of perchlorate. Peptides in this size range

have been reported for other fungi as a result of secondary metabolism, in which some cyclic peptides are produced in the presence of chemical stress by fungi in the genus *Penicillium*; in this case, the fungus started to produce these peptides as chelators to deal with high concentrations of manganese and copper cations (FILL *et al.*, 2016). Considering the high magnesium concentration in the tested samples, the fungus *R. smilis* may also use peptide chelators to deal with these cations. However, the increase in the production of peptides in fungi in the presence of perchlorate ions was reported only in our study. Another possible explanation, considering that plants and fungi have similar biological processes, is the production of these molecules as salinity stress signaling agents. NAKAMINAMI *et al.* (2018) observed that plants produce linear peptides of this size as peptide hormones that signal cascades to help with salinity stress caused by sodium chloride.

Many other feature molecules had their production increased (Table S1.5), although the annotation was limited due to the lack of MS/MS spectra of microbial metabolites deposited in dedicated mass spectrometry databases. However, it is worth noting that the reported annotated molecules had their production increased only under perchlorate salt conditions, indicating that they are a starting point for choosing which molecules are interesting to identify in perchlorate brines on Mars.

2.2.5 - Conclusion

From the standpoint of potential life on present Mars, perchlorate-resistant features will be important for microbial survival on Mars's regoliths and brine environment. Thus, this study provides, for the first time, insight into the growth and resistance of the black fungus *Rhinocladiella similis* to magnesium perchlorate and the combined effect of ionizing radiation. The investigation of the variation in protein profiles under perchlorate brine conditions supported the morphological aspects and showed that the fungus activated several pathways in response to osmotic and antioxidant stress caused by perchlorate salt. Defensive mechanisms to cope with the chaotropic action were also observed. The metabolites found in the simulated experiment with magnesium perchlorate, such as proline-derived osmolites and peptides, may aid in the identification of molecules to be sought by the new generation of rovers and mass spectrometers that will possibly be sent to Mars in the future.

This study advances the frontier of knowledge in astrobiology and sets a precedent for the continuous exploration of life in extreme environments, whether on Earth or beyond. The findings presented herein promote a better understanding of the extremophilic

capabilities of terrestrial microorganisms, paving the way for the exploration of life beyond the boundaries of our planet.

CHAPTER 3 - NEW INSIGHTS INTO THE USE OF HALOPHILIC BACTERIA TO UNDERSTAND LIFE ON ENCELADUS

3.1 - INVESTIGATING POLYEXTREMOPHILIC BACTERIA IN AL WAHBAH CRATER, SAUDI ARABIA: A TERRESTRIAL MODEL FOR LIFE ON SATURN'S MOON ENCELADUS[3]

3.1.1 - Introduction

Astrobiology is an emerging interdisciplinary field that investigates the origin, evolution, and distribution of life in the universe, both on Earth and beyond, including the possibility that life exists in other planetary bodies in our solar system (https://www.astrobiologyprimer.org; SCHULTZ *et al.*, 2023b). The discovery of extraterrestial environments that are analogous to some extreme environments on Earth and the study of the organisms that inhabit them have produced results that further support the plausibility of life beyond Earth (WAGNER *et al.*, 2022). Extremophilic microorganisms isolated from these terrestrial environments have become the main models for possible extraterrestrial life in harsh environments (LOPEZ *et al.*, 2019; MERINO *et al.*, 2019; SCHULTZ *et al.*, 2023b).

Haloalkaliphilic organisms are particularly attractive models in astrobiology because they are evolutionarily ancient, physiologically versatile, and capable of surviving in diverse extreme planetary environments. Of these organisms, polyextremophilic characteristics, such as tolerance to high salinity, anaerobic conditions, high levels of ionizing ultraviolet radiation, and temperatures ranging from subzero to >120 °C, make these organisms an ideal model for studying the possibility of life on the icy moon of Saturn, Enceladus (WAGNER *et al.*, 2022). Observations of the Cassini–Huygens and Galileo spacecraft have revealed that Enceladus has a significant ocean of liquid water beneath its icy crust (KIVELSON *et al.*, 2000; WAITE *et al.*, 2009). The use of many scientific instruments coupled with the Cassini spacecraft has shown that the ocean of Enceladus is highly alkaline, with a pH around 10-12, and rich in phosphate salts, demonstrated to be 100 times richer in phosphate than Earth's oceans (POSTBERG *et al.*, 2023). Additionally, it is known that the bottom of this ocean is potentially dominated by hydrothermal sources and governed by volcanic activity (DEAMER & DAMER, 2017). Recent studies have shown that the ocean of

[3] This section is an adapted version of the paper:

Santos, A.; Schultz, J.; Trapp, M. A.; Modolon, F.; Romanenko, A.; Jaiswal, A. k.; Gomes, L.; Rodrigues-Filho, E. & Rosado, A. S. Investigating polyextremophilic bacteria in Al Wahbah crater, Saudi Arabia: a terrestrial model for life on Saturn's moon Enceladus. *Astrobiology*, 24(**8**): 824-838, 2024. DOI: 10.1089/ast.2024.0017.

Enceladus contains macromolecules of up to 200 Da, in addition to small molecules (MORA *et al.*, 2022; POSTBERG *et al.*, 2018). These observations have sparked discussions within the scientific community about the possibility of these molecules being associated with microbial activity. Consequently, several space agencies are now focused on finding life in the ocean of Enceladus (BROCKWELL *et al.*, 2016; DEAMER & DAMER, 2017; NEVEU *et al.*, 2020). To better understand icy moons, astrobiologists and planetary scientists are highly interested in finding remote locations on Earth with physicochemical conditions similar to those present in Enceladus' subglacial ocean and aim to conduct fieldwork to exploit their microbiomes in search for novel biological models (KANIK & VERA, 2021; STEINLE *et al.*, 2018).

Saudi Arabia has many volcanoes and extensive basaltic lava fields, known as harrats, located along the western part of the Arabian Shield subparallel to the Red Sea (WAHAB *et al.*, 2014). Notably, the Al Wahbah crater within the Harrat Kishb volcanic area emerges as a significant site for extraterrestrial analog studies and a potential new source of astrobiological resources such as extremophiles. Despite its Earth-bound location, the Al Wahbah crater is an intriguing analog for studying microbial life akin to that possibly present on Enceladus. The similarities between Enceladus's physical and chemical environments – particularly its ocean and hydrothermal vents – and the phosphate-rich, highly alkaline soil of the Al Wahbah crater are striking. The crater comprises soil with a high concentration of sodium phosphates and chlorates, being highly alkaline. These chemical characteristics arise due to leaching processes and the formation of a temporary lake in the middle of the crater during rainy periods. This seasonal lake in Al Wahbah exhibits pH and salinity levels parallel those of Enceladus's ocean. Soil analysis at the crater's center reveals high phosphate and chloride concentrations, with a pH between 9 and 10 (WAHAB *et al.*, 2014). Similarly, Enceladus's ocean is considered alkaline, with a pH between 9 and 12, and replete with various ions, suggesting that potential microbial inhabitants would need to be halophilic and alkali-tolerant. The moon's potential for hosting microbial life is especially high near its hydrothermal vents, where volcanic activities could foster favorable life-sustaining conditions (REH *et al.*, 2016). The volcanic nature of Al Wahbah, characterized by basaltic minerals, phosphate crystals, and olivines, coupled with the desert's elevated temperatures, renders it an exemplary terrestrial counterpart for Enceladus's potentially habitable environments. Furthermore, a molecular study revealed a diverse microbial community capable of thriving in these saline and alkaline conditions (ALBOKARI *et al.*, 2018). Given the physicochemical similarities between Enceladus's ocean and the alkaline clay in Al Wahbah, this crater

represents a prime location for exploring thermohaloalkaliphilic (heat, salt, and alkali-loving) microorganisms, serving as biological proxies for life on Enceladus.

Although the microbial metabolism of potential extraterrestrial living organisms may differ from that of terrestrial microorganisms, the search for molecular biosignatures in other worlds can be initiated by characterizing micromolecules and their respective metabolic pathways in organisms that inhabit extreme conditions on Earth. With the current advancement in instrumental techniques, particularly mass spectrometry (MS), and the popularity of platforms for annotating organic molecules, such as Global Natural Products Social (GNPS), it has become easier to propose classes or families of compounds produced by microorganisms cultivated under various conditions (WANG *et al.*, 2015; SEYLER *et al.*, 2020).

Currently, we are aware that in the coming years, new mass spectrometers generation will be sent to the gas giants of our solar system, aiming to investigate the possibility of life on their icy moons (AREVALO *et al.*, 2020). One of these instruments, the Mass Spectrometer for Planetary Exploration/Europa (MASPEX), is scheduled to be sent in 2024 on the Europa Clipper mission. MASPEX is a time-of-flight mass spectrometer, known for its high resolution and sensitivity, allowing for the detection of traces (ppb) of organic compounds. Selected by NASA for the Europa Clipper mission, MASPEX will analyze samples of the sprayed atmosphere on the moon's surface to evaluate any evidence of habitability and life (BROCKWELL *et al.*, 2016; SEPHTON *et al.*, 2018). This same technology and approach are being considered for use in missions investigating organic molecules in the oceans of Enceladus in the coming decades (REH *et al.*, 2016). Additionally, other mass spectrometers are being developed exclusively for use in astrobiology research, such as the CosmoOrbitrap, featuring an Orbitrap analyzer, the same as used in our study presented here. This equipment will have the capability to produce results of the same excellence as the equipment used in Earth's laboratories (AREVALO *et al.*, 2018; AREVALO *et al.*, 2023).

Given the imminent deployment of mass spectrometers to Enceladus, understanding the molecules potentially present on the moon through laboratory experiments that integrate extremophilic microorganisms with the physicochemical conditions of these extraterrestrial oceans can provide valuable insights into the possible molecular signatures. This approach is crucial for advancing our understanding of life’s limits and detecting environments as extreme as those found on Enceladus.

Motivated by the extreme characteristics of the Al Wahbah crater in Saudi Arabia and their resemblance to those of Enceladus, along with the growing emphasis on genomic characterization in bacterial taxonomy and functionalities for astrobiological purposes, we aimed to isolate and characterize extremophilic bacteria from the crater's samples. Our isolates spanned 11 distinct bacterial genera and belonged to three phyla: *Actinomycetota*, *Bacillota*, and *Pseudomonadota*. Moreover, the genomes of two thermohaloalkaliphilic strains were sequenced and compared with those of closely related species available in public databases. Herein, we present an in-depth analysis of genomic characterization, metabolic potential, and chemical profiles of the bacterial strains cultured from the Al Wahbah crater, and focus on the searching of novel biosignatures potentially useful in a search for life on Enceladus. For this study, we hypothesized that microorganisms isolated from the Al Wahbah crater could provide insights into the existence of life on Enceladus. The unique features of the thermohaloalkaliphilic strains, indicate their potential compatibility with the extreme conditions of Enceladus' subglacial ocean. Genomic and chemical analyses of these microorganisms can broaden our understanding of extremophilic life on Earth, serve as a biological model for hypothesizing about the nature of extraterrestrial life forms, and lay the groundwork for future astrobiological explorations to identify biosignatures on celestial bodies. The goal of our research is to enhance our understanding of potential life forms in the Enceladus' ocean.

3.1.2 - Materials and Methods

3.1.2.1 - Study Site And Sampling Strategy

Sampling was performed at different locations in the Al Wahbah crater (lat. 22.90632, lon. 41.13849), located on the Harrat Kishb basalt plateau in the Hejazi region of Saudi Arabia, in February 2023. A total of nine samples were collected from three sites: (i) site with a high concentration of sodium phosphate salt, (ii) a dry part at the edge of the site with salt, and (iii) a clay-rich area in the middle of the crater (Figure 3.1). Approximately 500 g of soil was collected from each sampling point (in triplicate) at 0–10-cm depth, placed into sterile plastic bags, and stored at 4 °C until processing in the laboratory.

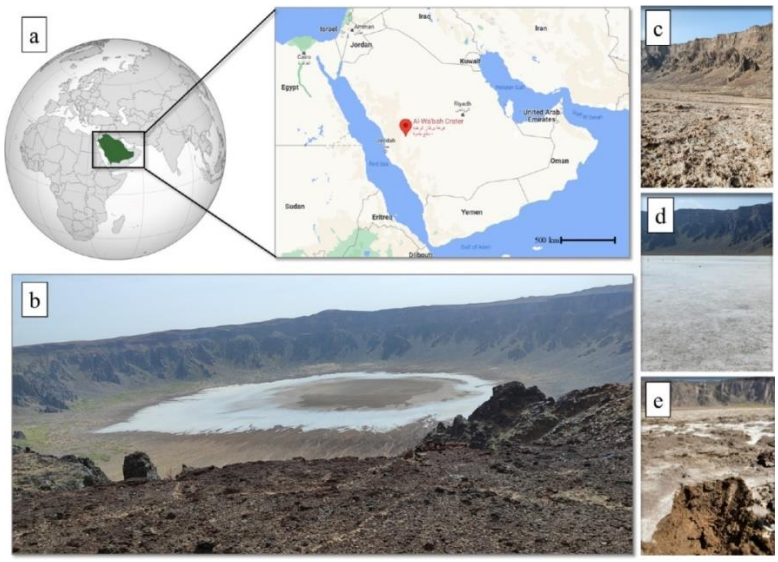

FIGURE 3.1 – (a) Map of the Harrat Kishb region, located west of Taif, in Saudi Arabia. (b) Overview of the Al Wahbah crater. The samples were collected from three specific locations at the bottom of the crater: (c) soil from the edges of the salty region, (d) salty crust, and (e) salt clay from the center of the crater.

3.1.2.2 - Physicochemical Characterization

To characterize the collected soil samples, we evaluated the physicochemical parameters of the soils, including pH, electrical conductivity, and elemental analysis. The analyses were performed in the Analytical Core Laboratory of the King Abdullah University of Science and Technology (ACL/KAUST). Concentrations of 14 major elements were analyzed. Si, Al, Fe, K, Na, Ca, Mg, Ti, P, and Mn concentrations were determined using inductively coupled plasma-optical emission spectroscopy (Agilent 5110 ICP-OES, Agilent, Santa Clara, CA, US). First, the microwave-digestion method, according to the US EPA 3051A protocol, was used to prepare soil samples in triplicate. After digestion, the samples were diluted with deionized water up to 20 mL, of which 10 mL was used for the analysis. Blank, standard, and quality-control samples were also prepared. The blanks consisted of 10 mL of 1% nitric acid, and the standard consisted of 1 mL of 100 ppm of each element analyzed in a total volume of 10 mL. The 25-, 10-, and 1-ppm standards were prepared from the 100-ppm standard. Commercially available multi-element standards were used to prepare quality-control samples for all elements. A Flash 2000 Series CHNS/O Automatic Elemental Analyzer using the dry-combustion method was used to determine carbon, hydrogen, and nitrogen concentrations. A 10-mg amount of homogenized sample (inverted by hand) was weighed in tin capsules and sealed. Standards with known concentrations for calibration and

quality control were weighed and sealed in tin capsules. The standards and samples were prepared and loaded into the instrument for analysis.

3.1.2.3 - Isolation and Growth Conditions

To retrieve the culturable fraction of bacteria from the soils of the Al Wahbah Crater, a soil-sprinkling strategy in agar Petri dishes was applied. Four different culture media were used: Horikoshi alkaline medium (final pH, 10.0), modified marine medium (final pH, 10.3), halophilic medium (final pH, 9.0), and Bushnell–Haas medium (final pH, 7.4) (the media compositions are presented in Table S2.1). For the sprinkling methodology, soil samples were homogenized, and 100 mg of each soil sample was sprinkled onto four culture media in triplicate and incubated at 35 °C and 55 °C as growth temperatures for up to 72 h. After incubation, morphologically distinct colonies were isolated by streaking on their respective media.

Pure bacterial colonies from both strategies were transferred to their respective liquid medium (15 mL) and incubated at the isolation temperature with shaking (150 rpm) for up to 48 h. An aliquot of the microbial culture was placed in a cryogenic vial containing glycerol (20% v/v) in triplicate and stored at −80 °C. All isolated microbial strains from Al Wahbah crater were deposited in the Saudi Extreme Culture Collection of the Laboratory of Microbial Ecogenomics and Biotechnology, KAUST. A summary of the experimental design is shown in Figure S2.1.

3.1.2.4 - DNA Extraction, 16S rRNA Gene Sequencing, and Phylogenetic Analysis

A Wizard® Genomic DNA Purification Kit (Promega, United States) was used to extract total genomic DNA from the bacterial strains according to the manufacturer's instructions. Isolates were identified based on Sanger sequencing of the 16S rRNA gene for molecular identification. A Master Mix AmpliTaq 360 (Promega, United States) was used to amplify an approximately 1450-bp fragment of the 16S rRNA gene with universal primers 27F (5′-AGA-GTT-TGA-TCM-TGG-CTC-AG-3′) and 1492R (5′-TAC-GGY-TAC-CTT-GTT-ACG-ACT-T-3′) (WEISBURG *et al.*, 1991) via polymerase chain reaction (PCR), according to the manufacturer's instructions. The amplification was performed in a thermocycler as follows: an initial denaturation step was performed at 95 °C for 10 min followed by four consecutive cycles of 98 °C for 30 s, 98 °C for 1 min, and 72 °C for 1 min.

This step was followed by 30 cycles of 54 °C for 30 s, 72 °C for 1 min, and a final extension step at 72 °C for 15 min. PCR products were quantified using Qubit 4.0 with the Qubit® dsDNA HS Assay Kit (Life Technologies, United States); stained with Sybr Safe stain (Invitrogen, USA) in 1% agarose for examination; run at 90 V and 500 A for 45 min; and visualized using Gel Doc™ EZ System. The PCR products were then sent to Macrogen, Inc., Seoul, South Korea, for Sanger sequencing of the 16S rRNA gene. Subsequently, BioEdit (v.7.2.5) was used to check and trim the raw sequences, and align the sequences from both primers. BLAST was then used to compare the resulting sequences with homologous sequences in the National Center for Biotechnology Information (NCBI)-GenBank database. Aiming to check the evolutionary distance between our isolates, the neighbor-joining statistical method with 1,000 bootstrap replications was used to construct the phylogenetic tree in IQTREE (v.2.2.0.3; MINH *et al.*, 2020), and the interactive Tree Of Life (iTOL; v.6.7) was used for annotation and editing (LETUNIC & BORK, 2021).

3.1.2.5 - Whole-Genome Sequencing, Assembly, and Characterization

To better understand the taxonomy and functionalities of polyextremophilic bacteria for astrobiological purposes, two bacterial strains capable of growing under thermohaloalkalinophilic conditions were selected for whole-genome sequencing and in-depth characterization of their genomes. Hence, an amount of 5 μg/μL of gDNA was used to construct paired-end sequencing libraries (2 × 150 bp) of 350-bp inserts following the manufacturer's protocol for the Illumina TruSeq Nano DNA library preparation kit. Quality analysis of the final libraries was performed on an Agilent 2100 bioanalyzer (Agilent Technologies). The bacterial sample was sequenced on the Illumina NovaSeq6000 platform, as recommended by the manufacturer, with a minimum data output of 10 Gb per sample.

For genome assembly, FastQC (ANDREWS, 2010) was used to check the quality of the raw reads, and SPAdes (v.3.13.0) (BANKEVICH *et al.*, 2012) and Unicycler (v.0.4.8) (WICK *et al.*, 2017) were used to perform *de novo* assembly. Metrics to evaluate the quality and choose the best assembly were generated by QUAST (GUREVICH *et al.*, 2013). The *Bacillus halodurans* strain C-125 genome sequence from NCBI (accession BA000004.3) was used as the reference to generate a scaffold in CONTIGuator (GALARDINI *et al.*, 2011). MOB-suite (v3.0.3) (ROBERTSON & NASH, 2018) was used to screen plasmid sequences, and BLASTn was used to check plasmid contigs against the nonredundant database of NCBI. GFinisher (v.1.4) (GUIZELINI *et al.*, 2016) and GapBlaster (v.1.1.2) (SÁ *et al.*, 2016) were

used to fill gaps within genome and plasmid sequences. CheckM (PARKS *et al.*, 2015) was also used to check each assembly for completeness and contamination. The default parameters were used in all of the software.

To perform nucleotide-level comparisons of these two genomes within their respective genera, we used the NCBI command line tool datasets (v.15.23.0) and obtained all validly described representative genomes of this genus (https://github.com/ncbi/datasets). We then used JSpeciesWS to compute the pairwise Average Nucleotide Identity (ANI) computations with the novel strains as a query with representative genomes (RICHTER *et al.*, 2016). Furthermore, to estimate digital DNA–DNA hybridization (dDDH), we employed the Genome-to-Genome Distance Calculator (GGDC; v3.0) online tool with the recommended Formula 2 and the BLAST+ alignment tool (MEIER-KOLTHOFF *et al.*, 2013).

3.1.2.6 - Whole-Genome Sequencing (WGS)-Based Phylogeny

To validate the taxonomy and phylogeny placement of the two polyextremophilic strains within their respective genera, we generated two phylogenetic trees based on the pangenome analysis, that capture the complete genetic diversity within species. Hence, firstly, we used the OrthoFinder program that accepts *.faa* amino acid sequence fasta files for each genome to perform all-vs-all BLASTp to identify orthologous genes. OrthoFinder employs a Markov clustering algorithm (MCL) to group proteins to determine orthologous genes (EMMS & KELLY, 2015). We used 29 species (27 *Bacillus* species and 2 newly sequenced genomes, 3Ho3b and 4Ho3b) for the pangenome, core genome, and singletons calculation (Table S2.2). The newly sequenced genome strain 3Ho3b was used as the reference genome for the analysis with the default OrthoFinder parameter. Furthermore, we used our own *in-house* Perl script for the pangenome, core genome, and singleton set calculations. The extrapolations of the pangenes were calculated according to Heap's Law for both the open and closed pangenome (GUIMARÃES *et al.*, 2015; JAISWAL *et al.*, 2020; SOARES *et al.*, 2013), and the least-squares fit of the exponential regression decay for the core and singletons calculations. For the pangenome, core genome, and singleton, the methodology of JAISWAL *et al.* (2020) was used. Subsequently, the phylogenetic trees were constructed at the genus level (27 *Bacillus* species and 2 newly sequenced genomes 3Ho3b and 4Ho3b), and also based on the core genome proteins (shared by all of the species) obtained from the pangenome analysis. The species *Streptococcus agalactia* ATCC13813 and *S. gordonii* ATCC10558 were used as outgroups for tree construction. All species and their

protein sequences used for the analysis were downloaded from the NCBI genome database. Using GToTree (v.1.8.2), which is a command line tool using hidden Markov models, we aligned and identified single-copy genes from the entire genome and generated concatenated protein alignments (LEE, 2019). Because the strains were affiliated with *Bacillota*, 119 single-copy genes associated with Firmicutes were applied to position both strains. Next, we used IQTREE v.2.2.0.3 (MINH *et al.*, 2020) with ModelFinder-Plus (KALYAANAMOORTHY *et al.*, 2017) to construct the phylogenetic tree from the protein alignment generated by GToTree with 1,000 ultra-fast bootstrap replicates. Then, iTOL v.6.7 (LETUNIC & BORK, 2021) was used to visualize the WGS-based trees.

3.1.2.7 - Genome Annotation and in Silico Genome Mining to Search for Potential Biosignatures

Prokka (v.1.11) (SEEMANN, 2014) was used to perform annotation, and Subsystems Technology (RAST-tk) (AZIZ *et al.*, 2008) and rapid annotation of microbial genomes were used to perform functional annotations. The results were used to infer functions at the subsystem level. In addition, the NCBI clusters of orthologous genes (COG), PFAM, and KEGG databases in Anvi'o (v.7.1; EREN *et al.*, 2015) were used to analyze the predicted contigs. Manual filtration for data mining was performed in the functional tables generated by NCBI COG. To predict biosynthetic gene clusters, the web-based platforms antiSMASH 6.0 (BLIN *et al.*, 2021), BAGEL4 (VAN HEEL *et al.*, 2018), and PRISM 4.0 (SKINNIDER *et al.*, 2015) were used. To identity prophage sequences, Phage Search Tool Enhanced Release (PHASTER) was used (ARNDT *et al.*, 2016).

3.1.2.8 - Cultivation and Extraction of Metabolites from Polyextremophilic Bacteria

Initially, a sterile loop was used to plate the two bacterial strains isolated at a temperature of 55 °C onto R2A culture medium plates in quintuplicate and supplemented with 15 g/L of sodium bicarbonate and 15 g/L of sodium chloride to simulate the chemical conditions of Enceladus' ocean. The bacteria were incubated at 55 °C for 7 days, and after incubation, the bacteria were completely scraped from the culture medium. In addition, five 10-mm agar plugs were placed in a solution of ethanol and methanol acetate (1:1 v/v). The solution was then placed in an ultrasonic bath for 45 min. The obtained extract was dried in a rotary evaporator in vacuum. Subsequently, the dried samples were suspended in high-

pressure liquid chromatography (HPLC)-grade methanol, centrifuged, and transferred to vial flasks for ultra-HPLC-Q-Orbitrap high-resolution MS.

3.1.2.9 - Mass Spectrometry Analysis and Data Processing

An untargeted screening study of the crude extracts of thermohaloalkalophilic bacteria was conducted that used ultra-HPLC coupled to an Orbitrap ID-X MS (UHPLC-Orbitrap ID-X MS). Electrospray ionization in positive (ESI+) and negative (ESI−) modes was applied to the studied compounds, and the following parameters were used: vaporized temperature = 100 °C, voltage = 3500 V, sheath gas = 30 L/min, auxiliary gas = 15 L/min, ion-source fragmentation = 35 V, and capillary temperature = 300 °C. The equipment was set to perform automated operations. A 10-µL aliquot of each sample was injected through a loop injector into a C18 column (Acquity CSH 100 × 2.1 mm, 1.7 µm). The 5-µL samples were pumped through the UHPLC system along with the mobile phase and separated on a C18 column. The flow rate was set to 0.5 mL/min, and a 15-min gradient was used to achieve the required separation.

A molecular network was created using the online workflow (https://ccms-ucsd.github.io/GNPSDocumentation/) on the GNPS website (http://gnps.ucsd.edu). The data were filtered by removing all MS/MS fragment ions within ±17 Da of the precursor *m/z*. MS/MS spectra were window-filtered by choosing only the top six fragment ions in the ±50-Da window throughout the spectrum. The precursor ion mass tolerance was set to 0.02 Da, and the MS/MS fragment ion tolerance was set to 0.02 Da. A network was then created in which edges were filtered to have a cosine score >0.65 and more than four matched peaks. Furthermore, edges between two nodes were kept in the network if and only if each of the nodes appeared in each other's respective top-10 most similar nodes. Finally, the maximum size of a molecular family was set to 50, and the lowest-scoring edges were removed from the molecular families until the molecular family size was below this threshold. The spectra in the network were then searched against the GNPS spectral libraries. The library spectra were filtered in the same manner as used for the input data. All matches between network and library spectra were required to have a score >0.65 and at least four matched peaks.

3.1.2.10 - Data Availability

All Sanger sequences were deposited in NCBI GenBank under accession numbers OR888764–OR888811 in the BioProject PRJNA1047907 (Table 3.1). The BioSample accession numbers for the assembled genomes described here are SAMN38599447 (strain 3Ho3b) and SAMN38599448 (strain 4Ho3b). The genomes used for comparison are listed in Table S2.2. The data obtained through MS using a molecular networking approach are publicly available for reference and use by the scientific community. For the ESI+ MS-technique-acquired data, interested parties can use GNPS with the identifier ID = b609721100ce491e9cde0cced1909f84 to access them. The ESI-MS data are available in the same repository, and the identifier ID = f36714ac5bd54798982cab5afda5cb97 can be used for access.

3.1.3 - Results

3.1.3.1 - Physicochemical Parameters of the Al Wahbah Crater

The pH and electrical conductivity values were 8.9 and 66.22 dS/m in the salt-crust, 9.1 and 28.6076 dS/m in the clay soil, and 9.4 and 42.8028 dS/m in the dry edge of the salt-crust soil sample, respectively. The clay-soil sample had the highest number of elements with the highest concentrations, including Fe, C, Ca, Mg, Ti, and P. The highest concentrations of Al, K, Na, and N were in the soil with salt crust, whereas the highest concentration of Si was in the soil-only sample. The salt-crust soil sample had the highest concentration of sodium (59.92 g/kg) compared with 28.14 g/kg in the soil-only sample and 23.21 g/kg in the clay-soil sample. In contrast, the Mg concentration was higher in the clay-soil sample (32.88 g/kg) than in the samples with only soil (15.38 g/kg) and salt crust (12.72 g/kg). The total nitrogen content was 0.21 g/kg in the soil-only and clay-soil samples and 0.3 g/kg in the samples with salt crust. The total carbon concentration was highest in the clay soil (11.37 g/kg), followed by salt-crust (9.75 g/kg) and soil-only (7.17 g/kg) samples (Table 3.1).

TABLE 3.1 – Physicochemical properties and elemental composition of Al Wahbah crater soil samples.

	Al Wahbah crater soil samples (g/Kg)		
Elements	**Soil (AWS)**	**Soil with salt crust (AWR)**	**Clay (AWC)**
pH	9.363	8.914	9.119
EC (dS/m)	42.8028	66.2267	28.6076
Si	0.62 ± 0.09	0.48 ± 0.15	0.54 ± 0.02
Al	21.57 ± 1.50	24.99 ± 1.36	22.03 ± 3.34
Fe	26.97 ± 1.41	27.17 ± 1.24	29.8 ± 4.90
C	7.17 ± 0.16	9.75 ± 0.38	11.37 ± 1.14
K	4.78 ± 0.08	6.17 ± 0.46	4.83 ± 0.12
Na	28.14 ± 1.42	59.92 ± 5.79	23.21 ± 2.60
Ca	26.49 ± 1.36	28.51 ± 1.46	32.88 ± 4.07
Mg	12.72 ± 0.87	15.38 ± 0.77	22.76 ± 2.73
Ti	0.7 ± 0.02	0.59 ± 0.03	0.81 ± 0.01
N	0.21 ± 0.01	0.3 ± 0.01	0.21 ± 0
P	0.46 ± 0	0.46 ± 0.04	0.64 ± 0.02
Mn	0.39 ± 0.01	0.39 ± 0.03	0.4 ± 0

Data are presented as the mean (±95% confidence level) of a triplicate

3.1.3.2 - Culturing Haloalkaliphilic Bacteria from the Al Wahbah Volcanic Crater

A total of 48 bacterial isolates, spanned into three families, were obtained from the soil samples collected from three sites at the Al Wahbah crater (Figure 3.2a, Table S2.3). The phylogenetic tree showed four clearly distinct clusters (Figure 3.2b), with three large clades comprising the *Bacillota* phylum. The clay soil yielded the highest number of strains and generic diversity (25 isolates), followed by the salt crust soil sample (20 isolates). Most of the cultured strains belonged to family *Bacillaceae*, with more representatives of the genera *Evansella* (n = 18) and *Alkalihalobacillus* (n = 10). Moreover, strains of *Kocuria* and *Pseudomonas* genera were isolated only from soil samples containing salt crust. The majority of bacteria (n = 43) were isolated at 35 °C, whereas five strains were recovered at 55 °C, including members of *Halalkalibacterium*, *Alkalihalophilus*, and *Amphibacillus* genera. Two

of them were exclusively cultured in thermophilic conditions, identified as *Anaerobacillus alkalidiazotrophicus* strains 3Ho3b and 4Ho3b based on 16SrDNA sequencing (Figure 3.2b), and were further selected for WGS, and taxonomic and functional analyses.

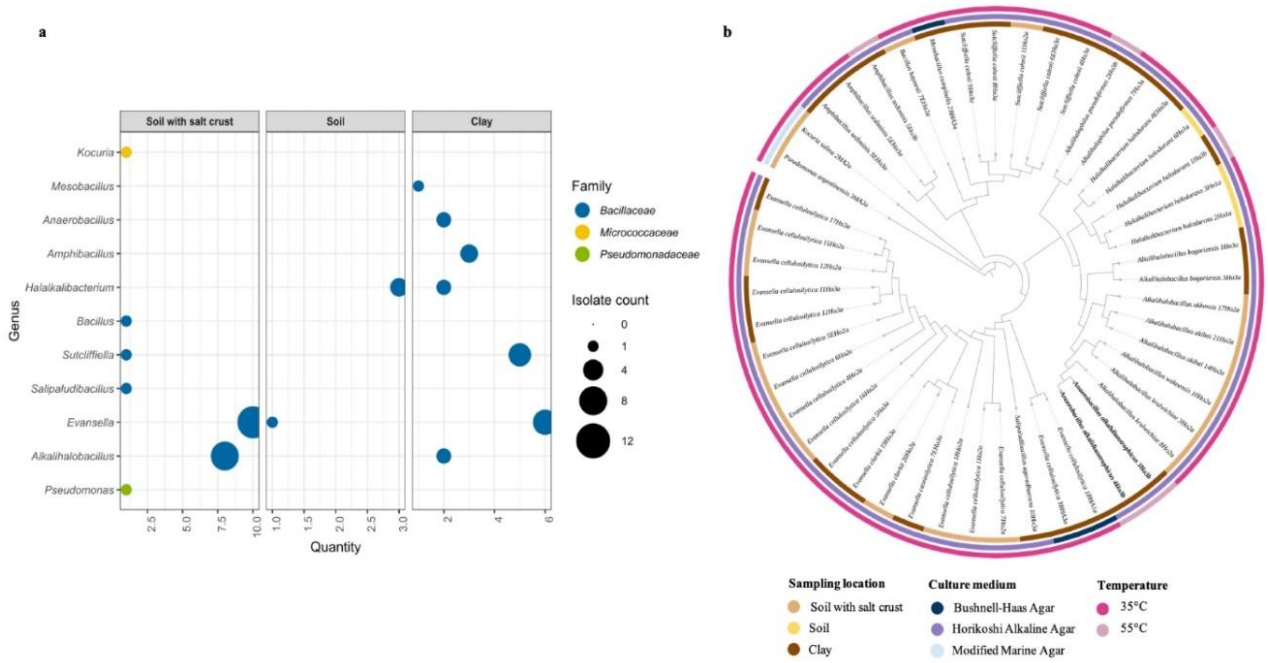

FIGURE 3.2 – (a) Genus- and family-level assignment of bacterial isolates retrieved from the three sampling sites in the Al Wahbah crater, Saudi Arabia. The average relative abundance of each genus isolated from the crater bacterial community is shown on the x-axis. (b) Phylogenetic tree based on rrs gene sequences is showing the relationship between the bacterial strains isolated from the Al Wahbah crater. Colors in the outer circles indicate the sampling location, the culture media employed to isolate the strains and the temperature of incubation. The neighbor-joining method was used to construct the phylogenetic trees, and bootstrap analyses using 1,000 repetitions were performed.

3.1.3.3 - Genomic Features and Relatedness Indices

The genomes of strains 3Ho3b and 4Ho3b, both cultured from clay-soil samples in Horikoshi alkaline agar at 55 °C, were assembled *de novo*. The genome size was approximately 4.4 Mb, with 43.4% GC content and ~4,530 protein-coding sequences in 48 and 49 contigs, respectively. The general genomic features of the two strains 3Ho3b and 4Ho3b are summarized in Table 3.2. Their circularized genomes with additional information of the contigs, GC%, CDS on both strands and gene content are shown in Figure S2.3.

TABLE 3.2 – General features of the genome of strains 3Ho3b and 4Ho3b.

Strain	Genome size (bp)	Contigs	GC content	Completeness	Coverage	Coding sequences	RNA	WGS accession number
3Ho3b	4,385.928	48	43.40%	99.3%	503	4,534	79	JAXIWI000000000
4Ho3b	4,385.548	49	43.41%	99.3%	483	4,520	79	JAXIWJ000000000

Aiming to confirm the identity of the bacterial strains, we performed ANI and dDDH analyses with the closest species from the public database (accession number GCF_000011145.1), and both strains, 3Ho3b and 4Ho3b, were closely related to *Halalkalibacterium halodurans*, with 99% similarity for ANIb and 94.5% for dDDH (Table S2.4). Moreover, ANI indices (<95%) and dDDH values (<70%) were above the threshold levels of bacterial species identity, confirming that the examined Al Wahbah crater strains belonged to *Halalkalibacterium halodurans* species.

3.1.3.4 - Phylogenomic Analysis of Halalkalibacterium Halodurans Strains

We generated whole-genome-based phylogenies to identify closely related species in the isolated genomes. For that, firstly, pangenome analysis was performed with our 2 newly sequenced genomes—3Ho3b and 4Ho3b—and 27 genomes from family *Bacillaceae* (selected on the basis of their core proteins analyses), aiming to capture the complete genetic diversity within species. Based on the resulting pangenome, core genome, and singleton analysis (Figure S2.4, Table S2.5), we identified a total of 15,752 genes as a pangenome and 879 genes were identified as the core genome, keeping genome 3Ho3b as a reference. We also identified approximately 537 genes as part of the core genome and 29 genes as singletons of our novel strains of *Halalkalibacterium halodurans* (Figure S2.4, Table S2.5).

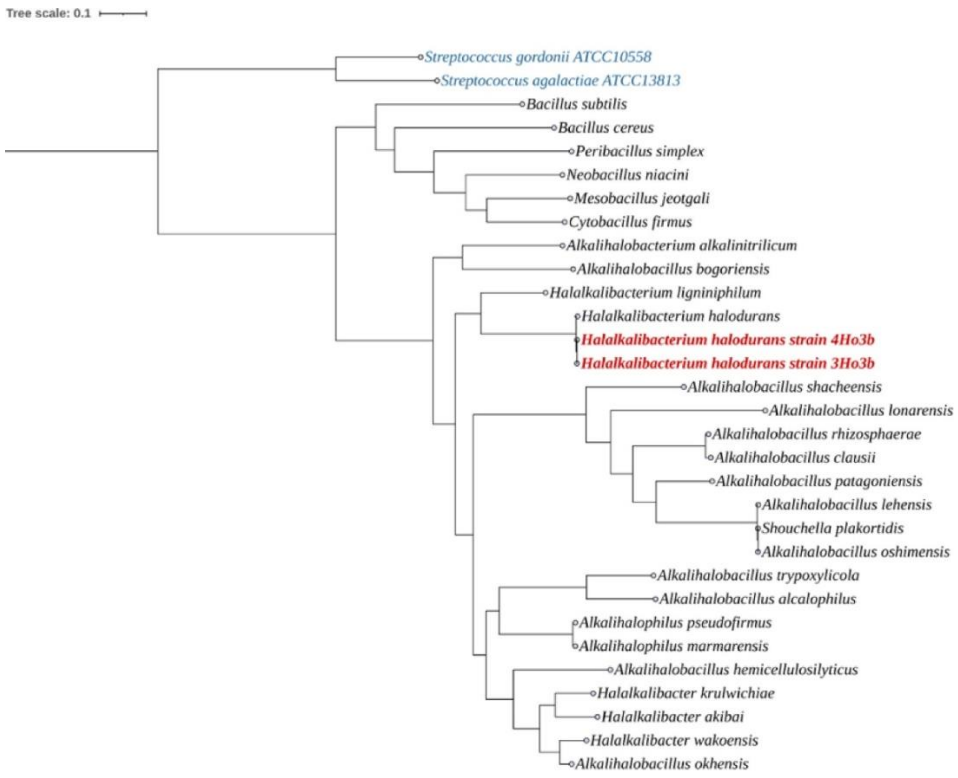

FIGURE 3.3 – Whole genome sequencing phylogenetic tree of our newly sequenced genomes from 3Ho3b and 4Ho3b strains.

The phylogenetic tree was constructed using the protein sequences of halophilic bacteria (27 Bacillus species) that were downloaded from the NCBI genome server, and our two genomes from 3Ho3b and 4Ho3b strains. Species from Streptococcus were used as outgroups. A total of 119 single-copy genes associated with Bacillota were applied to position both strains. ModelFinder-Plus was used to construct the phylogenetic tree from the protein alignment with 1,000 ultra-fast bootstrap replicates.

Subsequently, we created two phylogenetic trees that were based on the whole genome of 27 species and 2 newly sequenced genomes of family Bacillaceae (Figure 3.3) and based on core proteins, keeping strain 3Ho3b as the reference genome for the core protein (Figure S2.2). We found that newly sequenced genomes 3Ho3b and 4Ho3b were in the same clade as the species *Halalkalibacterium ligniniphilum* and *Halalkalibacterium halodurans*. Similarly, the phylogenetic tree based on the core protein exhibited the same pattern, confirming the phylogeny placement of our strains into *Halalkalibacterium halodurans* species.

3.1.3.5 - Functional Characterization and Data Mining for Genes with Potential Applications in Astrobiology

To investigate the genetic characteristics of the two polyextremophilic strains, we used RAST-tk and NCBI COG to perform a comprehensive genome annotation. The subsystem mapping resulted in 455 subsystems for both *Halalkalibacterium halodurans* strains (3Ho3b and 4Ho3b). Among the annotated subsystems, the top categories based on average gene counts were related to amino acids and their derivatives, carbohydrates, cofactors, vitamins, prosthetic groups, pigments, and protein metabolism, which showed the highest numbers of assigned genes in descending order. With COG, 4,317 genes were predicted for the 4Ho3b strain and 4,315 for the 3Ho3b strain.

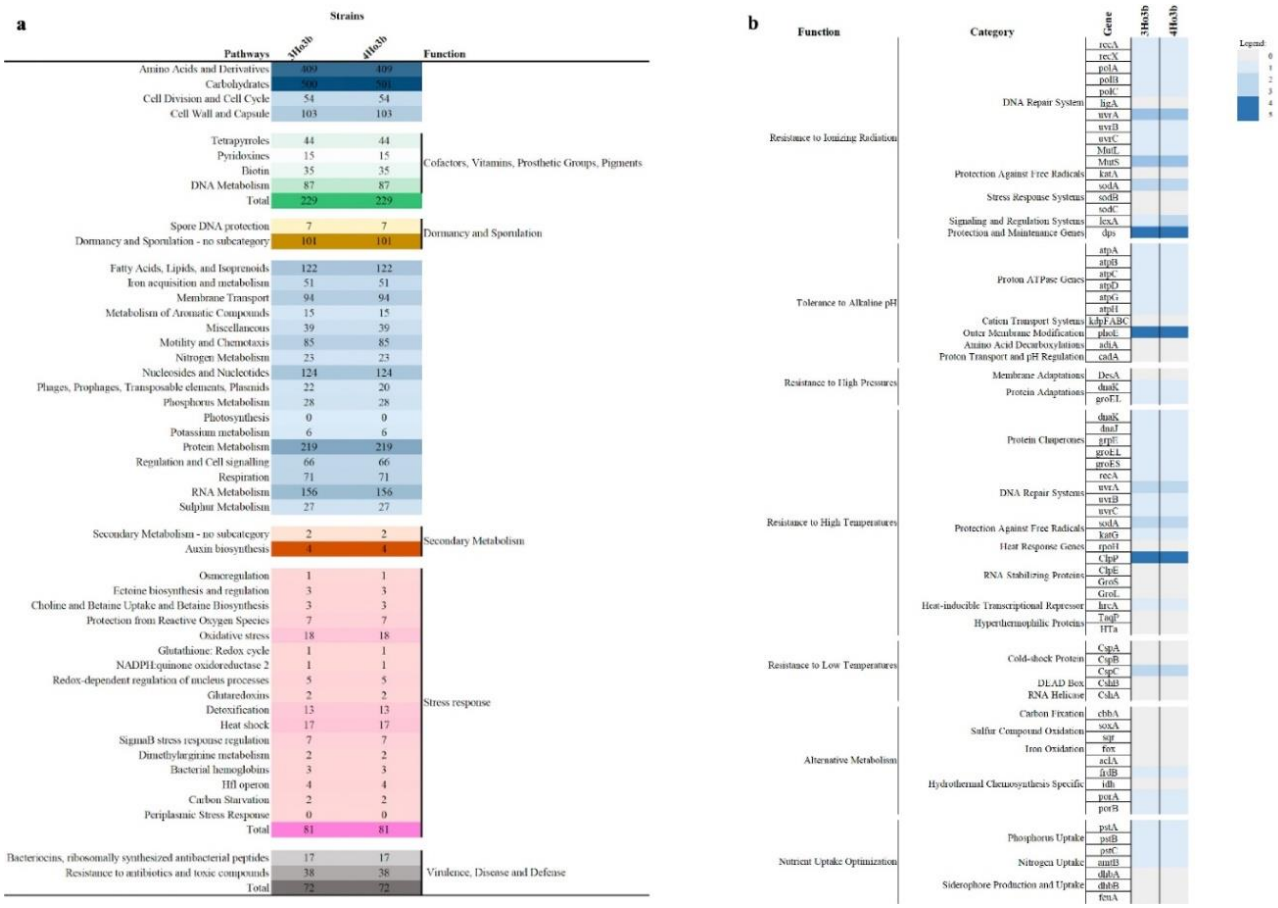

FIGURE 3.4 – Annotated genes of metabolisms from *Halalkalibacterium halodurans* strains (3Ho3b and 4Ho3b).

Panel (a) is displaying the general functional annotation, using RAST-tk, antiSMASH, BAGEL, and PRISM tools, and in panel (b) NCBI COG were used to detect the genes. COG,clusters of orthologous genes; NCBI, National Center for Biotechnology Information.

To explore the potential for producing secondary metabolites in the newly discovered strains of the Al Wahbah crater, we used antiSMASH, BAGEL, and PRISM tools

to predict secondary metabolites. This analysis revealed a total of eight gene clusters in both analyzed genomes, two of which exhibited 100% similarity with lantibiotic haloduracin and bacillopaline, and the other six clusters were similar to ectoine, schizokinen (NI siderophore), fengycin (betalactone), 7-deoxypactamycin (T3PKS), and RiPP-like and cyclic lactone autoinducer. Additionally, PRISM 4 detected three clusters, including the same types observed with antiSMASH-class II lanthipeptide, ectoine, and NI siderophore, whereas with BAGEL, haloduracin was identified in one area of interest (Figure 3.4a). Analysis with the PHASTER program detected only one intact prophage sequence in the genomes, which was related to *Staphylococcus* with a GC content of 40.41%, a 38.8-kb region length, and four incomplete prophages with similarity to *Bacillus* and *Peanebacillus* phages.

To more deeply understand the applicability of the analyzed strains from the Al Wahbah crater to the field of astrobiology, we conducted further investigations into the metabolic potential of these strains by manually mining genes of interest for different functionalities in the strain genomes, such as resistance to ionizing radiation, tolerance to alkalinity and extreme temperatures, resistance to high pressure, the presence of alternative metabolisms, and optimization of nutrient uptake. We then made some noteworthy observations (Figure 3.4b). Overall, we used COG to predict genes related to genome stabilization, DNA repair systems, and adaptation to high temperature and alkaline conditions. A complete list of detected genes is presented in Table S2.6.

Regarding the adaptation of the strains to thermal stress, both genomes exhibited chaperones involved in repairing heat-induced protein damage, DnaK and DnaJ, as well as small Hsps (hsp20), htpX, and ClpP genes, and GroEL and GroES. Genes related to DNA repair systems, such as recA, uvrA, uvrB, and uvrC, and those that protect against free radicals, sodA and katG, were also detected. Genes associated with cold-shock proteins were not commonly detected, and only the ClpC gene was observed in the analyzed genomes. Genes involved in adaptation to alkaline pH were identified, including the antiporter NhaC, proton ATPase genes atpA to atpH, and phoE, which is a gene involved in outer-membrane modification. To protect against ionizing radiation, the genes recA, recX, polA-C, uvrA-C, MutL, and MutS, which are involved in DNA repair, and sodA, lexA, and dps, which are involved in the stress-response system, were identified. Interestingly, many genes involved in carbon, sulfur, iron, and nitrogen metabolism were absent. We predicted hydrothermal chemosynthesis-specific genes, such as frdB, porA, and porB, and genes related to phosphorus (pstA, pstB, and pstC) and amtB for nitrogen uptake were observed.

3.1.3.6 - Molecular Network-Based Dereplication of Microbial Extracts

To analyze the chemical inventory of *Halalkalibacterium halodurans* strains, we used tandem MS (MS–MS) data processed on the GNPS platform. This approach enabled the execution of detailed chemical annotations and creation of a global molecular network. The integration of GNPS with dereplication, assisted by a natural products library, facilitated the identification of various chemical structural classes and their analogs. As indicated in Table 3.3, the molecules were annotated in accordance with level-2 identification, consistent with the Metabolomics Standards Initiative guidelines by SUMNER *et al.* (2007).

TABLE 3.3 – Compounds of *Halalkalibacterium halodurans* strains annotated via the GNPS database: Molecular families, ionization mode, retention time, and detected masses.

Molecular family	**Compounds**	**Ionizaton mode**	**RT (min)**	***m/z***
Nucleotide derivatives	Uridine 5'-monophosphate	neg	2.48	323.029
Nucleotide derivatives	Cytidine-3'-monophosphate	neg	1.04	322.045
Nucleotide derivatives	2'-Deoxyadenosine-5'-monophosphate	neg	2.05	330.061
Cyclopeptides	Versicoloritide A	pos	4.23	560.271
Cyclopeptides	cyclo(D-Trp-L-Pro)	pos	5.31	284.139
Lipoaminoacid and lysine derivatives	Lys-Ile-PyroGlu	pos	2.98	371.229
Lipoaminoacid and lysine derivatives	Lys-C12:0	pos	6.68	329.28
Lipoaminoacid and lysine derivatives	Lys-Ile	pos	0.89	260.197
Lipoaminoacid and lysine derivatives	Lys-C16:0	pos	8.72	385.343
Lipoaminoacid and lysine derivatives	Lys-C15:0	pos	8.24	371.328
Amino acid derivatives	N-Acetyl-L-glutamic acid	neg	1.66	188.056
Amino acid derivatives	N-Acetyl-L-aspartic acid	neg	1.44	174.041
Amino acid derivatives	L-alanyl-L-alanine	neg	0.75	159.078
Phospholipids	Hexadecanoyl-sn-glycero-3-phosphoethanolamine	pos	9.3	907.579
Phospholipids	1-Myristoyl-2-hydroxy-sn-glycero-3-phosphoethanolamine	pos	8.45	426.263
Phospholipids	1-Palmitoyl-2-hydroxy-sn-glycero-3-phosphoethanolamine	pos	9.18	454.282
Phospholipids	1-(9-Octadecenoyl)-sn-glycero-3-phosphoethanolamine	neg	9.57	478.294
Phospholipids	PE (16:1/0:0)	neg	8.77	450.263

Phospholipids	PE (17:1/0:0)	neg	9.14	464.279
Pyridoxine derivatives	4-Pyridoxic acid	neg	2.18	182.046
Tryptophan derivatives	N-Acetyltryptophan	neg	5.57	245.093

GNPS, Global Natural Products Social.

The use of a molecular network was crucial for differentiating chemical species within the same molecular family, organizing them into clusters based on fragmentation spectral-alignment algorithms, independent of retention times (tR). This methodology significantly expedited the annotation of known molecules. Figure 3.5 shows the resulting global molecular network, with data from both the negative-ionization mode (Figure 3.5a) and positive-ionization mode (Figure 3.5b). The molecular networks reveal various chemical entities, accounting for approximately 710 nodes in the negative mode and 737 nodes in the positive mode. Specific clusters are formed for both ionization modes (Figure 3.5). By comparing the spectra obtained with those deposited in the GNPS database, it was possible to annotate some clusters according to molecular family categories. This is observed, for example, in the five clusters identified in the negative mode (phospholipids, nucleotide derivatives, nonproteinogenic amino acids, pyridoxine derivatives, and tryptophan derivatives) and three clusters in the positive mode (phospholipids, lipoamino acids, and cyclopeptides).

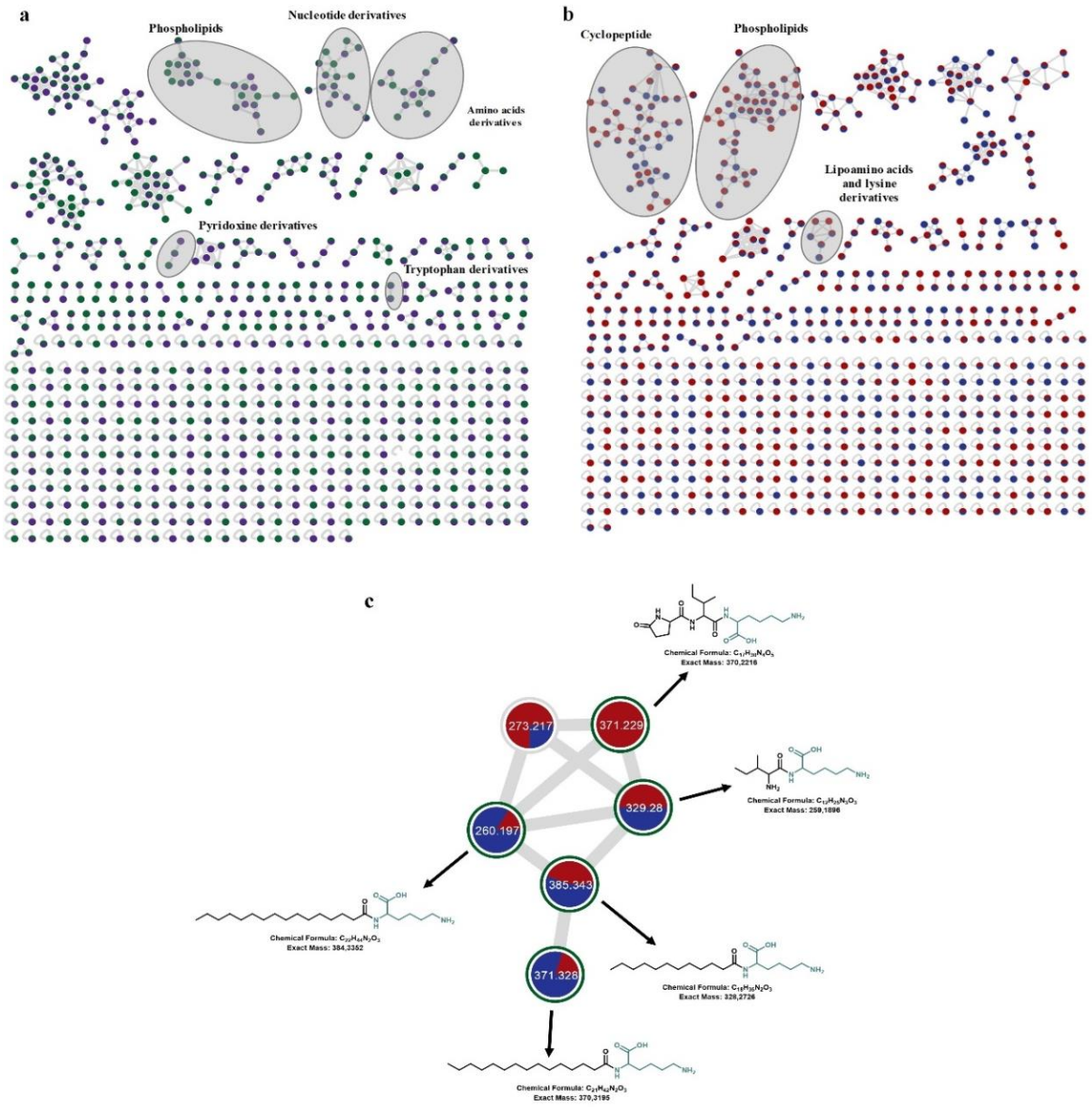

FIGURE 3.5 – Global molecular network of the methanolic extracts obtained from the two strains of *Halalkalibacterium halodurans*.

Each node represents the MS/MS spectrum of a feature (high-resolution mass and retention times). **(a)** Data from the negative-ion mode was used to construct the molecular network. The green nodes indicate MS/MS spectrum associated with molecules from strain 3Ho4b, whereas the purple nodes represent MS/MS spectrum derived from strain 3Ho3b. **(b)** Data from the positive-ion mode were used to construct the molecular network. The red nodes correspond to strain 3Ho3b, whereas the blue nodes represent strain 3Ho4b. **(c)** Molecular cluster of the lipoamino acids and lysine derivatives. MS, mass spectrometry.

In the analysis of the molecular network, some entities are specific to a single strain. The Venn diagram (Figure S2.5) shows that, for the negative-ionization mode, 16% of the nodes belong exclusively to strain 3Ho3b, 15% belong only to strain 3Ho4b, and 69% represent chemical entities that appear in both bacteria. Similarly, for the positive-ionization

mode, 19% of the nodes belong exclusively to strain 3Ho3b, 18% belong only to strain 3Ho4b, and 63% are chemical entities present in both strains.

3.1.4 - Discussion

Saudi Arabia harbors vast extreme environments with the potential to be exploited as analog habitats of extraterrestrial environments, such as Enceladus. The extremophilic microbiome thriving in these environments could be used for astrobiological applications, but no research of this type has been conducted so far. With the aim of characterizing potential novel biological models, this study is the first to assess the culturable bacterial fraction of the Al Wahbah crater with a focus on its habitability on Enceladus.

Due to the tidal forces exerted by Saturn, Enceladus's core is active, allowing for volcanic activity on the ocean floor. Additionally, recent discoveries indicate that Enceladus' ocean possess high concentrations of phosphate ions, which is highly unusual compared to Earth's oceans, with about 100x to 500x the average abundance of phosphate (POSTBERG *et al.*, 2023). This alkaline and saline environment, presenting high temperatures, offers a mystery regarding the potential life, and types of polyextremophilic microorganisms that could be thriving there. On our planet, environments with this combination of physicochemical factors are quite rare. Recently, the shallow lakes of Last Chance and Goodenough were considered as a potential environmental analog to understand the origin of life and possible forms of life on Enceladus, which have with similar chemical characteristics and presenting high phosphate concentrations and elevated pH (HAAS *et al.*, 2024).

In this sense, the search for other environments that exhibit these characteristics becomes of great importance to the astrobiology community. Therefore, the Al Wahbah crater, visually different from the icy moon, emerges as a very interesting environment to seek microbial models for Enceladus's ocean and possible hydrothermal sources. Our physicochemical results of the Al Wahbah soils (Table 3.1), along with the studies of WAHAB *et al.* (2014), show that the crater presents high concentration of phosphates and presence of crystals at the bottom of the crater, also high pH, and temperatures that can exceed 50 °C in the summer. It is worth noting that during the rainy season, the interior of the crater becomes flooded, giving rise to a temporary lake. Moreover, ALBOKARI *et al.* (2018), using independent-cultivation techniques detected a great diversity

of halophilic and alkaline-tolerant microorganisms in the crater's soils, exibhiting an interesting and diverse extremofilic microbial community.

Using different culture media (SCHULTZ *et al.*, 2023a), we isolated >48 strains from three sites. Phylogenetic analysis classified most isolates as belonging to *Bacillaceae*. Members of this family present distinct morphological and physiological characteristics, such as the formation of heat-resistant endospores, which enables them to thrive under extreme conditions, such as extreme environments in Saudi Arabia and potentially on Enceladus. Upon examining Al Wahbah bacterial strains, two polyextremophilic strains capable of growing under extreme temperatures, high salinity, and alkaline pH (conditions similar to potential hydrothermal sources in the subterranean ocean of Enceladus (WAITE *et al.*, 2017) were selected for deeper genomic characterization and chemical profile analysis with a focus on astrobiology. Both were phylogenetically close to *Halalkalibacterium halodurans*, a bacterium living in alkaline saline conditions that was first described by BOYER *et al.* (1973), isolated from dried sewage sludge, and later reclassified by JOSHI *et al.* (2021). Our strains, 3Ho3b and 4Ho3b, of *Halalkalibacterium halodurans* matched haloduracin, a two-peptide lantibiotic described as having potent antimicrobial activity (OMAN & VAN DER DONK, 2009), and bacillopaline, a metallophore used to acquire trace metals from the environment, respectively (REITZ & MEDEMA, 2022). Moreover, clusters similar to ectoine, schizokinen, fengycin, T3PKS, and RiPP-like and cyclic lactone autoinducer were observed in both strains. These natural products may have a role when encountering unfavorable environmental conditions.

Considering the possible physicochemical conditions, such as high pressure, excess salts, alkaline pH, and elevated temperatures, of potential hydrothermal vents on the Enceladus ocean, the metabolism of any potential microbial community there must meet specific requirements to survive in that environment. Looking at specific genes and metabolism interesting for astrobiology, genome mining led to the identification of key functional genes related to stress response and survival strategy. Our strains of *Halalkalibacterium halodurans* can flourish under thermophilic, highly saline, and alkaline conditions, and for that, they developed different approaches aiming to survive in extreme environments. To thrive under harsh thermal conditions, strategies related to DNA-stabilizing mechanisms, efficient DNA repair systems, and adapted proteins are required (WANG *et al.*, 2016), and our strains exhibit these modifications. Genes related to protein-folding under high temperatures (dnaK, dnaJ, groEL, and groES) and genes encoding DNA repair and protection against free radicals (recA, uvr, sodA, and katG) were detected. They are crucial in

maintaining the functioning and integrity of the microbial system (COKER, 2019; PAULINO-LIMA *et al.*, 2013; SOMAYAJI *et al.*, 2022). Genes encoding cold-shock proteins were also analyzed because of their wider role in stress tolerance both in cold tolerance and in osmotic stress (SCHMID *et al.*, 2009); however, only the CspC protein was observed. When facing a temperature downshift, the bacterial cells might counteract some harmful effects (PHADTARE, 2004). Additionally, proton ATPase genes and phoE encoding a phosphate-limitation-inducible outer-membrane pore protein were observed in our strains. These genes are crucial for maintaining intracellular pH under alkaline conditions, helping to pump protons into the cell (PADAN *et al.*, 2005). In addition, in response to adverse environmental conditions, microorganisms enduring numerous physicochemical stresses may adopt reversible metabolic strategies, such as dormancy and spore formation (LEUNG *et al.*, 2020).

Screening of the chemical profile of *Halalkalibacterium halodurans* strains using the molecular network approach revealed that the bacteria also differ minimally in their metabolite composition, as expected. However, the analysis showed several molecular classes essential for bacterial life that could be used as biosignatures. The plan to send again mass spectrometers to Enceladus is becoming increasingly close to reality. We know that the next generation of these instruments, aimed at searching for biosignatures, is very similar to the mass spectrometers used in Earth's laboratories (AREVALO *et al.*, 2020). With this advancement in space exploration, it will soon be possible to integrate bioinformatics tools for annotating natural products to help identify molecules from other celestial bodies. The approach of generating a molecular network from MS/MS spectra, along with comparison with spectral libraries, is very efficient for obtaining a preliminary understanding of an unknown sample. Thus, having an idea of the possible complex molecules that we could detect there, as a result of the metabolism of extremophilic microorganisms cultivated under similar conditions, would greatly assist in future missions (LOPEZ *et al.*, 2019).

Notably, a phospholipid cluster was detected in both ionization modes in our study. As fundamental components of bacterial cell membranes, these molecules form the base structure of the lipid bilayer, which significantly contributes to the maintenance of structural integrity and membrane fluidity and facilitates selective substance transport (PARSONS & O ROCK, 2014). Another detected class was nucleotides and their derivatives, which are omnipresent in all life domains and have key roles in DNA synthesis, enzyme regulation, and energy transport, as in ATP and GTP cases. In addition, the production of pyridoxine derivatives (vitamin B6) was observed. These molecules are critical cofactors in various enzymatic reactions, particularly in amino acid synthesis and degradation. Because of

their chemical structure similar to that of some osmolytes, it is possible that pyridoxine may also be biosynthesized by bacteria for this purpose (SLEATOR & HILL, 2002).

Two molecular classes have attracted considerable interest: cyclopeptides and lipoamino acids or lipoampeptides. Cyclopeptides are notable for their variety of biological activities. In the literature, these molecules are often associated with biological control and the capture of certain metabolic cations, acting as chelators (GISIN *et al.*, 1978; KUBIK, 2022; RIBEIRO *et al.*, 2022). Lipoamino acids, illustrated in the molecular cluster in Figure 3.4c, are molecules that feature one or more amino acid units linked to a fatty acid, usually attached to the amino group. These molecules demonstrate the ability to confer stability to macromolecules under chemical and thermal stress conditions (VICENTE-GARCIA & COLOMER, 2023). The presence of a hydrophobic chain differentiates them from peptides and amino acids, thereby endowing them with amphiphilic properties. Thus, these molecules can act in micelle formation to protect nutrients and other cellular molecules in alkaline and saline environments (VICENTE-GARCIA & COLOMER, 2023).

Although the molecules presented are not novel, their identification in microorganisms isolated from the Al Wahbah crater is novel. Analyzing the chemical profile of these strains reveals the importance of investing in studies on metabolites produced by extremophilic microorganisms. Our study showed that even using specialized databases, it was possible to annotate <10% of the entities detected in the extracts. This finding indicates that exploring the secondary metabolism of extremophiles is a promising field that, if further explored, can broaden our understanding of astrobiology and the molecular diversity produced by microorganisms in extreme environments on our planet. In the search for extraterrestrial life, identification of these molecules as biological markers in upcoming space missions could be significant, particularly if their patterns are not easily attributable to nonbiological processes. Detection of these molecules in the oceans of Enceladus could suggest the presence of microbial activity.

3.1.5 - Conclusion

In summary, the study findings broaden the range of analogous extraterrestrial environments in astrobiology, including the Al Wahbah crater in Saudi Arabia. We investigated and characterized cultivable bacteria from the crater to uncover potential biological models and biosignatures pertinent to the search for extraterrestrial life, particularly on Enceladus, an icy moon of Saturn. Specific attention was devoted to exploring the

distinctive attributes of *Halalkalibacterium halodurans* strains 3Ho3b and 4Ho3b, which led to demonstrating their ability to thrive under thermohaloalkaliphilic conditions, and provided valuable insights into the adaptations necessary for survival in extreme environments. The molecules reported by chemical profile analysis show that the MS analytical technique can be useful for identifying the components that characterize life in an astrobiological context. Furthermore, chemical profile MS analysis underscores the potential of this technique as a powerful tool for identifying life-associated components in an astrobiological context. The molecules identified through this analysis open avenues for further research, emphasizing the need for a more extensive exploration of metabolite production by extremophilic microorganisms. However, the quest to understand the production of metabolites by extremophilic microorganisms remains challenging and underinvestigated because of the scarcity of chemical annotations.

Overall, these initial insights from integrated omics data, encompassing both genomics and metabolomics, suggest bacterial strains isolated from the Al Wahbah crater in Saudi Arabia may serve as terrestrial proxies for hypothetical microbes on Enceladus. This comparison provides a foundation for identifying potential biosignatures, potentially offering biosignatures for use in the search for life beyond Earth.

CHAPTER 4 - FINAL CONSIDERATIONS

This thesis presented an in-depth analysis of the use of extremophilic microorganisms as eukaryotic models for astrobiological research, with a focus on the fungus *Rhinocladiella similis*. When subjected to simulated Martian regolith and perchlorate conditions, the fungus demonstrated remarkable metabolic and morphological adaptations, revealing survival mechanisms in environments of extreme chemical and physical stress. The production of biosignatures, such as oxylipins and indolic compounds, underscores the potential of this organism as a model in the search for extraterrestrial life. The multi-omics approach was essential in providing greater robustness to these results.

Additionally, the investigation of polyextremophilic bacteria, isolated from the Al Wahbah crater, demonstrated the adaptation of these species to conditions analogous to those found in subsurface oceans of icy celestial bodies, such as Enceladus, a moon of Saturn. These bacteria exhibited an extraordinary ability to survive in environments with high salinity, alkalinity, elevated phosphate levels, and high temperatures, offering new perspectives on the viability of life in extraterrestrial environments, placing Saudi Arabia on the astrobiological map as a location of interest for extraterrestrial analog environments.

Thus, this thesis contributes significantly to the advancement of astrobiology, providing new insights into the molecular and metabolic strategies of extremophilic organisms and their potential applications in missions exploring life on Mars and other celestial bodies. The use of genomic and metabolomic approaches has established a solid foundation for future investigations into the limits of life under extreme conditions, both on Earth and in other environments in the Solar System. Furthermore, it serves as a promising tool for creating new biosignatures as targets in the search for life beyond Earth.

REFERENCES

ABDULAZIZ HURAYSI ALBOKARI, M.; MOHAMMAD, A. A. A.-N. & IBRAHIM, M. Niche for high abundant extremophilic microbial communities in an ancient crater. *International Journal of Astrobiology*, 17(**4**): 345-355, 2018. DOI: 10.1017/S1473550417000295.

ABRAHAMSSON, V. & KANIK, I. In situ organic biosignature detection techniques for space applications. *Frontiers in Astronomy and Space Sciences*, **9**: 959670, 2022. DOI: 10.3389/fspas.2022.959670.

AISLABIE, J. M. & MCLEOD, M. P. Dominant bacteria in soils of marble point and wright valley, Victoria Land, Antarctica. *Soil Biology and Biochemistry*, 38(**10**): 3041-3056, 2006. DOI: 10.1016/j.soilbio.2006.02.018.

ALAZARD, D.; DUKAN, S.; URIOS, A. *et al.* Desulfovibrio hydrothermalis sp. nov., a novel sulfate-reducing bacterium isolated from hydrothermal Vents. *International Journal of Systematic and Evolutionary Microbiology*, 53(**1**): 173-178, 2003. DOI: 10.1099/ijs.0.02323-0.

ALTAIR, T.; AVELLAR, M. G. B.; RODRIGUES, F. *et al.* Microbial habitability of Europa sustained by radioactive sources. *Scientific Reports*, 8(**1**): 260, 2018. DOI: 10.1038/s41598-017-18470-z.

ALVES, F. L.; STEVENSON, A.; BAXTER, E. *et al.* Concomitant osmotic and chaotropicity-induced stresses in Aspergillus wentii: compatible solutes determine the biotic window. *Current Genetics*, **61**: 457-477, 2015. DOI: 10.1007/s00294-015-0496-8.

ANDREWS, S. *FastQC: a quality control tool for high throughput sequence data*, 2010. http://www.bioinformatics.babraham.ac.uk/projects/fastqc.

ANISIMOVA, M. & GASCUEL, O. Approximate likelihood-ratio test for branches: a fast, accurate, and powerful alternative. *Systematic Biology*, 55(**4**): 539-552, 2006. DOI: 10.1080/10635150600755453.

ANSARI, A. H. Detection of organic matter on Mars, results from various Mars missions, challenges, and future strategy: a review. *Frontiers in Astronomy and Space Sciences*, **10**: 1075052, 2023. DOI: 10.3389/FSPAS.2023.1075052/BIBTEX.

AOUIDA, M.; LEDUC, A.; POULIN, R. *et al.* AGP2 encodes the major permease for high affinity polyamine import in Saccharomyces cerevisiae. *Journal of Biological Chemistry*, 280(**25**): 24267-24276, 2005. DOI: 10.1074/jbc.M503071200.

AREVALO, R. J.; SELLIEZ, L.; BRIOIS, C. *et al.* An Orbitrap-based laser desorption/ablation mass spectrometer designed for spaceflight. *Rapid Communications in Mass Spectrometry*, 32(**21**): 1875-1886, 2018. DOI: 10.1002/rcm.8244.

AREVALO, R.; NI, Z. & DANELL, R. M. Mass spectrometry and planetary exploration: a brief review and future projection. *Journal of Mass Spectrometry*, 55(**1**): e4454, 2020. DOI: 10.1002/JMS.4454.

AREVALO, R.; WILLHITE, L.; BARDYN, A. *et al.* Laser desorption mass spectrometry with an Orbitrap analyser for in situ astrobiology. *Nat Astron*, **7**: 359-365, 2023. DOI: 10.1038/s41550-022-01866-x.

ARNDT, D.; GRANT, J. R.; MARCU, A. *et al.* PHASTER: a better, faster version of the PHAST phage search tool. *Nucleic Acids Research*, 44(**W1**): W16-W21, 2016. DOI: 10.1093/nar/gkw387.

ASTASHYN, A.; TVEDTE, E. S.; SWEENEY, D. *et al.* Rapid and sensitive detection of genome contamination at scale with FCS-GX. *bioRxiv : The Preprint Server for Biology*, 543519, 2023. DOI: 10.1101/2023.06.02.543519.

AZIZ, R. K.; BARTELS, D.; BEST, A. A. *et al.* The RAST server: rapid annotations using subsystems technology. *BMC Genomics*, **9**: 75, 2008. DOI: 10.1186/1471-2164-9-75.

BAKER, B. J. & BANFIELD, J. F. Microbial communities in acid mine drainage. *FEMS Microbiology Ecology*, 44(**2**): 139-152, 2003. DOI: 10.1016/S0168-6496(03)00028-X.

BAKER-AUSTIN, C. & DOPSON, M. Life in acid: pH homeostasis in acidophiles. *Trends in Microbiology*, 15(**4**): 165-171, 2007. DOI: 10.1016/j.tim.2007.02.005.

BANKEVICH, A.; NURK, S.; ANTIPOV, D. *et al.* SPAdes: a new genome assembly algorithm and its applications to single-cell sequencing. *Journal of Computational Biology : A Journal of Computational Molecular Cell Biology*, 19(**5**): 455-477, 2012. DOI: 10.1089/cmb.2012.0021.

BAPAT, N. V. & RAJAMANI, S. Distinguishing biotic vs. abiotic origins of 'bio'signatures: clues from messy prebiotic chemistry for detection of life in the universe. *Life*, 13(**3**): 766, 2023. DOI: 10.3390/LIFE13030766.

BARTON, L. E.; QUICKSALL, A. N. & MAURICE, P. A. Siderophore-mediated dissolution of hematite (α-Fe2O3): effects of nanoparticle size. *Geomicrobiology Journal*, 29(**4**): 314-322, 2012. DOI: 10.1080/01490451.2011.558566.

BEBLO-VRANESEVIC, K.; HUBER, H. & RETTBERG, P. High tolerance of Hydrogenothermus marinus to sodium perchlorate. *Frontiers in Microbiology*, 8(**JUL**): 1369, 2017. DOI: 10.3389/fmicb.2017.01369.

BEBLO-VRANESEVIC, K., BOHMEIER, M., SCHLEUMER, S., RABBOW, E., PERRAS, A. K., MOISSL-EICHINGER, C., SCHWENDNER, P., COCKELL, C. S., VANNIER, P., MARTEINSSON, V. T., MONAGHAN, E. P., RIEDO, A., EHRENFREUND, P., GARCIA-DESCALZO, L., GÓMEZ, F., MALKI, M., AMILS, R., GABOYER, F., HICKMAN-LEWIS, K., WESTALL, F., … RETTBERG, P. Impact of Simulated Martian Conditions on (Facultatively) Anaerobic Bacterial Strains from Different Mars Analogue Sites. *Current issues in molecular biology*, **38**, 103–122. 2020. https://doi.org/10.21775/cimb.038.103

BEECH, M. & COMTE, M. Life on Mars: past, present, and future. *Terraforming Mars*, 135-160, 2021. DOI: 10.1002/9781119761990.ch9.

BIJLANI, S.; PARKER, C.; SINGH, N. K. *et al.* Genomic characterization of the titan-like cell producing Naganishia tulchinskyi, the first novel eukaryote isolated from the international space station. *Journal of Fungi*, 8(**2**): 165. DOI: 10.3390/jof8020165.

BILLI, D.; FERNANDEZ, B. G.; FAGLIARONE, C. *et al.* Exploiting a perchlorate-tolerant desert cyanobacterium to support bacterial growth for in situ resource utilization on Mars. *International Journal of Astrobiology*, 20(**1**): 29-35, 2021. DOI: 10.1017/S1473550420000300.

BLIN, K.; SHAW, S.; KLOOSTERMAN, A. M. *et al.* antiSMASH 6.0: improving cluster detection and comparison capabilities. *Nucleic Acids Research*, 49(**W1**): W29-W35, 2021. DOI: 10.1093/nar/gkab335.

BLUM, M.; CHANG, H. Y.; CHUGURANSKY, S. *et al.* The InterPro protein families and domains database: 20 years on. *Nucleic Acids Research*, 49(**D1**): D344-D354, 2021. DOI: 10.1093/nar/gkaa977.

BOYER, E. W.; INGLE, M. B. & MERCER, G. D. Bacillus alcalophilus subsp. halodurans subsp. nov.: an alkaline amylase producing alkalophilic organism. *International Journal of Systematic Bacteriology*, 23(**3**): 238-242, 1973. DOI: 10.1099/00207713-23-3-238.

BROCK, T. D. & FREEZE, H. Thermus aquaticus gen. n. and sp. n., a Nonsporulating Extreme Thermophile. *Journal of Bacteriology*, 98(**1**): 289-297, 1969. DOI: 10.1128/jb.98.1.289-297.1969.

BROCKWELL, T. G.; MEECH, K. J.; PICKENS, K. *et al. The mass spectrometer for planetary exploration* (MASPEX). IEEE Aerospace Conference Proceedings. 2016.p. 1-17. DOI: 10.1109/AERO.2016.7500777.

BRODHUN, F. & FEUSSNER, I. Oxylipins in fungi. *The FEBS Journal*, 278(**7**): 1047-1063, 2011. DOI: 10.1111/j.1742-4658.2011.08027.x.

CANNON, K. M.; BRITT, D. T.; SMITH,T. M. *et al.* Mars global simulant MGS-1: a Rocknest-based open standard for basaltic martian regolith simulants. *Icarus*, **317**: 470-478, 2019. DOI: 10.1016/j.icarus.2018.08.019.

CARR, E. C.; BARTON, Q.; GRAMBO, S. *et al.* Characterization of a novel polyextremotolerant fungus, Exophiala viscosa, with insights into its melanin regulation and ecological niche. *G3*, 13(**8**): jkad110, 2023. DOI: 10.1093/g3journal/jkad110.

CARRÉ, L.; GONZALEZ, D.; GIRARD, É. *et al.* Effects of chaotropic salts on global proteome stability in halophilic archaea: Implications for life signatures on Mars. *Environmental Microbiology*, 25(**11**): 2216-2230, 2023. DOI: 10.1111/1462-2920.16451.

CASSARO, A.; PACELLI, C. & ONOFRI, S. Survival, metabolic activity, and ultrastructural damages of Antarctic black fungus in perchlorates media. *Frontiers in Microbiology*, **13**: 992077, 2022. DOI: 10.3389/FMICB.2022.992077/BIBTEX.

CHAN, M. A.; HINMAN, N. W.; POTTER-MCINTYRE, S. L. *et al.* Deciphering biosignatures in planetary contexts. *Astrobiology*, 19(**9**): 1075-1102, 2019. DOI: 10.1089/ast.2018.1903.

CHAN, P. P. & LOWE, T. M. tRNAscan-SE: Searching for tRNA genes in genomic sequences. *Methods in Molecular Biology*, **1962**: 1-14, 2019. DOI: 10.1007/978-1-4939-9173-0_1.

CHANDER, A. M.; TEIXEIRA, M. M.; SINGH, N. K. *et al.* Description and genome characterization of three novel fungal strains isolated from Mars 2020 mission-associated spacecraft assembly facility surfaces-recommendations for two new genera and one species. *Journal of Fungi*, 9(**1**): 31, 2022. DOI: 10.3390/jof9010031.

CHATTERJEE, S. Life beyond earth. In CHATTERJEE, S., *From stardust to first cells: the origin and evolution of early life* (p. 235-252). Cham: Springer International Publishing, 2023.

CHEN, F.; LY, C.; MIKELLIDES, I. *et al.* Mars 2020 mission biological return sample contamination control approach and verification. *Astrobiology*, 23(**8**): 862-879, 2023. DOI: 10.1089/ast.2022.0048.

CHOI, J.; PARK, J.; KIM, D. *et al.* Fungal secretome database: integrated platform for annotation of fungal secretomes. *BMC Genomics*, **11**: 105, 2010. DOI: 10.1186/1471-2164-11-105.

CHOU, L.; MAHAFFY, P.; TRAINER, M. *et al.* Planetary mass spectrometry for agnostic life detection in the Solar System. *Frontiers in Astronomy and Space Sciences*, **8**: 755100, 2021. DOI: 10.3389/fspas.2021.755100.

CHUN, S. C.; PARAMASIVAN, M. & CHANDRASEKARAN, M. Proline accumulation influenced by osmotic stress in arbuscular mycorrhizal symbiotic plants. *Frontiers in Microbiology*, **9**: 2525, 2018. DOI: 10.3389/fmicb.2018.02525.

CLARK, B. C.; KOLB, V. M.; STEELE, A. *et al.* Origin of life on Mars: suitability and opportunities. *Life*, 11(**6**): 539, 2021. DOI: 10.3390/life11060539.

COKER, J. A. Recent advances in understanding extremophiles. *F1000Research*, **8**: F1000, 2019. DOI: 10.12688/f1000research.20765.1.

COLEINE, C.; STAJICH, J. E. & SELBMANN, L. Fungi are key players in extreme ecosystems. *Trends in Ecology & Evolution*, 37(**6**): 517-528, 2022. DOI: 10.1016/j.tree.2022.02.002.

DACHWALD, B.; ULAMEC, S.; POSTBERG, F. *et al.* Key technologies and instrumentation for subsurface exploration of ocean worlds. *Space Science Reviews*, 216(**5**): 83, 2020. DOI: 10.1007/s11214-020-00707-5.

DEAMER, D. & DAMER, B. Can life begin on enceladus? A perspective from hydrothermal chemistry. *Astrobiology*, 17(**9**): 834-839, 2017. DOI: 10.1089/AST.2016.1610.

DELCHER, A. L.; HARMON, D.; KASIF, S. *et al.* Improved microbial gene identification with GLIMMER. *Nucleic Acids Research*, 27(**23**): 4636-4641, 1999. DOI: 10.1093/nar/27.23.4636.

DICK, S. J. Origins and development of NASA's exobiology program, 1958-1976. *Acta Astronautica*, 65(**1-2**): 1-5, 2009. DOI: 10.1016/j.actaastro.2009.01.058.

DIEHL, R. C.; GUINN, E. J.; CAPP, M. W. *et al.* Quantifying additive interactions of the osmolyte proline with individual functional groups of proteins: comparisons with urea and glycine betaine, interpretation of m-values. *Biochemistry*, 52(**35**): 5997-6010, 2013. DOI: 10.1021/bi400683y.

EMMS, D. M. & KELLY, S. OrthoFinder: solving fundamental biases in whole genome comparisons dramatically improves orthogroup inference accuracy. *Genome Biology*, **16**: 157, 2015. DOI: 10.1186/s13059-015-0721-2.

EREN, A. M.; ESEN, O. C.; QUINCE, C. *et al.* Anvi'o: an advanced analysis and visualization platform for 'omics data. *PeerJ*, **3**: e1319, 2015. DOI: 10.7717/peerj.1319.

EREN, A. M.; KIEFL, E.; SHAIBER, A. *et al.* Community-led, integrated, reproducible multi-omics with anvi'o. *Nature Microbiology*, 6(**1**): 3-6, 2021. DO: 10.1038/s41564-020-00834-3.

FILL, T. P.; PALLINI, H. F.; AMARAL, L. D. S. *et al.* Copper and manganese cations alter secondary metabolism in the fungus Penicillium brasilianum. *Journal of the Brazilian Chemical Society*, 27(**8**): 1444-1451, 2016. DOI: 10.5935/0103-5053.20160163.

FRITH, M. C. A new repeat-masking method enables specific detection of homologous sequences. *Nucleic Acids Research*, 39(**4**): e23, 2011. DOI: 10.1093/nar/gkq1212.

GALARDINI, M.; BIONDI, E. G.; BAZZICALUPO, M. *et al.* CONTIGuator: a bacterial genomes finishing tool for structural insights on draft genomes. *Source Code for Biology and Medicine*, **6**: 11, 2011. DOI: 10.1186/1751-0473-6-11.

GAO, J.; WENDEROTH, M.; DOPPLER, M. *et al.* Fungal melanin biosynthesis pathway as source for fungal toxins. *mBio*, 13(**3**): e0021922, 2022. DOI: 10.1128/mbio.00219-22.

GEVI, F.; LEO, P.; CASSARO, A. *et al.* Metabolomic profile of the fungus Cryomyces antarcticus under simulated martian and space conditions as support for life-detection missions on Mars. *Frontiers in Microbiology*, **13**: 749396, 2022. DOI: 10.3389/FMICB.2022.749396/BIBTEX.

GISIN, B. F.; TING-BEALL, H. P.; DAVIS, D. G. *et al.* Selective ion binding and membrane activity of synthetic cyclopeptides. *Biochimica et Biophysica* Acta, 509(**2**): 201-217, 1978. DOI: 10.1016/0005-2736(78)90041-X.

GLAVIN, D. P., FREISSINET, C., MILLER, K. E., EIGENBRODE, J. L., BRUNNER, A. E., BUCH, A., SUTTER, B., ARCHER JR., P. D., ATREYA, S. K., ... (). Evidence for perchlorates and the origin of chlorinated hydrocarbons detected by SAM at the Rocknest aeolian deposit in Gale Crater. Journal of Geophysical Research: Planets, 118(**10**), 1955-1973, 2013. https://doi.org/10.1002/jgre.20144

GLEIN, R. C. & WAITE, H. J. The carbonate geochemistry of Enceladus' Ocean. *Geophysical Research Letters*, 47(**3**): e2019GL085885, 2020. DOI: 10.1029/2019GL085885.

GRABHERR, M. G.; HAAS, B. J.; YASSOUR, M. *et al.* Full-length transcriptome assembly from RNA-Seq data without a reference genome. *Nature Biotechnology*, 29(**7**): 644-652, 2011. DOI: 10.1038/nbt.1883.

GUIMARÃES, L. C.; FLORCZAK-WYSPIANSKA, J.; JESUS, L. B. *et al.* Inside the pan-genome - methods and software overview. *Curr Genomics*, 16(**4**): 245-252, 2015. DOI: 10.2174/1389202916666150423002311.

GUIZELINI, D.; RAITTZ, R. T.; CRUZ, L. M. *et al.* GFinisher: a new strategy to refine and finish bacterial genome assemblies. *Scientific Reports*, **6**: 34963, 2016. DOI: 10.1038/srep34963.

GUREVICH, A.; SAVELIEV, V.; VYAHHI, N. *et al.* QUAST: quality assessment tool for genome assemblies. *Bioinformatics*, 29(**8**): 1072-1075, 2013. DOI: 10.1093/bioinformatics/btt086.

HAAS, B. J.; SALZBERG, S. L.; ZHU, W. *et al.* Automated eukaryotic gene structure annotation using EVidenceModeler and the Program to Assemble Spliced Alignments. *Genome Biology*, 9(**1**): R7, 2008. DOI: 10.1186/gb-2008-9-1-r7.

HAAS, S.; SINCLAIR, K. P. & CATLING, D. C. Biogeochemical explanations for the world's most phosphate-rich lake, an origin-of-life analog. *Commun Earth Environ*, **5**: 28, 2024. DOI: 10.1038/s43247-023-01192-8.

HECHT, M. H.; KOUNAVES, S. P.; QUINN, R. C. *et al.* Detection of perchlorate and the soluble chemistry of martian soil at the Phoenix Lander site. *Science*, 325(**5936**): 64-67, 2009. DOI: 10.1126/SCIENCE.1172466.

HEINZ, J.; DOELLINGER, J.; MAUS, D. *et al.* Perchlorate-specific proteomic stress responses of Debaryomyces hansenii could enable microbial survival in Martian brines. *Environmental Microbiology*, 24(**11**): 5051-5065, 2022. DOI: 10.1111/1462-2920.16152.

HEINZ, J.; KRAHN, T. & SCHULZE-MAKUCH, D. A new record for microbial perchlorate tolerance: fungal growth in NaClO4 brines and its implications for putative life on Mars. *Life*, 10(**5**): 53, 2020. DOI: 10.3390/LIFE10050053.

HEINZ, J.; WAAJEN, A. C.; AIRO, A. *et al.* Bacterial growth in chloride and perchlorate brines: halotolerances and salt stress responses of planococcus halocryophilus. *Astrobiology*, 19(**11**): 1377-1387, 2019. DOI: 10.1089/AST.2019.2069.

HUANG, W.; WANG, T.; PEREZ-FERNANDEZ, C. *et al.* Iron acquisition and mineral transformation by cyanobacteria living in extreme environments. *Materials Toda. Bio*, **17**: 100493, 2022. DOI: 10.1016/j.mtbio.2022.100493.

HUERTA-CEPAS, J.; SZKLARCZYK, D.; HELLER, D. *et al.* eggNOG 5.0: a hierarchical, functionally and phylogenetically annotated orthology resource based on 5090 organisms and 2502 viruses. *Nucleic Acids Research*, 47(**D1**): D309-D314, 2019. DOI: 10.1093/nar/gky1085.

HUIDOBRO, J.; ARAMENDIA, J.; ARANA, G. *et al.* Reviewing in situ analytical techniques used to research Martian geochemistry: From the Viking Project to the MMX future mission. *Analytica Chimica Acta*, **1197**: 339499, 2022. DOI: 10.1016/j.aca.2022.339499.

JAISWAL, A. K.; TIWARI, S.; JAMAL, S. B. *et al.* The pan-genome of *Treponema pallidumreveals* differences in genome plasticity between subspecies related to venereal and non-venereal syphilis. *BMC Genomics*, **21**: 33, 2020. DOI: 10.1186/s12864-019-6430-6.

JIN, L.; BI, Y.; HU, C. *et al.* A comparative study of evaluating missing value imputation methods in label-free proteomics. *Scientific Reports*, **11**: 1760, 2021. DOI: 10.1038/s41598-021-81279-4.

JOSHI, A.; THITE, S.; KARODI, P. *et al. Alkalihalobacterium elongatum* gen. nov. sp. nov.: an antibiotic-producing bacterium isolated from Lonar Lake and reclassification of the genus *Alkalihalobacillus* into seven novel genera. *Frontiers in Microbiology*, **12**: 722369-722369, 2021. DOI: 10.3389/fmicb.2021.722369.

JOSHUA, I. M. & HÖFKEN, T. Ste20 and Cla4 modulate the expression of the glycerol biosynthesis enzyme Gpd1 by a novel MAPK-independent pathway. *Biochemical and Biophysical Research Communications*, **517**: 611-616, 2019. DOI: 10.1016/j.bbrc.2019.07.072.

KALYAANAMOORTHY, S.; MINH, B. Q.; WONG, T. K. F. *et al.* ModelFinder: fast model selection for accurate phylogenetic estimates. *Nature Methods*, 14(**6**): 587-589, 2017. DOI: 10.1038/nmeth.4285.

KANIK, I. & VERA, J. P. Astrobiology of Mars, Europa, Titan and Enceladus: most likely places for alien life. *Frontiers in Astronomy and Space Sciences*, **8**: 643268, 2021. DOI: 10.3389/fspas.2021.643268.

KEJŽAR, A.; GOBEC, S.; PLEMENITAŠ, A. *et al.* Melanin is crucial for growth of the black yeast Hortaea werneckii in its natural hypersaline environment. *Fungal Biology*, 117(**5**): 368-379, 2013. DOI: 10.1016/j.funbio.2013.03.006.

KIVELSON, M. G.; KHURANA, K. K.; RUSSELL, C. T. *et al.* Galileo magnetometer measurements: a stronger case for a subsurface ocean at Europa. *Science*, 289(**5483**): 1340-1343, 2000. DOI: 10.1126/SCIENCE.289.5483.1340/SUPPL_FILE/1052879S2_THUMB.GIF.

KOGEJ, T.; STEIN, M.; VOLKMANN, M. *et al.* Osmotic adaptation of the halophilic fungus Hortaea werneckii: role of osmolytes and melanization. *Microbiology*, 153(**Pt 12**): 4261-4273, 2007. DOI: 10.1099/mic.0.2007/010751-0.

KORF, I. Gene finding in novel genomes. *BMC Bioinformatics*, 5: 59, 2004. DOI: 10.1186/1471-2105-5-59.

KOUNAVES, S. P.; CHANIOTAKIS, N. A.; CHEVRIER, V. F. *et al.* Identification of the perchlorate parent salts at the Phoenix Mars landing site and possible implications. *Icarus*, **232**: 226-231, 2014. DOI: 10.1016/J.ICARUS.2014.01.016.

KUBIK, S. Synthetic receptors based on abiotic cyclo(pseudo)peptides. *Molecules*, 27(**9**): 2821, 2022. DOI: 10.3390/molecules27092821.

KUZICHEVA, E. A. & GONTAREVA, N. B. Exobiological investigations on russian spacecrafts. *Astrobiology*, 3(**2**): 253-261, 2003. DOI: 10.1089/153110703769016352.

LEE, J.; LEE, B.; SHIN, D. *et al.* Carnitine uptake by AGP2 in yeast Saccharomyces cerevisiae is dependent on Hog1 MAP kinase pathway. *Mol Cells*, 13(**3**): 407-412, 2002. DOI: 10.1016/S1016-8478(23)15052-7.

LEE, M. D. GToTree: a user-friendly workflow for phylogenomics. *Bioinformatics*, 35(**20**): 4162-4164, 2019. DOI: 10.1093/bioinformatics/btz188.

LETUNIC, I. & BORK, P. Interactive tree of life (iTOL) v5: an online tool for phylogenetic tree display and annotation. *Nucleic Acids Research*, 49(**W1**): W293-W296, 2021. DOI: 10.1093/nar/gkab301.

LEUNG, P. M.; BAY, S. K.; MEIER, D. V. *et al.* Energetic basis of microbial growth and persistence in desert ecosystems. *mSystems*, 5(**2**): e00495-19, 2020. DOI: 10.1128/mSystems.00495-19.

LI, H. Minimap2: pairwise alignment for nucleotide sequences. *Bioinformatics*, 34(**18**): 3094-3100, 2018. DOI: 10.1093/bioinformatics/bty191.

LIU, H.; ZHANG, X.; CHEN, W. *et al.* The regulatory functions of oxylipins in fungi: A review. *Journal of Basic Microbiology*, 63(**10**): 1073-1084, 2023. DOI: 10.1002/jobm.202200721.

LIU, S.; YOUNGCHIM, S.; ZAMITH-MIRANDA, D. *et al.* Fungal melanin and the mammalian immune system. *Journal of Fungi*, 7(**4**): 264, 2021. DOI: 10.3390/jof7040264.

LOMSADZE, A. Gene identification in novel eukaryotic genomes by self-training algorithm. *Nucleic Acids Research*, **33**: 6494-6506, 2005. DOI: 10.1093/nar/gki937.

LOPEZ, J. V.; PEIXOTO, R. S. & ROSADO, A. S. Inevitable future: space colonization beyond Earth with microbes first. *FEMS Microbiology Ecology*, 95(**10**): fiz127, 2019. DOI: 10.1093/femsec/fiz127.

MARTÍNEZ, G. M. & RENNO, N. O. Water and brines on mars: Current evidence and implications for MSL. *Space Science Reviews*, 175(**1-4**): 29-51, 2013. DOI: 10.1007/S11214-012-9956-3.

MAWJI, E.; GLEDHILL, M.; WORSFOLD, P. J. *et al.* Collision-induced dissociation of three groups of hydroxamate siderophores: ferrioxamines, ferrichromes and coprogens/fusigens. *Rapid Communications in Mass Spectrometry*, 22(**14**): 2195-2202, 2008. DOI: 10.1002/rcm.3604.

MEIER-KOLTHOFF, J. P.; AUCH, A. F.; KLENK, H. P. *et al.* Genome sequence-based species delimitation with confidence intervals and improved distance functions. *BMC Bioinformatics*, **14**: 60, 2013. DOI: 10.1186/1471-2105-14-60.

MERINO, N.; ARONSON, H. S.; BOJANOVA, D. P. *et al.* Living at the extremes: extremophiles and the limits of life in a planetary context. *Frontiers in Microbiology*, 10(**MAR**): 447668, 2019. DOI: 10.3389/FMICB.2019.00780/BIBTEX.

MINH, B. Q.; NGUYEN, M. A. & VON HAESELER, A. Ultrafast approximation for phylogenetic bootstrap. *Molecular Biology and Evolution*, 30(**5**): 1188-1195, 2013. DOI: 10.1093/molbev/mst024.

MINH, B. Q.; SCHMIDT, H. A.; CHERNOMOR, O. *et al.* IQ-TREE 2: new models and efficient methods for phylogenetic inference in the genomic era. *Molecular Biology and Evolution*, 37(**5**): 1530-1534, 2020. DOI: 10.1093/molbev/msaa015.

MIRARAB, S.; NGUYEN, N.; GUO, S. *et al.* PASTA: ultra-large multiple sequence alignment for nucleotide and amino-acid sequences. journal of computational biology : a

journal of computational molecular cell biology, *Journal of Computational Biology*, 22(**5**): 377-386, 2015. DOI: 10.1089/cmb.2014.0156.

MISTRY, J.; CHUGURANSKY, S.; WILLIAMS, L. *et al.* Pfam: the protein families database in 2021. *Nucleic Acids Research*, 49(**D1**): D412-D419, 2021. DOI: 10.1093/nar/gkaa913.

MOL, M. L. Astrobiology in space: a comprehensive look at the solar system. *Life*, 13(**3**): 675, 2023. DOI: 10.3390/life13030675.

MORA, M. F.; KOK, M. G. M.; NOELL, A. *et al.* Detection of biosignatures by capillary electrophoresis mass spectrometry in the presence of salts relevant to Ocean Worlds Missions. *Astrobiology*, 22(**8**): 914-925, 2022. DOI: 10.1089/AST.2021.0091.

NADAL, M., GARCÍA-PEDRAJAS, M. D., & GOLD, S. E. Dimorphism in fungal plant pathogens. *FEMS microbiology letters*, 284(2), 127–134, 2008. https://doi.org/10.1111/j.1574-6968.2008.01173.x

NAKAMINAMI, K., OKAMOTO, M., HIGUCHI-TAKEUCHI, M., YOSHIZUMI, T., YAMAGUCHI, Y., FUKAO, Y., SHIMIZU, M., OHASHI, C., TANAKA, M., MATSUI, M., SHINOZAKI, K., SEKI, M., & HANADA, K. AtPep3 is a hormone-like peptide that plays a role in the salinity stress tolerance of plants. *Proceedings of the National Academy of Sciences of the United States of America*, 115(22), 5810–5815, 2018. https://doi.org/10.1073/pnas.1719491115

NASCIMENTO-DIAS, B. L. & MARTINEZ-FRIAS, J. Brief review about History of Astrobiology. *International Journal of Astrobiology*, 22(**1**): 67-78, 2023. DOI: 10.1017/S1473550422000386.

NEVEU, M.; ANBAR, A. D.; DAVILA, A. F. *et al.* Returning samples from enceladus for life detection. *Frontiers in Astronomy and Space Sciences*, **7**: 539960, 2020. DOI: 10.3389/FSPAS.2020.00026/BIBTEX.

NIU, M.; STEFFAN, B. N.; FISCHER, G. J. *et al.* Fungal oxylipins direct programmed developmental switches in filamentous fungi. *Nat Commun*, **11**: 5158, 2020. DOI: 10.1038/s41467-020-18999-0.

NOIRUNGSEE, N.; CHANGKHONG, S.; PHINYO, K. *et al.* Genome-scale metabolic modelling of extremophiles and its applications in astrobiological environments. *Environmental Microbiology Reports*, 16(**1**): e13231, 2024. DOI: 10.1111/1758-2229.13231.

NOSANCHUK, J. D.; STARK, R. E. & CASADEVALL, A. Fungal melanin: what do we know about structure? *Frontiers in Microbiology*, **6**: 1463, 2015. DOI: 10.3389/fmicb.2015.01463.

OMAN, T. J. & VAN DER DONK, W. A. Insights into the mode of action of the two-peptide lantibiotic haloduracin. *ACS Chemical Biology*, 4(**10**): 865-74, 2009. DOI: 10.1021/cb900194x.

ONOFRI, S., DE LA TORRE, R., DE VERA, J. P., OTT, S., ZUCCONI, L., SELBMANN, L., SCALZI, G., VENKATESWARAN, K. J., RABBOW, E., SÁNCHEZ IÑIGO, F. J., &

HORNECK, G. (). Survival of rock-colonizing organisms after 1.5 years in outer space. *Astrobiology*, 12(5), 508–516, 2012. https://doi.org/10.1089/ast.2011.0736

ONOFRI, S.; BARRECA, D.; SELBMANN, L. *et al.* Resistance of antarctic black fungi and cryptoendolithic communities to simulated space and Martian conditions. *Studies in Mycology*, **61**: 99-109, 2008. DOI: 10.3114/sim.2008.61.10.

ONOFRI, S.; PACELLI, C.; SELBMANN, L. *et al.* The amazing journey of Cryomyces antarcticus from Antarctica to space. In SECKBACH, J. & STAN-LOTTER, H. (eds.), *Extremophiles as Astrobiological Models* (p. 237-254).Wiley, 2020.

ONOFRI, S.; SELBMANN, L.; PACELLI, C. *et al.* Survival, DNA, and ultrastructural integrity of a cryptoendolithic antarctic fungus in Mars and lunar rock analogs exposed outside the International Space Station. *Astrobiology*, **19**: 170-182, 2019. DOI: 10.1089/ast.2017.1728.

OROSEI, R.; LAURO, S. E.; PETTINELLI, E. *et al.* Radar evidence of subglacial liquid water on Mars. *Science*, 361(**6401**): 490-493, 2018. DOI: 10.1126/science.aar7268.

PADAN, E.; BIBI, E.; ITO, M. *et al.* Alkaline pH homeostasis in bacteria: new insights. *Biochim Biophys Acta*, 1717(**2**): 67-88, 2005. DOI: 10.1016/j.bbamem.2005.09.010.

PALMER, J. M. & STAJICH, J. E. Funannotate v1.8.1: eukaryotic genome annotation, 2020. DOI: 10.5281/zenodo.1134477.

PARKS, D. H.; IMELFORT, M.; SKENNERTON, C. T. *et al.* CheckM: assessing the quality of microbial genomes recovered from isolates, single cells, and metagenomes. *Genome Research*, 25(**7**): 1043-1055, 2015. DOI: 10.1101/gr.186072.114.

PARSONS, J. B., & ROCK, C. O. Bacterial lipids: metabolism and membrane homeostasis. Progress in lipid research, 52(3), 249–276, 2013 https://doi.org/10.1016/j.plipres.2013.02.002

PATEL, R. K. & JAIN, M. NGS QC Toolkit: a toolkit for quality control of next generation sequencing data. *PloS One*, 7(**2**): e30619, 2012. DOI: 10.1371/journal.pone.0030619.

PATHANIA, S.; SOLANKI, P.; PUTATUNDA, C. *et al.* Adaptation to cold environment: the survival strategy of psychrophiles. In GOEL, R.; SONI, R.; SUYAL, D. C. & KHAN, M. (eds.), *Survival strategies in cold-adapted microorganisms* (p. 87-111). Wiley, 2022.

PAULINO-LIMA, I. G.; AZUA-BUSTOS, A.; VICUÑA, R. *et al.* Isolation of UVC-tolerant bacteria from the hyperarid atacama desert, Chile. *Microbial Ecology*, 65(**2**): 325-335, 2013. DOI: 10.1007/s00248-012-0121-z.

PECORARO, L.; WANG, X.; SHAH, D. *et al.* Biosynthesis pathways, transport mechanisms and biotechnological applications of fungal siderophores. *Journal of Fungi*, 8(**1**): 21, 2021. DOI: 10.3390/jof8010021.

PHADTARE, S. Recent developments in bacterial cold-shock response. *Current Issues in Molecular Biology*, 6(**2**): 125-136. PMID: 15119823.

POSTBERG, F.; KHAWAJA, N.; ABEL, B. *et al.* Macromolecular organic compounds from the depths of Enceladus. *Nature*, 558(**7711**): 564-568, 2018. DOI: 10.1038/s41586-018-0246-4.

POSTBERG, F.; SEKINE, Y.; KLENNER, F. *et al.* Detection of phosphates originating from Enceladus's ocean. *Nature*, 618(**7965**): 489-493, 2023. DOI: 10.1038/s41586-023-05987-9.

PRAKASH, P. Y., & BHARGAVA, K. A modified micro chamber agar spot slide culture technique for microscopic examination of filamentous fungi. Journal of microbiological methods, 123, 126–12, 2016. https://doi.org/10.1016/j.mimet.2016.02.015

PRICE, A.; MACEY, M. C.; PEARSON, V. K. *et al.* Oligotrophic growth of nitrate-dependent Fe2+-oxidising microorganisms under simulated early martian conditions. *Frontiers in Microbiology*, **13**: 800219, 2022. DOI: 10.3389/fmicb.2022.800219.

PULSCHEN, A. A.; ARAUJO, G. G.; CARVALHO, A. C. S. R. *et al.* Survival of extremophilic yeasts in the stratospheric environment during balloon flights and in laboratory simulations. *Applied and Environmental Microbiology*, 84(**23**): e01942-18, 2018. DOI: 10.1128/AEM.01942-18.

PULSCHEN, A. A.; RODRIGUES, F.; DUARTE, R. T. D. *et al.* UV-resistant yeasts isolated from a high-altitude volcanic area on the Atacama Desert as eukaryotic models for astrobiology. *MicrobiologyOpen*, 4(**4**): 574, 2015. DOI: 10.1002/MBO3.262.

RAMALHO, T. P.; CHOPIN, G.; SALMAN, L. *et al.* On the growth dynamics of the cyanobacterium Anabaena sp. PCC 7938 in Martian regolith. *NPJ Microgravity*, 8(**1**): 43, 2022. DOI: 10.1038/s41526-022-00240-5.

RAWLINGS, N. D.; BARRETT, A. J.; THOMAS, P. D. *et al.* The MEROPS database of proteolytic enzymes, their substrates and inhibitors in 2017 and a comparison with peptidases in the PANTHER database. *Nucleic Acids Research*, 46(**D1**): D624-D632, 2018. DOI: 10.1093/nar/gkx1134.

REH, K.; SPILKER, L.; LUNINE, J. I. *et al. Enceladus life finder: the search for life in a habitable moon*. IEEE Aerospace Conference. Big Sky, MT, USA, 2016. p. 1-8. DOI: 10.1109/AERO.2016.7500813.

REITZ, Z. L. & MEDEMA, M. H. Genome mining strategies for metallophore discovery. *Current Opinion in Biotechnology*, **77**: 102757, 2022. DOI: 10.1016/j.copbio.2022.102757.

RIBEIRO, R.; PINTO, E.; FERNANDES, C. *et al.* Marine cyclic peptides: antimicrobial activity and synthetic strategies. *Marine Drugs*, 20(**6**): 397, 2022. DOI: 10.3390/md20060397.

RICHTER, M.; ROSSELLÓ-MÓRA, R.; GLÖCKNER F. O. *et al.* SpeciesWS: a web server for prokaryotic species circumscription based on pairwise genome comparison. *Bioinformatics*, 32(**6**): 929-931, 2016. DOI: 10.1093/bioinformatics/btv681.

ROBERTSON, J. & NASH, J. H. E. MOB-suite: software tools for clustering, reconstruction and typing of plasmids from draft assemblies. *Microbial Genomics*, 4(**8**): e000206, 2018. DOI: 10.1099/MGEN.0.000206/CITE/REFWORKS.

RZYMSKI, P., PONIEDZIAŁEK, B., HIPPMANN, N., & KACZMAREK, Ł. Screening the Survival of Cyanobacteria Under Perchlorate Stress. Potential Implications for Mars In Situ Resource Utilization. *Astrobiology*, 22(**6**), 672–684, 2022https://doi.org/10.1089/ast.2021.0100

SÁ, P. H.; MIRANDA, F.; VERAS, A. *et al.* GapBlaster-A graphical gap filler for prokaryote genomes. *PLoS One*, 11(**5**): e0155327, 2016. DOI: 10.1371/journal.pone.0155327.

SANTOS, A. & RODRIGUES-FILHO, E. New Δ8,9-pregnene steroids isolated from the extremophile fungus Exophiala oligosperma. *Natural Product Research*, 35(**15**): 2598-2601, 2019. DOI: 10.1080/14786419.2019.1684277.

SANTOS, A.; RODRIGUES-FILHO, E. & HOMEM, M. G. P. Analysis of microbial lipids deposited on Mars Global Simulant (MGS-1) by geomatrix-assisted laser desorption/ionization-mass spectrometry. *International Journal of Astrobiology*, 20(**3**): 234-240, 2021. DOI: 10.1017/S1473550421000100.

SAV, H.; OZAKKAS, F.; ALTINBAS, R. *et al.* Virulence markers of opportunistic black yeast in Exophiala. *Mycoses*, 59(**6**): 343-350, 2016. DOI: 10.1111/myc.12478.

SCHAIBLE, M. J.; SZEINBAUM, N.; BOZDAG, G. O. *et al.* Chapter the Astrobiology primer 3.0. *Astrobiology*, 24(**S1**): S4-S39, 2024. DOI: 10.1089/ast.2021.0129.

SCHMID, B.; KLUMPP, J.; RAIMANN, E. *et al.* Role of cold shock proteins in growth of Listeria monocytogenes under cold and osmotic stress conditions. *Applied and Environmental Microbiology*, 75(**6**): 1621-1627, 2009. DOI: 10.1128/AEM.02154-08.

SCHULTZ, J.; MODOLON, F.; PEIXOTO, R. S. *et al.* Shedding light on the composition of extreme microbial dark matter: alternative approaches for culturing extremophiles. *Frontiers in Microbiology*, **14**: 1167718, 2023a. DOI: 10.3389/fmicb.2023.1167718.

SCHULTZ, J.; SANTOS, A.; PATEL, N. *et al.* Life on the edge: bioprospecting extremophiles for Astrobiology. *Journal of the Indian Institute of Science*, 103(**3**): 721-737, 2023b. DOI: 10.1007/S41745-023-00382-9.

SEEMANN, T. Prokka: rapid prokaryotic genome annotation. *Bioinformatics*, 30(**14**): 2068-2069, 2014. DOI: 10.1093/bioinformatics/btu153.

SEPHTON, M. A.; WAITE, J. H. & BROCKWELL, T. G. How to detect life on icy moons. *Astrobiology*, 18(**7**): 843-855, 2018. DOI: 10.1089/ast.2017.1656.

SEPPEY, M.; MANNI, M. & ZDOBNOV, E. M. BUSCO: assessing genome assembly and annotation completeness. *Methods in Molecular Biology*, **1962**: 227-245, 2019. DOI: 10.1007/978-1-4939-9173-0_14.

SEYEDMOUSAVI, S.; NETEA, M. G.; MOUTON, J. W. *et al.* Black yeasts and their filamentous relatives: principles of pathogenesis and host defense. *Clinical Microbiology Reviews*, 27(**3**): 527-542, 2014. DOI: 10.1128/CMR.00093-13.

SEYLER, L.; KUJAWINSKI, E. B.; AZUA-BUSTOS, A. *et al.* Metabolomics as an emerging tool in the search for Astrobiologically relevant biomarkers. *Astrobiology*, 20(**10**); 1251-1261, 2020. DOI: 10.1089/ast.2019.2135.

SIMÃO, F. A.; WATERHOUSE, R. M.; IOANNIDIS, P. *et al.* BUSCO: assessing genome assembly and annotation completeness with single-copy orthologs. *Bioinformatics*, 31(**19**): 3210-3212, 2015. DOI: 10.1093/bioinformatics/btv351.

SIMÕES, M. F.; CORTESÃO, M.; AZUA-BUSTOS, A. *et al.* The relevance of fungi in astrobiology research – Astromycology. *Mycosphere*, 14(**1**): 1190-1253, 2023. DOI: 10.5943/mycosphere/14/1/13.

SIMPSON, A. C.; EEDARA, V. V. R.; SINGH, N. K. *et al.* Comparative genomic analysis of Cohnella hashimotonis sp. nov. isolated from the International Space Station. *Frontiers in Microbiology*, **14**: 1166013, 2023. DOI: 10.3389/fmicb.2023.1166013.

SINGH, M.; KAUR, K.; SHARMA, A. *et al.* Genome-wide characterization of peptidyl-prolyl cis-trans isomerases in Penicillium and their regulation by salt stress in a halotolerant P. oxalicum. *Scientific Reports*, 11(**1**): 12292, 2021. DOI: 10.1038/s41598-021-91602-8.

SKINNIDER, M. A.; DEJONG, C. A.; REES, P. N.; JOHNSTON, C. W.; LI, H.; WEBSTER, A. L.; WYATT, M. A. & MAGARVEY, N. A. Genomes to natural products PRediction Informatics for Secondary Metabolomes (PRISM). *Nucleic Acids Research*, 43(**20**): 9645-9662, 2015. DOI: 10.1093/nar/gkv1012.

SLEATOR, R. D. & HILL, C. Bacterial osmoadaptation: the role of osmolytes in bacterial stress and virulence. *FEMS Microbiology Reviews*, 26(**1**): 49-71, 2002. DOI: 10.1111/J.1574-6976.2002.TB00598.X.

SOARES, S. C.; SILVA, A.; TROST, E. *et al.* The pan-genome of the animal pathogen *Corynebacterium pseudotuberculosis* reveals differences in genome plasticity between the biovar ovis and equi strains. *PLoS One*, 8(**1**): e53818, 2013. DOI: 10.1371/journal.pone.0053818.

SOLÉ-DOMÈNECH, S., JOHANSSON, B., SCHALLING, M., MALM, J., & SJÖVALL, P. Analysis of opioid and amyloid peptides using time-of-flight secondary ion mass spectrometry. *Analytical chemistry*, 82(**5**), 1964–1974, 2010. https://doi.org/10.1021/ac902712f

SOMAYAJI, A.; DHANJAL, C. R.; LINGAMSETTY, R. *et al.* An insight into the mechanisms of homeostasis in extremophiles. *Microbiol Research*, **263**:127115, 2022. DOI: 10.1016/j.micres.2022.127115.

STAJICH J, P. J. Stajichlab/AAFTF: automated assembly for the fungi. 2019. DOI: 10.5281/zenodo.1658103.

STEENWYK, J. L.; BUIDA, T. J.; LI, Y.; SHEN, X. X. *et al.* ClipKIT: a multiple sequence alignment trimming software for accurate phylogenomic inference. *PLoS Biology*, 18(**12**): e3001007, 2020. DOI: 10.1371/journal.pbio.3001007.

STEINLE, L.; KNITTEL, K.; FELBER, N. *et al.* Life on the edge: active microbial communities in the Kryos MgCl2-brine basin at very low water activity. *The ISME Journal*, 12(**6**): 1414-1426, 2018. DOI: 10.1038/s41396-018-0107-z.

SUMNER, L. W.; AMBERG, A.; BARRETT, D. *et al.* Proposed minimum reporting standards for chemical analysis Chemical Analysis Working Group (CAWG) Metabolomics Standards Initiative (MSI). *Metabolomics: Official Fournal of the Metabolomic Society*, 3(**3**): 211-221, 2007. DOI: 10.1007/s11306-007-0082-2.

TESEI, D. Black fungi research: out-of-this-world implications. *Encyclopedia 2*, 212-229, 2022. DOI: 10.3390/encyclopedia2010013.

TESTA, A. C.; HANE, J. K.; ELLWOOD, S. R. *et al.* CodingQuarry: highly accurate hidden Markov model gene prediction in fungal genomes using RNA-seq transcripts. *BMC Genomics*, 16(**1**): 170, 2015. DOI: 10.1186/s12864-015-1344-4.

THITLA, T.; KUMLA, J.; HONGSANAN, S. *et al.* Exploring diversity rock-inhabiting fungi from northern Thailand: a new genus and three new species belonged to the family Herpotrichiellaceae. *Frontiers in Cellular and Infection Microbiology*, **13**: 1252482, 2023. DOI: 10.3389/fcimb.2023.1252482.

VAGO, J. L. & WESTALL, F. Habitability on early Mars and the search for biosignatures with the ExoMars rover. *Astrobiology*, 17(**6-7**): 471-510, 2017. DOI: 10.1089/ast.2016.1533.

VAN HEEL, A. J.; JONG, A.; SONG, C. *et al.* BAGEL4: a user-friendly web server to thoroughly mine RiPPs and bacteriocins. *Nucleic Acids Research*, 46(**W1**): W278-W281, 2018. DOI: 10.1093/nar/gky383.

VICENTE-GARCIA, C. & COLOMER, I. Lipopeptides as tools in catalysis, supramolecular, materials and medicinal chemistry. *Nature Reviews Chemistry*, 7(**10**): 710-731, 2023. DOI: 10.1038/s41570-023-00532-8.

WADSWORTH, J. & COCKELL, C. S. Perchlorates on Mars enhance the bacteriocidal effects of UV light. *Scientific Reports*, 7(**1**): 4662, 2017. DOI: 10.1038/s41598-017-04910-3.

WAGNER, N. Y.; ANDERSEN, D. T.; HAHN, A. S. *et al.* Survival strategies of an anoxic microbial ecosystem in Lake Untersee, a potential analog for Enceladus. *Scientific Reports*, **12**: 7376, 2022. DOI: 10.1038/s41598-022-10876-8.

WAHAB, A. A.; MAATY, M. A. A.; STUART, F. M. *et al.* The geology and geochronology of Al Wahbah maar crater, Harrat Kishb, Saudi Arabia. *Quaternary Geochronology*, **21**: 70-76, 2014. DOI: 10.1016/j.quageo.2013.01.008.

WAITE, J. H.; GLEIN, C. R.; PERRYMAN, R. S. *et al.* Cassini finds molecular hydrogen in the Enceladus plume: evidence for hydrothermal processes. *Science*, 356(**6334**): 155-159, 2017. DOI: 10.1126/science.aai8703.

WAITE, J. H.; LEWIS, W. S.; MAGEE, B. A. *et al.* Liquid water on Enceladus from observations of ammonia and 40Ar in the plume. *Nature*, 487-490, 2009. DOI: 10.1038/nature08153.

WALKER, B. J.; ABEEL, T.; SHEA, T. *et al.* Pilon: an integrated tool for comprehensive microbial variant detection and genome assembly improvement. *PloS One*, 9(**11**): e112963, 2014. DOI: 10.1371/journal.pone.0112963.

WANG, M.; CARVER, J. J.; PHELAN, V. V. *et al.* Sharing and community curation of mass spectrometry data with Global Natural Products Social Molecular Networking. *Nature Biotechnology*, **34**: 828-837, 2016. DOI: 10.1038/nbt.3597.

WANG, Q.; CEN, Z. & ZHAO, J. The survival mechanisms of thermophiles at high temperatures: an angle of omics. *Physiology*, **30**: 97-106, 2015. DOI: 10.1152/physiol.00066.2013.

WANG, Y.; XIANG, Q.; ZHOU, Q. *et al.* Mini review: advances in 2-haloacid dehalogenases. *Frontiers in Microbiology*, **12**: 758886, 2021. DOI: 10.3389/fmicb.2021.758886.

WEBER, J. M.; MARLIN, T. C.; PRAKASH, M. *et al.* A review on hypothesized metabolic pathways on Europa and Enceladus: space-flight detection considerations. *Life*, 13(**8**): 1726, 2023.

WEISBURG, W. G.; BARNS, S. M.; PELLETIER, D. A. *et al.* 16S ribosomal DNA amplification for phylogenetic study. *Journal of Bacteriology*, 173(**2**): 697-703, 1991. DOI: 10.1128/jb.173.2.697-703.1991.

WICK, R. R.; JUDD, L. M.; GORRIE, C. L. *et al.* Unicycler: resolving bacterial genome assemblies from short and long sequencing reads. *PLOS Computational Biology*, **13**: e1005595, 2017. DOI: 10.1371/journal.pcbi.1005595.

WILHELM, M. B.; DAVILA, A. F.; EIGENBRODE, J. L. *et al.* Xeropreservation of functionalized lipid biomarkers in hyperarid soils in the Atacama Desert. *Organic Geochemistry*, **103**: 97-104, 2017. DOI: 10.1016/j.orggeochem.2016.10.015.

WILLIAMS, J. P. & HALLSWORTH, J. E. Limits of life in hostile environments: no barriers to biosphere function? *Environmental Microbiology*, **11**: 3292-3308, 2009. DOI: 10.1111/j.1462-2920.2009.02079

XU, X.; CHEN, Y.; LI, B. *et al.* Arginine methyltransferase PeRmtC regulates development and pathogenicity of penicilliumexpansum via mediating key genes in conidiation and secondary metabolism. *Journal of Fungi*, 7(**10**): 807, 2021. DOI: 10.3390/jof710080.

YADAV, A.; GUPTA, S.; ISTVAN, P. *et al.* Effects of perchlorate and other groundwater inorganic co-contaminants on aerobic RDX degradation. *Microorganisms*, 10(**3**): 663, 2022. DOI: 10.3390/microorganisms10030663.

YUZON, J. D.; SCHULTZHAUS, Z. & WANG, Z. Transcriptomic and genomic effects of gamma-radiation exposure on strains of the black yeast Exophiala dermatitidis evolved to display increased ionizing radiation resistance. *Microbiology Spectrum*, 11(**5**): e0221923, 2023. DOI: 10.1128/spectrum.02219-23.

ZOROV, D. B., JUHASZOVA, M., & SOLLOTT, S. J. Mitochondrial reactive oxygen species (ROS) and ROS-induced ROS release. Physiological reviews, 94(**3**), 909–950, 2014. https://doi.org/10.1152/physrev.00026.2013

APPENDIX A

SUPPLEMENTARY INFORMATION - 1

1.1 - RHINOCLADIELLA SIMILIS: A MODEL EUKARYOTIC ORGANISM FOR ASTROBIOLOGICAL STUDIES ON MICROBIAL INTERACTIONS WITH MARTIAN SOIL ANALOGS

TABLE S1.1 – Genomic characteristics of the analyzed strains in this study.

Species	***R. similis***	***R. similis***	***E. oligosperma***	***E. spinifera***	***E. xenobiotica***	***E. sideris***
Strain	LABIOMMI 1217	Poitiers	CBS72588	BMU00051	CBS118157	CBS121828
Locus tag	RBB50	POITI	ExoOl	ExoSp	ExoXe	ExoSi
Assembly Size	34,715,284 bp	34,259,553 bp	38,224,514 bp	32,380,025 bp	31,405,760 bp	29,505,589 bp
Largest Scaffold	2,943,420 bp	5,475,506 bp	4,470,873 bp	6,251,722 bp	5,554,269 bp	9,941,542 bp
Average Scaffold	433,941 bp	2,854,963 bp	267,304 bp	4,625,718 bp	2,093,717 bp	5,901,118 bp
Number of Scaffolds	80	12	143	7	15	5
Scaffold N50	1,238,920 bp	4,787,646 bp	3,385,568 bp	4,872,376 bp	5,039,080 bp	7,897,194 bp
GC (%)	50,98%	50,98%	50,01%	51,92%	51,52%	50,63%
Number of Genes	12.908	12.903	13.683	11.405	11.454	11.41
Number of Proteins	12.857	12.867	13.646	11.367	11.415	11.385
Number of tRNA	51	36	37	38	39	25
Unique Proteins	175	146	1.611	968	1.158	1.294
Proteins with at least 1 ortholog	12.666	12.71	11.736	10.336	10.15	9.965
Single-copy orthologs	5.974	5.974	5.974	5.974	5.974	5.974

TABLE S1.2 – Interpro/Pfam of astrobiological interest

[Data set]. Zenodo. https://doi.org/10.5281/zenodo.13947687

TABLE S1.3 – Features table of mass spectrometry data

[Data set]. Zenodo. https://doi.org/10.5281/zenodo.13947687

TABLE S1.4 – Assession number of the conserved genes used for MLSA analysis

[Data set]. Zenodo. https://doi.org/10.5281/zenodo.13947687

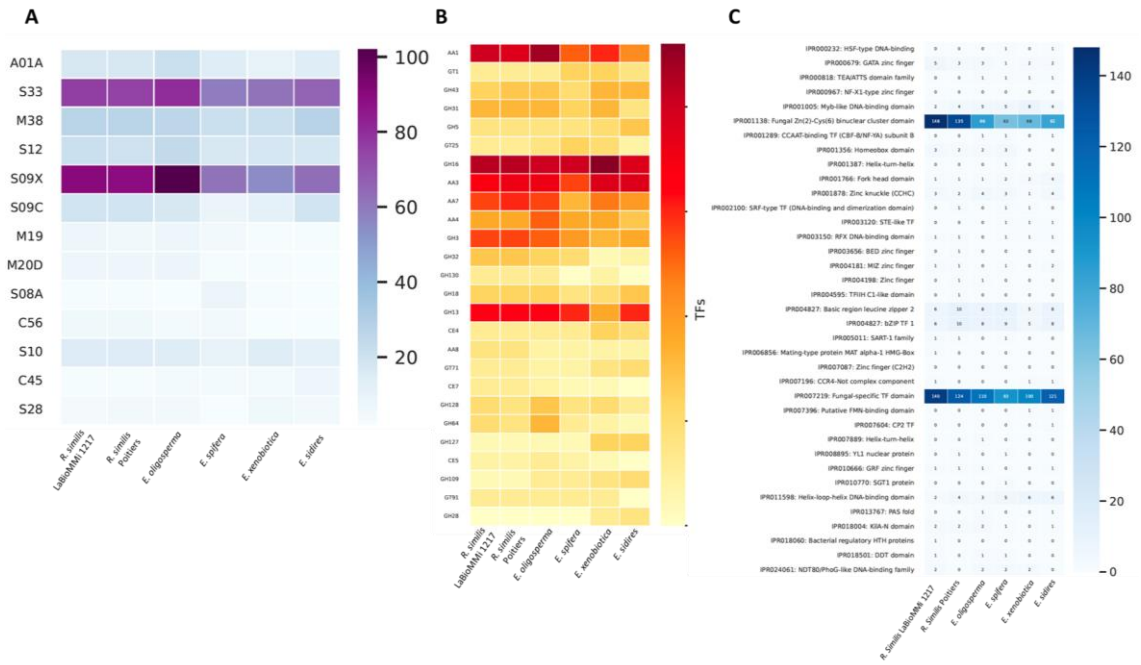

FIGURE S1.1 – Heatmaps illustrating protein families that show significant differences between species of the genera *Exophiala* and *Rhinocladiella* used in this study.

(A) Merops: Proteases involved in protein degradation processes. (B) CAZymes: Carbohydrate-active enzymes associated with the breakdown and modification of carbohydrates. (C) Transcription Factors: Proteins that regulate the transcription of specific genes.

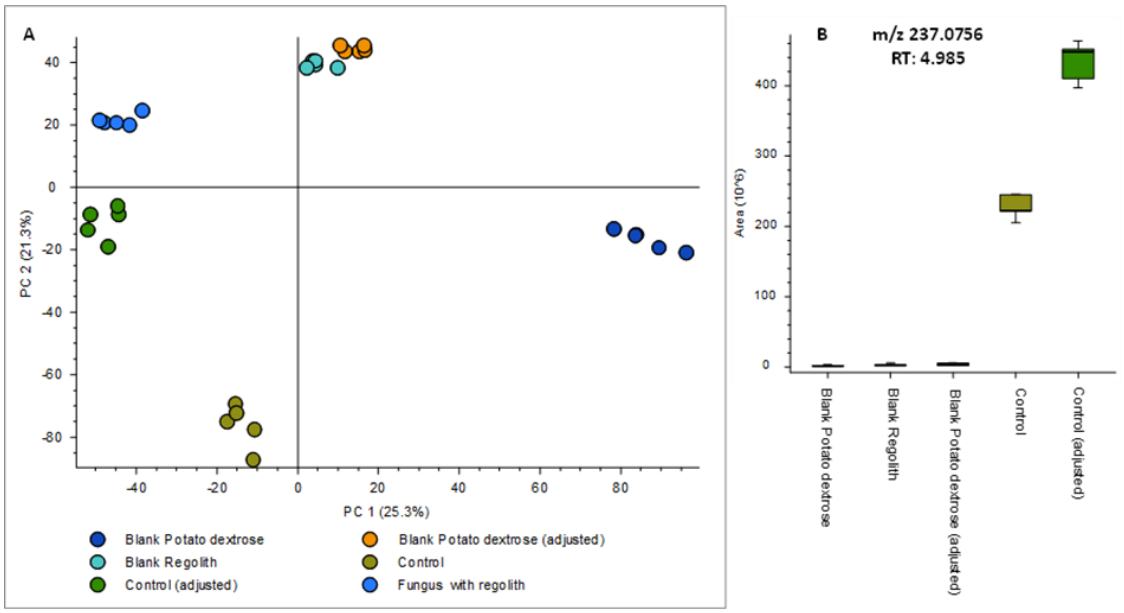

FIGURE S1.2 – (A) PCA of all groups, demonstrating the difference caused by adding regolith to the control experiment during the extraction process. (B) Illustration of the matrix effect using a Box plot for the areas of the feature with *m/z* 237.0756 RT: 4.985.

The extraction of this feature was enhanced by the use of regolith.

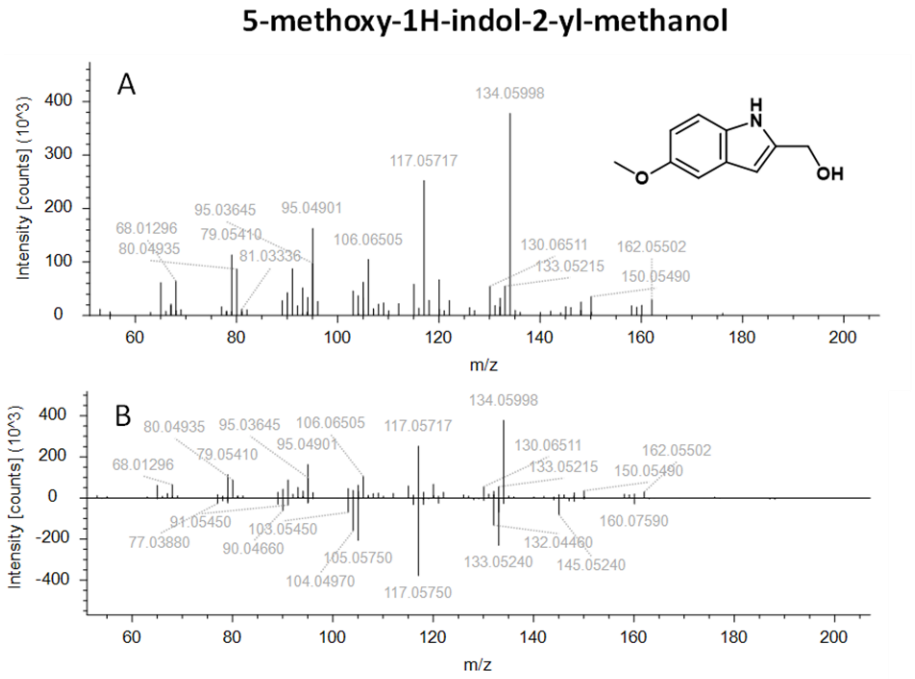

FIGURE S1.3 – (A) MS/MS spectrum of the ion with *m/z* 178.08624. (B) Spectral comparison between the obtained spectrum and the spectrum of 5-methoxy-1H-indol-2-yl-methanol deposited in the MzVault library.

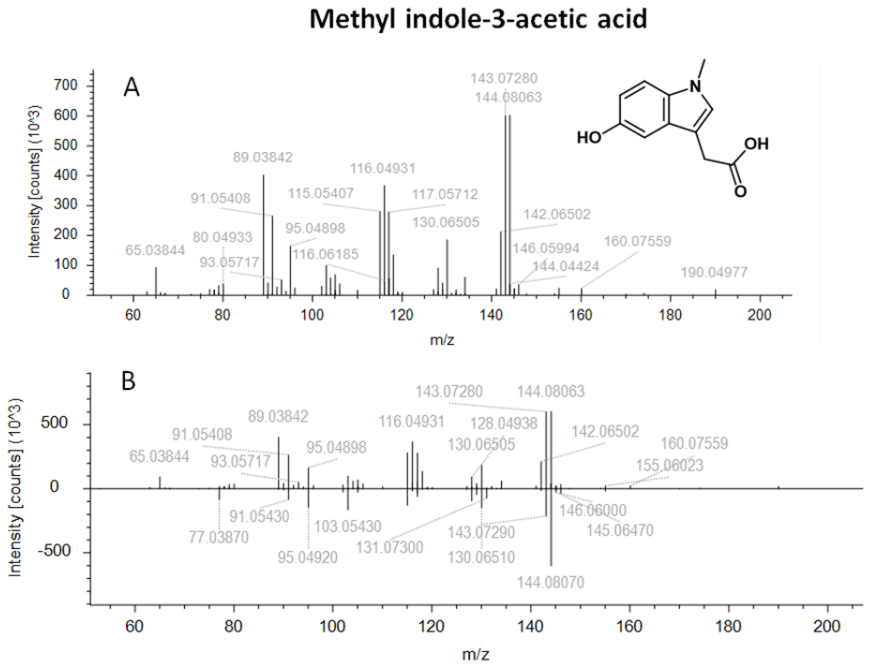

FIGURE S1.4 – (A) MS/MS spectrum of the ion with *m/z* 190.0862. (B) Spectral comparison between the obtained spectrum and the spectrum of 5-Methyl indole-3-acetic acid stored in the MzVault library.

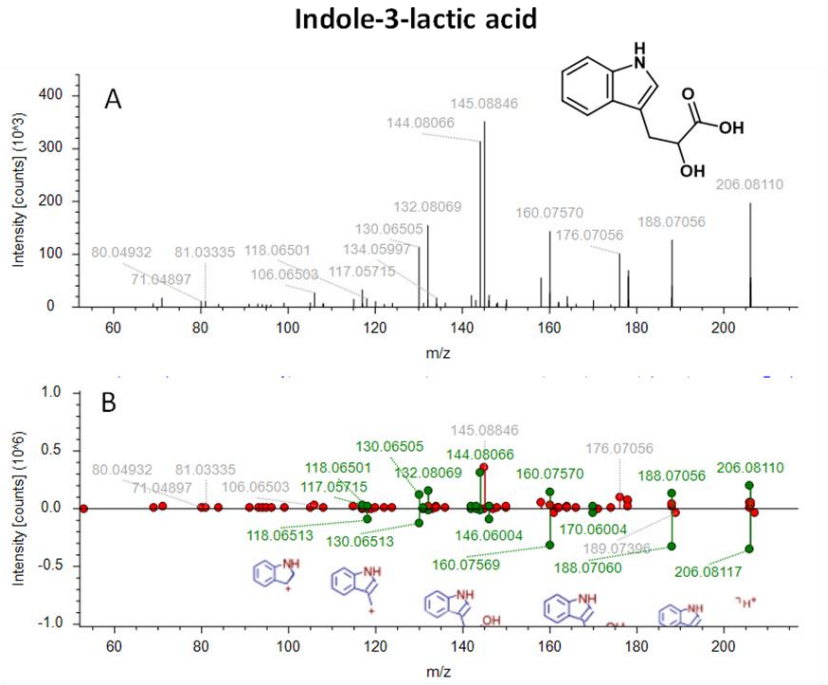

FIGURE S1.5 – (A) MS/MS spectrum of the ion with *m/z* 206.8101. (B) Spectral comparison between the obtained spectrum and the spectrum of Indole-3-lactic acid stored in the MZCloud library.

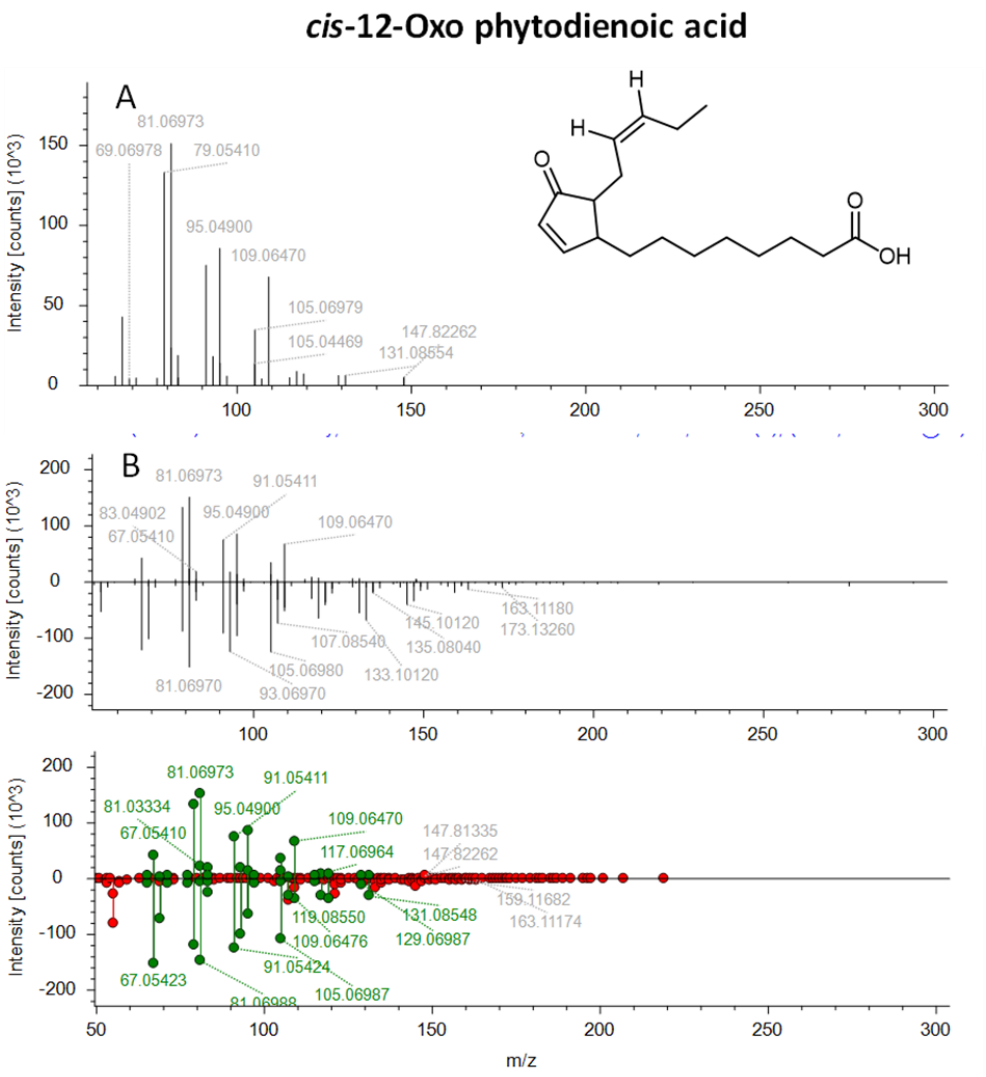

FIGURE S1.6 – (A) MS/MS spectrum of the ion with *m/z* 293.2111. (B) Spectral comparison between the obtained spectrum and the spectrum of cis-12-Oxo phytodienoic acid deposited in the MzVault and MZCloud library.

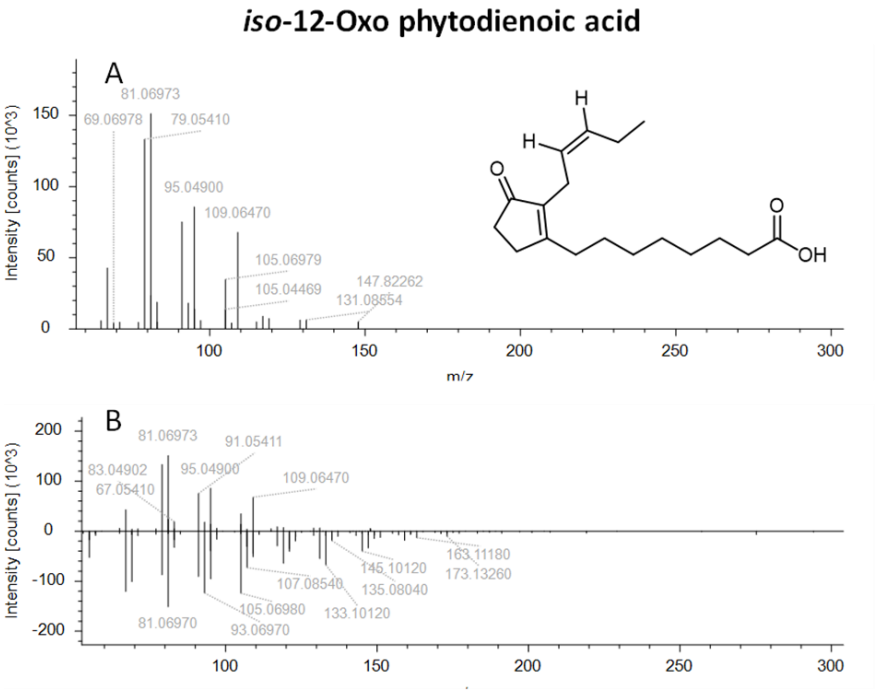

FIGURE S1.7 – (A) MS/MS spectrum of the ion with *m/z* 293.2111. (B) Spectral comparison between the obtained spectrum and the spectrum of cis-12-Oxo phytodienoic acid deposited in the MzVault.

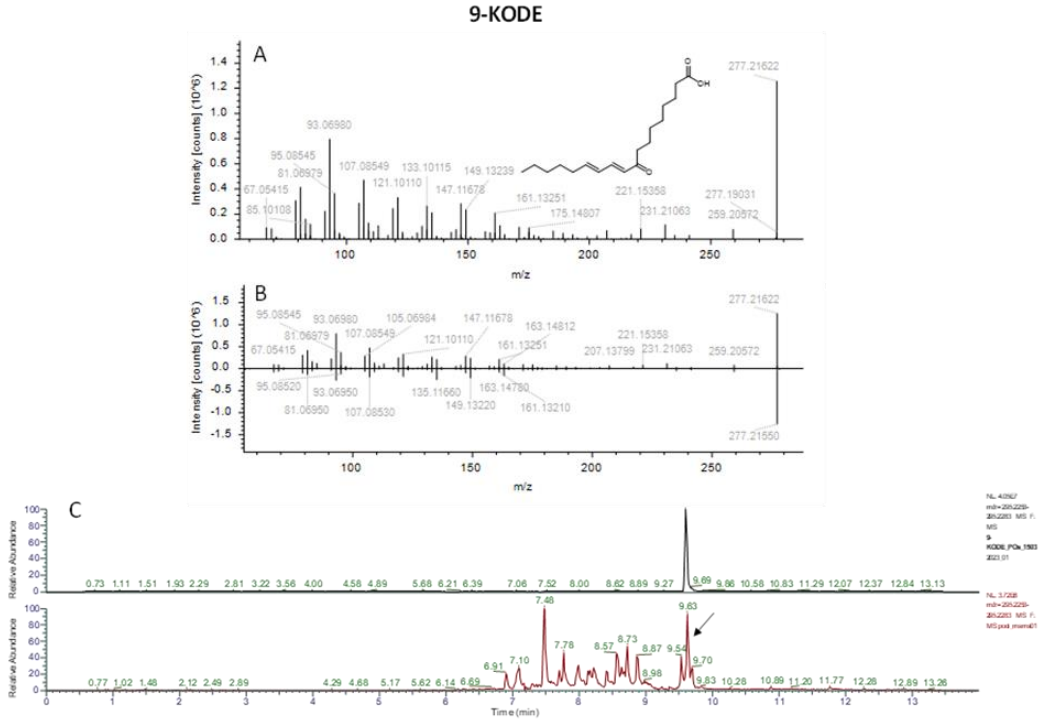

FIGURE S1.8 – (A) MS/MS spectrum of the ion with *m/z* 295.2268. (B) Spectral comparison between the obtained spectrum and the spectra of 9-KODE stored in the MzVault library. (C) Comparison of the retention time of the ion with *m/z* 295.2268 with the analytical standard of 9-KODE.

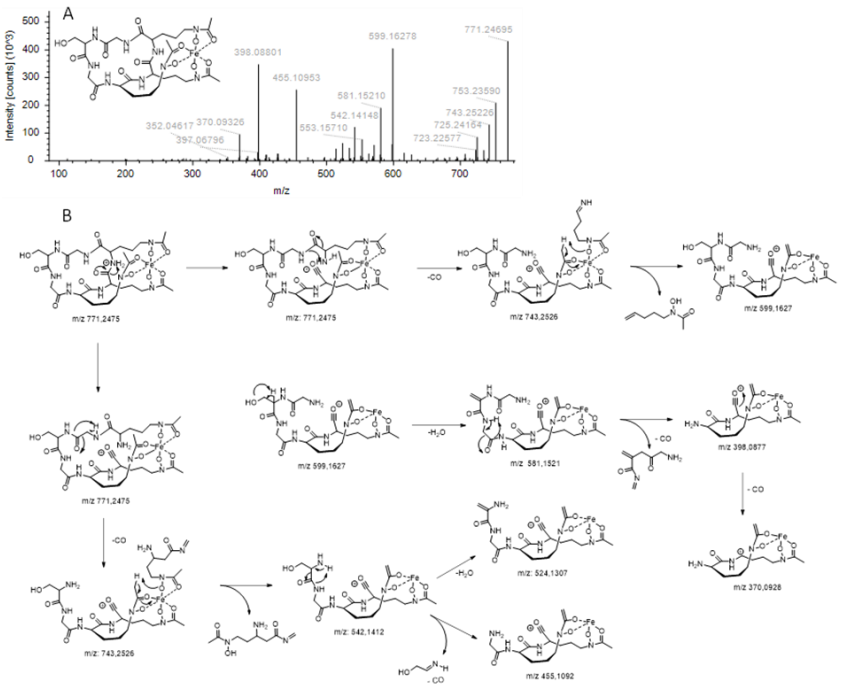

FIGURE S1.9 – (A) MS/MS spectrum of the ion with *m/z* 771.2469. (B) Proposed fragmentation pathway for the most intense ions.

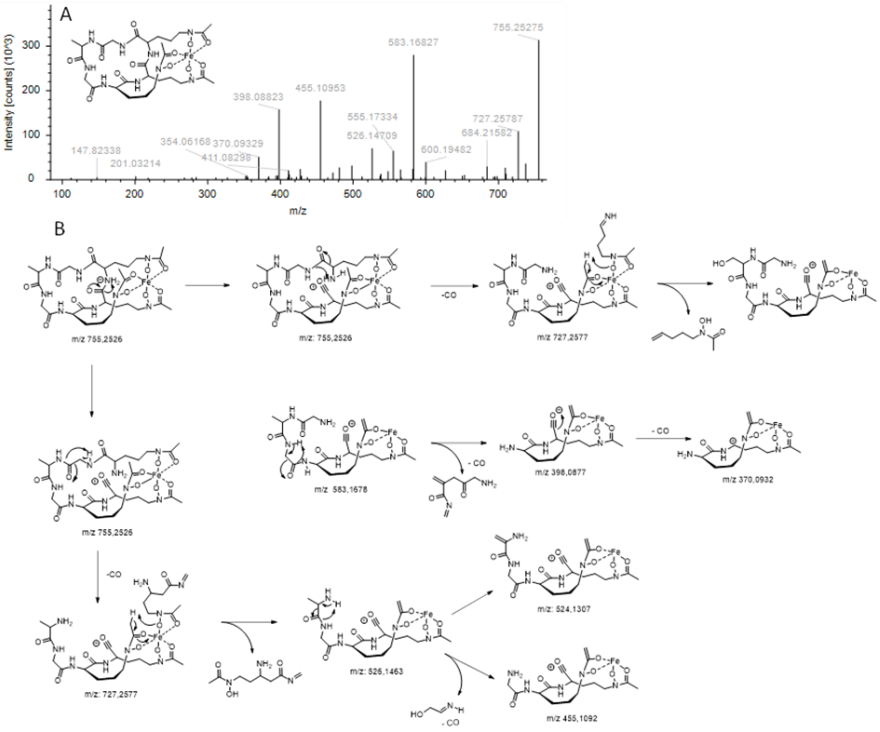

FIGURE S1.10 – (A) MS/MS spectrum of the ion with *m/z* 755.2527. (B) Proposed fragmentation pathway for the most intense ions.

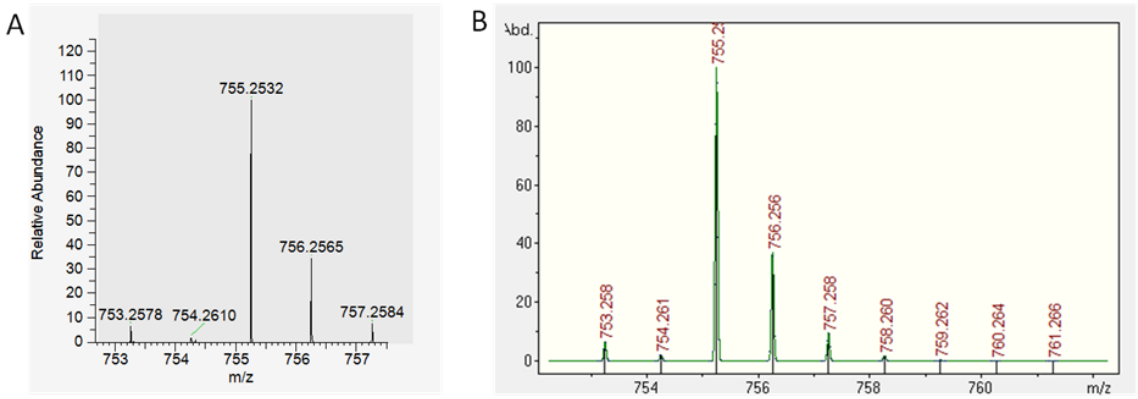

FIGURE S1.11 – (A) Full scan MS spectrum showing the isotopic pattern of the ion at *m/z* 755.2527 obtained. (B) Simulation of the isotopic pattern by the IsotopePattern Bruker software for the ion at *m/z* 755.2527.

1.2 - SURVIVING MARS: RHINOCLADIELLA SIMILIS AND LIFE IN PERCHLORATE-RICH ENVIRONMENTS

TABLE S1.5 – Table of features after statistical treatment performed in MetaboAnalyst.

[Data set]. Zenodo. https://doi.org/10.5281/zenodo.13947687

TABLE S1.6 – The table shows the annotated proteins, the up- and downregulated proteins, and the proteins from the enrichment analysis.

[Data set]. Zenodo. https://doi.org/10.5281/zenodo.13947687

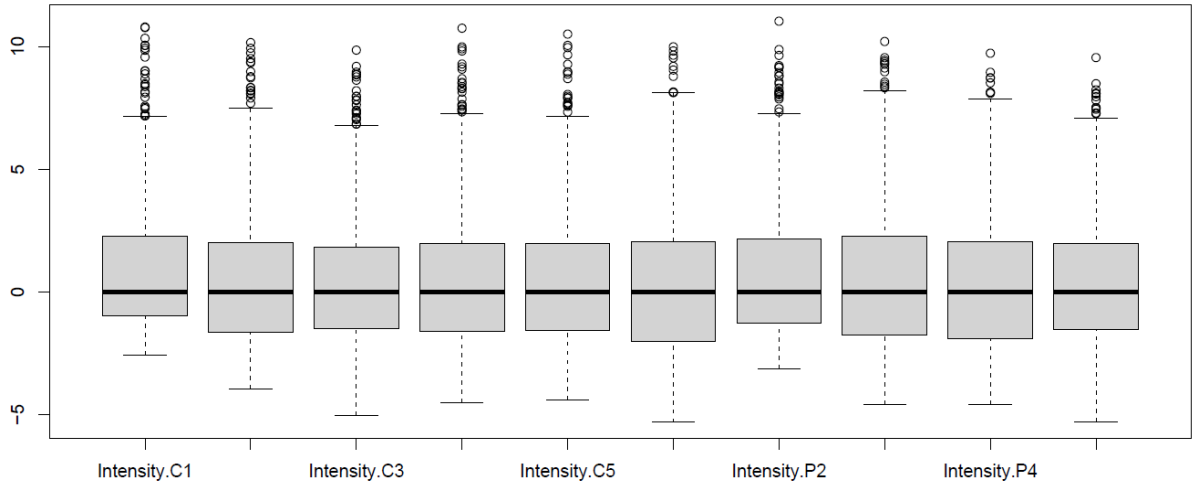

FIGURE S1.12 – Box plot of normalized proteomics data.

This graph shows the median of each biological replicate. The normalized quantification values were used to build this graph.

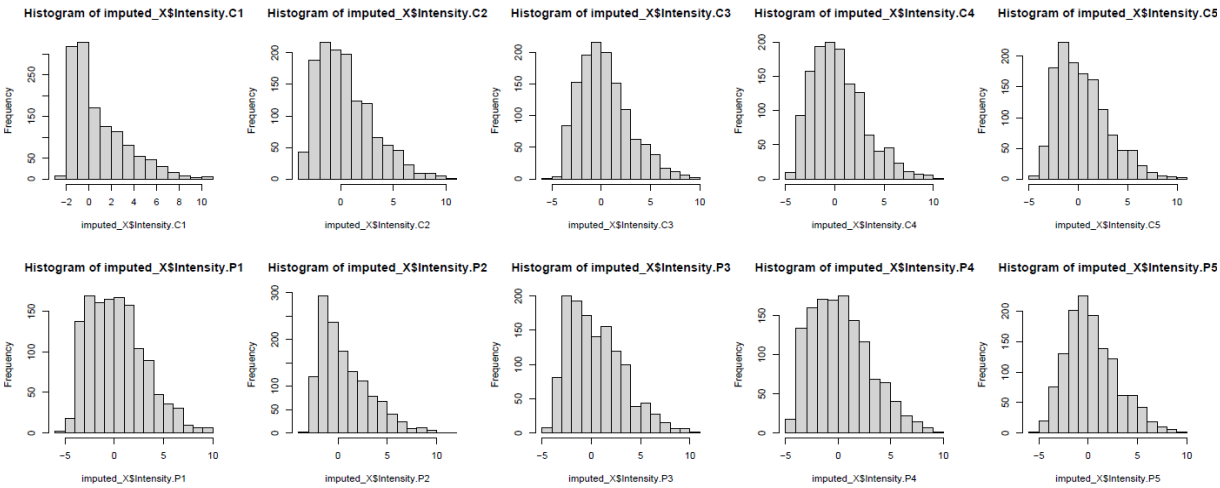

FIGURE S1.13 – Histogram of normalized proteomics data.

Each histogram represents the normal distribution of each biological replicate. The normalized quantification values were used to build this graph.

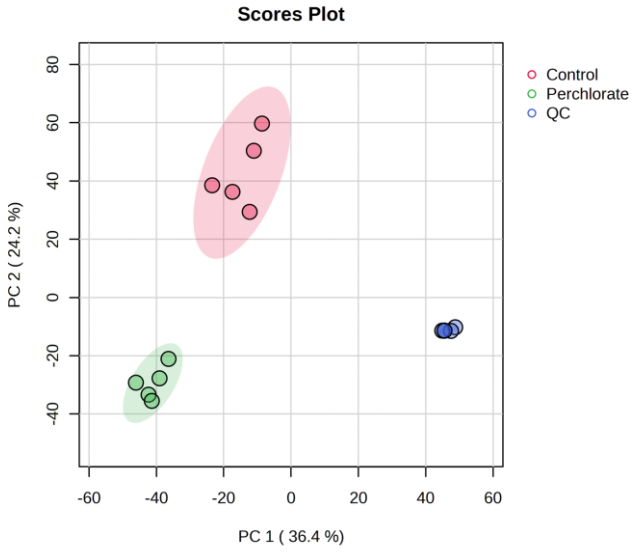

FIGURE S1.14 – Principal component analysis (PCA) showing data variance and clustering among metabolomics samples: Perchlorate (500 mM $Mg(ClO_4)_2$), Control (culture medium only), and QC (quality control, pool of all samples).

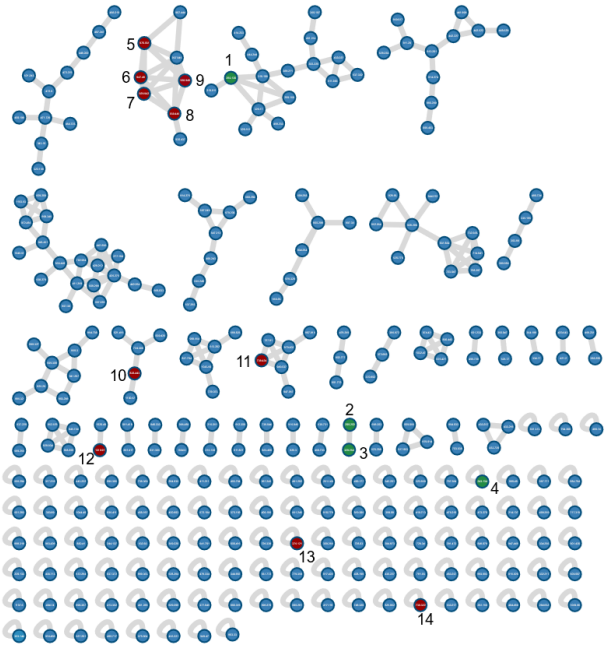

FIGURE S1.15 – The molecular network of features is upregulated in the presence of magnesium perchlorate generated by the GNPS platform.

The nodes represent the chemical identities, each characterized by its MS/MS spectrum. Connections between nodes indicate the similarity between MS/MS spectra, assessed by the cosine value. In the figure, the nodes in green are the chemical identities the platform has annotated. The nodes in red represent the features among the top 10 in terms of production increase, evaluated by the $\log_2$ (FC) value.

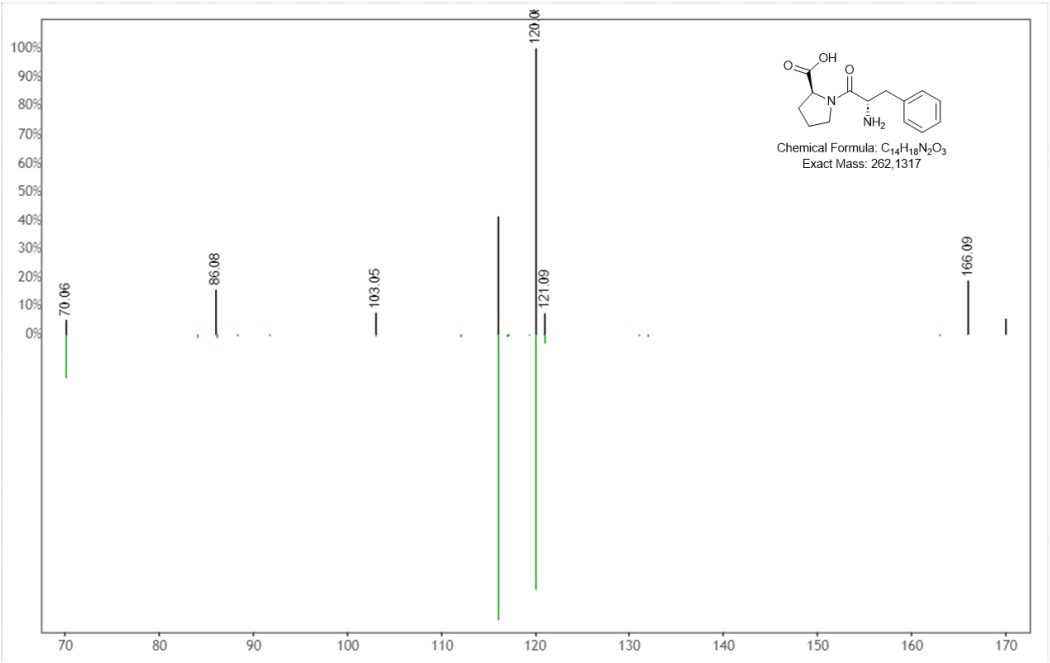

FIGURE S1.16 – MS/MS spectra comparison between the obtained spectrum and the spectrum of decanoylarginine (*m/z* 263.1382) deposited in the GNPS database.

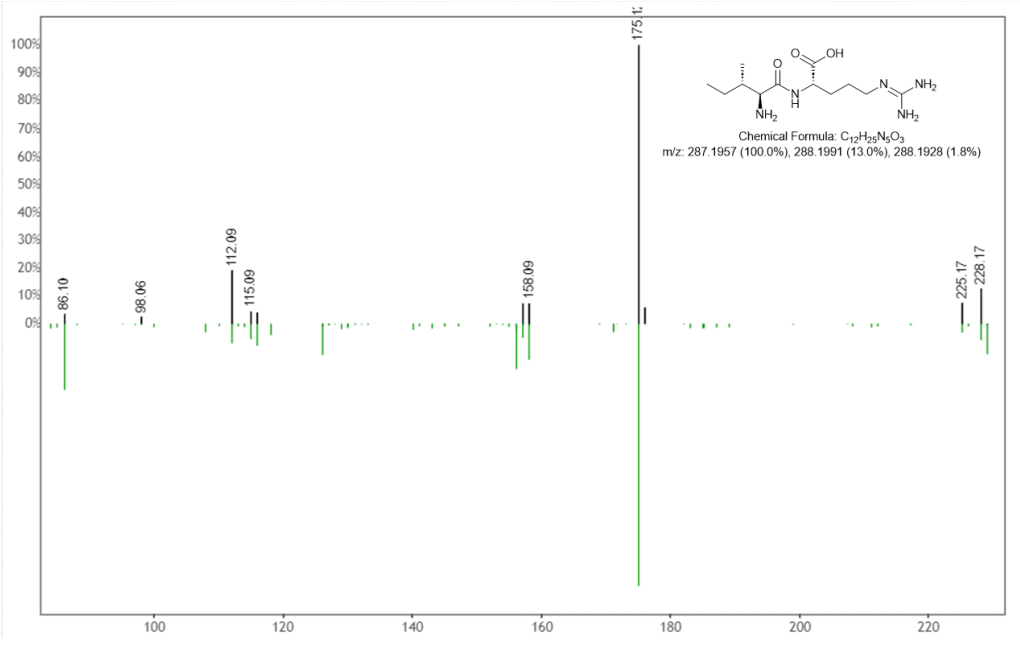

FIGURE S1.17 – MS/MS spectra comparison between the obtained spectrum and L-phenylalanyl-L-proline spectrum (*m/z* 288.2015) deposited in the GNPS database.

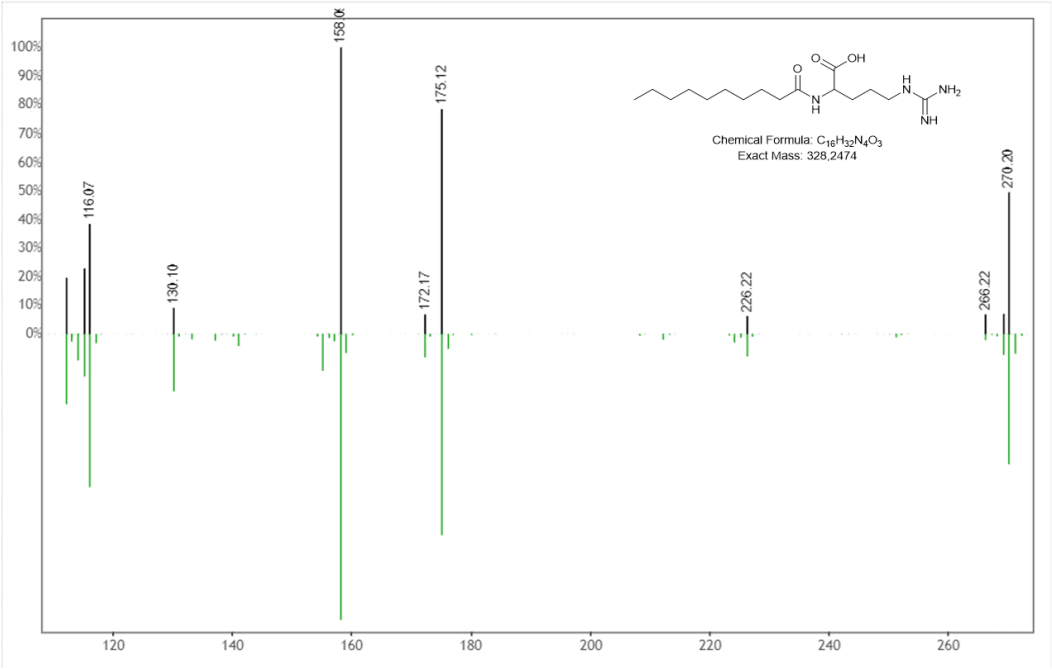

FIGURE S1.18 – MS/MS spectra comparison between the obtained spectrum and the spectrum of N,N-dimethylarginine (*m/z* 329.2535) deposited in the GNPS database.

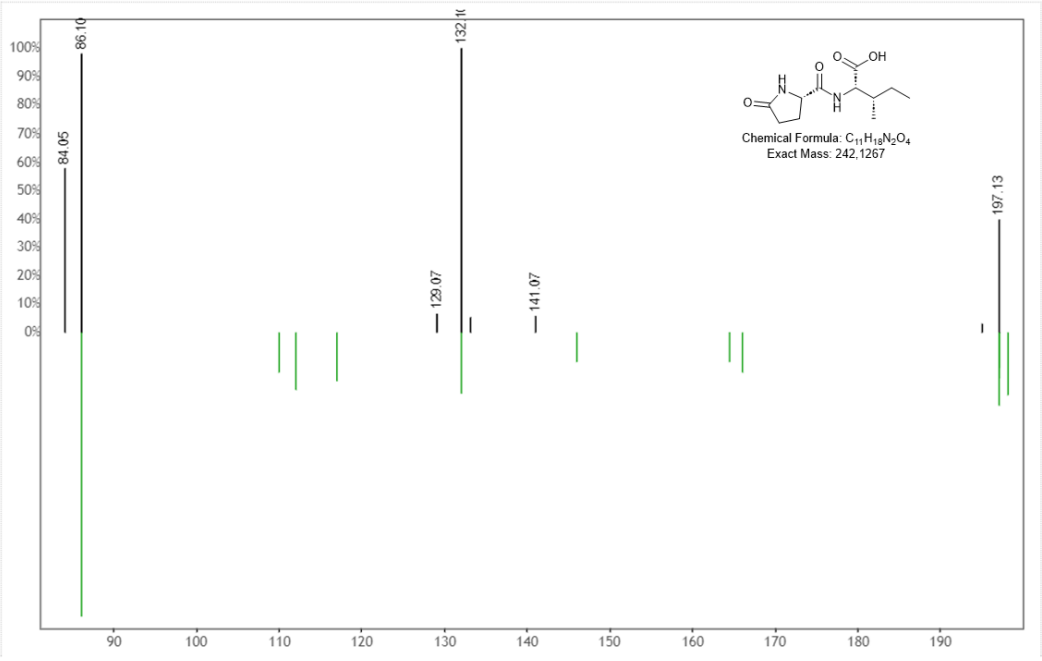

FIGURE S1.19 – MS/MS spectra comparison between the obtained spectrum and the spectrum of 5-oxopyrrolidine-2-carbonyl-L-isoleucine (*m/z* 243.13357) deposited in the GNPS database.

SUPPLEMENTARY INFORMATION - 2

2.1 - INVESTIGATING POLYEXTREMOPHILIC BACTERIA IN AL WAHBAH CRATER, SAUDI ARABIA: A TERRESTRIAL MODEL FOR LIFE ON SATURN'S MOON ENCELADUS

TABLE S2.1 – Composition of the culture media used to cultivate the bacterial isolates from the Al Wahbah crater, Saudi Arabia.

Culture media	Composition	Reference*
Modified marine agar	5-g peptone, 1-g yeast extract, 0.1-g ferric citrate, 19.450-g sodium chloride, 8.8-g Magnesium chloride, 3.240-g sodium sulfate, 1.800-g calcium chloride, 0.550-g potassium chloride, 0.160-g sodium bicarbonate, 0.080-g potassium bromide, 0.034-g strontium chloride, 0.022-g boric acid, 0.004-g sodium silicate, 0.0024-g sodium fluorate, 0.0016-g ammonium nitrate, 0.008-g disodium phosphate, 10-g sodium carbonate, 15-g Agar, 1000-mL distilled water	Zobell C. E. (1941). Studies on marine bacteria. I the cultural requirements of heterotrophic aerobes. *J. Mar. Res.* 4 (01-06), 41–75
Horikoshi alkaline	Glucose: 10 g, Yeast extract: 5 g, Peptone: 5g Dipotassium hydrogen phosphate: 1 g, Magnesium sulfate: 0.2 g, Sodium carbonate: 10 g, Distilled water: 1000 mL, Agar: 15 g	Horikoshi K. Alkaliphiles: some applications of their products for biotechnology. Microbiol Mol Biol Rev. 1999 Dec;63(4):735-50, table of contents. doi: 10.1128/MMBR.63.4.735-750.1999.
Bushnell–Hass agar	Calcium chloride dihydrate: 0.02 g, Magnesium sulfate heptahydrate: 0.2 g, Dipotassium hydrogen phosphate: 1 g, Potassium dihydrogen phosphate: 1 g, Ammonium nitrate: 1 g, Ferric chloride dihydrate: 0.05 g, Agar: 15 g, Distilled water: 1000 mL	L.D. Bushnell, H.F. Haas The utilization of certain hydrocarbons by microorganisms J. Bacteriol., 41 (1941), pp. 653-673
Halophilic medium	Magnesium chloride hexahydrate: 20 g, Potassium sulfate: 5 g, Calcium chloride dihydrate: 0.1 g, Yeast extract: 0.1 g, Ammonium chloride: 0.5 g, Potassium dihydrogen phosphate: 0.05 g, Sucrose: 0.5 g, Sodium chloride: 180 g, 4-(2-Hydroxyethyl)piperazine-1-ethanesulfonic acid (HEPES): 6 g, Agar: 15 g, Distilled water: 1000 mL	https://www.dsmz.de/microorganisms/medium/pdf/DSMZ_Medium1125.pdf

TABLE S2.2 – Genomes that were used for comparison in the present study.

Genomes	NCBI Ref Seq Assembly Accession	Status
Alkalihalobacillus alcalophilus	GCF_004802515.1	Scaffold
Alkalihalobacillus bogoriensis	GCF_000621445.1	Scaffold
Alkalihalobacillus clausii	GCA_002272085.1	Contig
Alkalihalobacillus hemicellulosilyticus	GCA_000513115.1	Contig
Alkalihalobacillus lehensis	GCA_004375095.1	Scaffold
Alkalihalobacillus lonarensis	GCA_900096965.1	Scaffold
Alkalihalobacillus okhensis	GCA_000787375.1	Contig
Alkalihalobacillus oshimensis	GCF_002019765.1	Scaffold
Alkalihalobacillus patagoniensis	GCF_002019705.1	Scaffold
Alkalihalobacillus rhizosphaerae	GCF_900142675.1	Scaffold
Alkalihalobacillus shacheensis	GCF_001484965.1	Scaffold
Alkalihalobacillus trypoxylicola	GCA_001592025.1	Contig
Alkalihalobacterium alkalinitrilicum	GCF_002019605.1	Scaffold
Alkalihalophilus marmarensis	GCA_000474275.2	Contig
Alkalihalophilus pseudofirmus	GCF_029094545.1	Complete
Bacillus cereus	GCA_900177005.1	Scaffold
Bacillus subtilis	GCA_000009045.1	Complete
Cytobacillus firmus	GCA_900445365.1	Contig
Halalkalibacter akibai	GCF_000513135.1	Contig
Halalkalibacter krulwichiae	GCF_001591945.1	Contig
Halalkalibacter wakoensis	GCF_000513095.1	Contig
Halalkalibacterium halodurans	GCF_005671335.1	Complete
Halalkalibacterium ligniniphilum	GCF_000334155.1	Contig
Mesobacillus jeotgali	GCF_002874535.1	Chromosome
Neobacillus niacini	GCF_001591505.1	Contig
Peribacillus simplex	GCF_002243645.1	Complete
Shouchella plakortidis	GCF_001420645.1	Scaffold
Streptococcus agalactiae ATCC13813	GCA_000186445.1	Scaffold

Streptococcus gordonii ATCC10558	GCF_001469295.1	Scaffold

TABLE S2.3 – List of Al Wahbah crater bacterial strains cultured via different culturing strategies and their molecular identification based on their 16S rRNA gene.

Number	Strain code	Sampling source	Isolation method	Incubation temp.	Culture medium	Species (NCBI taxonomy)	Total Score	Identity	Accession number
1	1Ho3a	Clay	Sprinkling	35°C	Horikoshi Alkaline Agar	*Alkalihalobacillus bogoriensis*	2392	97.38%	OR888779
2	3Ho3a	Clay	Sprinkling	35°C	Horikoshi Alkaline Agar	*Alkalihalobacillus bogoriensis*	2412	97.66%	OR888791
3	4Ho3a	Clay	Sprinkling	35°C	Horikoshi Alkaline Agar	*Sutcliffiella cohnii*	2597	99.65%	OR888796
4	5Ho3a	Clay	Sprinkling	35°C	Horikoshi Alkaline Agar	*Evansella cellulosilytica*	2499	98.72%	OR888800
5	7Ho3a	Clay	Sprinkling	35°C	Horikoshi Alkaline Agar	*Alkalihalophilus pseudofirmus*	2588	99.72%	OR888808
6	8Ho3a	Clay	Sprinkling	35°C	Horikoshi Alkaline Agar	*Sutcliffiella cohnii*	2508	98.39%	OR888810

7	9Ho3a	Clay	Sprinkling	35°C	Horikoshi Alkaline Agar	*Sutcliffiella cohnii*	2477	98.10%	OR888811
8	10Ho3a	Clay	Sprinkling	35°C	Horikoshi Alkaline Agar	*Salipaludibacillus agaradhaerens*	2590	99.10%	OR888765
9	11Ho3a	Clay	Sprinkling	35°C	Horikoshi Alkaline Agar	*Evansella cellulosilytica*	2344	96.36%	OR888767
10	12Ho3a	Clay	Sprinkling	35°C	Horikoshi Alkaline Agar	*Evansella cellulosilytica*	2311	96.06%	OR888769
11	17Ho3a	Clay	Sprinkling	35°C	Horikoshi Alkaline Agar	*Evansella cellulosilytica*	2459	97.83%	OR888774
12	19Ho3a	Clay	Sprinkling	35°C	Horikoshi Alkaline Agar	*Evansella clarkii*	2588	99.17%	OR888776
13	1Ho2a	Salt Crust	Sprinkling	35°C	Horikoshi Alkaline Agar	*Evansella cellulosilytica*	2459	97.76%	OR888778

14	3Ho2a	Salt Crust	Sprinkling	35°C	Horikoshi Alkaline Agar	*Alkalihalobacillus krulwichiae*	2351	97.40%	OR888790
15	4Ho2a	Salt Crust	Sprinkling	35°C	Horikoshi Alkaline Agar	*Evansella cellulosilytica*	2449	98.56%	OR888795
16	6Ho2a	Salt Crust	Sprinkling	35°C	Horikoshi Alkaline Agar	*Evansella cellulosilytica*	2501	98.32%	OR888804
17	7Ho2a	Salt Crust	Sprinkling	35°C	Horikoshi Alkaline Agar	*Evansella cellulosilytica*	2442	97.81%	OR888807
18	8Ho2a	Salt Crust	Sprinkling	35°C	Horikoshi Alkaline Agar	*Alkalihalobacillus krulwichiae*	2331	97.24%	OR888809
19	10Ho2a	Salt Crust	Sprinkling	35°C	Horikoshi Alkaline Agar	*Alkalihalobacillus wakoensis*	2233	98.65%	OR888764
20	11Ho2a	Salt Crust	Sprinkling	35°C	Horikoshi Alkaline Agar	*Sutcliffiella cohnii*	2549	99.29%	OR888766

21	12Ho2a	Salt Crust	Sprinkling	35°C	Horikoshi Alkaline Agar	*Evansella cellulosilytica*	2462	98.09%	OR888768
22	14Ho2a	Salt Crust	Sprinkling	35°C	Horikoshi Alkaline Agar	*Alkalihalobacillus akibai*	2545	99.36%	OR888770
23	15Ho2a	Salt Crust	Sprinkling	35°C	Horikoshi Alkaline Agar	*Evansella cellulosilytica*	2459	97.89%	OR888771
24	16Ho2a	Salt Crust	Sprinkling	35°C	Horikoshi Alkaline Agar	*Evansella cellulosilytica*	2440	98.41%	OR888772
25	17Ho2a	Salt Crust	Sprinkling	35°C	Horikoshi Alkaline Agar	*Alkalihalobacillus okhensis*	2518	98.53%	OR888773
26	18Ho2a	Salt Crust	Sprinkling	35°C	Horikoshi Alkaline Agar	*Evansella cellulosilytica*	2161	97.92%	OR888775
27	20Ho2a	Salt Crust	Sprinkling	35°C	Horikoshi Alkaline Agar	*Evansella clarkii*	2521	98.47%	OR888781

28	21Ho2a	Salt Crust	Sprinkling	35°C	Horikoshi Alkaline Agar	*Alkalihalobacillus akibai*	2388	97.49%	OR888782
29	2Ho1a	Soil	Sprinkling	35°C	Horikoshi Alkaline Agar	*Halalkalibacterium halodurans*	2590	99.51%	OR888784
30	3Ho1a	Soil	Sprinkling	35°C	Horikoshi Alkaline Agar	*Halalkalibacterium halodurans*	2494	98.58%	OR888789
31	6Ho1a	Soil	Sprinkling	35°C	Horikoshi Alkaline Agar	*Halalkalibacterium halodurans*	2590	99.86%	OR888803
32	1Ho3b	Clay	Sprinkling	55°C	Horikoshi Alkaline Agar	*Halalkalibacterium halodurans*	2591	99.65%	OR888780
33	2Ho3b	Clay	Sprinkling	55°C	Horikoshi Alkaline Agar	*Alkalihalophilus pseudofirmus*	2588	99.79%	OR888785
34	**3Ho3b**	**Clay**	**Sprinkling**	**55°C**	**Horikoshi Alkaline Agar**	***Anaerobacillus alkalidiazotrophicus***	**2351**	**97.07%**	**OR888792**

35	**4Ho3b**	**Clay**	**Sprinkling**	**55°C**	**Horikoshi Alkaline Agar**	***Anaerobacillus alkalidiazotrophicus***	**2311**	**96.64%**	**OR888797**
36	5Ho3b	Clay	Sprinkling	55°C	Horikoshi Alkaline Agar	*Amphibacillus sediminis*	2604	99.37%	OR888801
37	3EHo3a	Clay	Sprinkling	35°C	Horikoshi Alkaline Agar	*Amphibacillus sediminis*	2447	99.77%	OR888788
38	4EHo3a	Clay	Sprinkling	35°C	Horikoshi Alkaline Agar	*Halalkalibacterium halodurans*	2601	99.72%	OR888794
39	5EHo3a	Clay	Sprinkling	35°C	Horikoshi Alkaline Agar	*Amphibacillus sediminis*	2606	99.37%	OR888799
40	6EHo3a	Clay	Sprinkling	35°C	Horikoshi Alkaline Agar	*Sutcliffiella cohnii*	2484	98.51%	OR888802
41	7EHo3a	Clay	Sprinkling	35°C	Horikoshi Alkaline Agar	*Evansella caseinilytica*	2608	99.79%	OR888806

42	5EHo2a	Salt Crust	Sprinkling	35°C	Horikoshi Alkaline Agar	*Evansella cellulosilytica*	2466	97.77%	OR888798
43	7EHo2a	Salt Crust	Sprinkling	35°C	Horikoshi Alkaline Agar	*Bacillus haynesii*	2368	100.00%	OR888805
44	2BHA3a	Clay	Sprinkling	35°C	Bushnell Haas Agar	*Mesobacillus campisalis*	2514	98.73%	OR888783
45	3BHA3a	Clay	Sprinkling	35°C	Bushnell Haas Agar	*Evansella cellulosilytica*	2359	96.56%	OR888787
46	1BHA1a	Clay	Sprinkling	35°C	Bushnell Haas Agar	*Evansella cellulosilytica*	2237	95.14%	OR888777
47	2MA10_10_2a	Salt Crust	Sprinkling	35°C	Marine Agar, 10% NaCl and pH 10 (10 g of NaCO2)	*Kocuria salina*	2462	98.50%	OR888786
48	3MA10_10_2a	Salt Crust	Sprinkling	35°C	Marine Agar, 10% NaCl and pH 10 (10 g of NaCO2)	*Pseudomonas argentinensis*	2551	99.86%	OR888793

Strains in bold were selected for whole-genome sequencing.

TABLE S2.4 – Whole-genome, ANI, and dDDH values between strains 3Ho3b and 4Ho3b and the nearest neighbor, *Halalkalibacterium halodurans*.

Strain	**Closest species**	**WGS accession**	**ANI (%)**	**dDDH (%)**
3Ho3b	*Halalkalibacterium halodurans*	GCF_000011145.1	99	94.5
4Ho3b	*Halalkalibacterium halodurans*	GCF_000011145.1	99	94.5

TABLE S2.5 – The pangenome calculation and species used for the calculation.

[Pangenome_Calculation.xlsx]

TABLE S2.6 – Mined genes for astrobiology from annotated metabolisms of the Al Wahbah strains using clusters of orthologous genes (COG) annotation output.

Function	Category	Gene	3Ho3b strain	4Ho3b strain
Resistance to Ionizing Radiation	DNA Repair System	recA	1	1
	DNA Repair System	recX	1	1
	DNA Repair System	polA	1	1
	DNA Repair System	polB	1	1
	DNA Repair System	polC	1	1
	DNA Repair System	ligA	0	0
	DNA Repair System	ligB	0	0
	DNA Repair System	ligC	0	0
	DNA Repair System	uvrA	2	2
	DNA Repair System	uvrB	1	1
	DNA Repair System	uvrC	1	1
	DNA Repair System	MutL	1	1
	DNA Repair System	MutS	3	3
	Protection Against Free Radicals	katA	0	0
	Protection Against Free Radicals	katB	0	0
	Protection Against Free Radicals	katC	0	0
	Stress Response Systems	sodA	2	2
	Stress Response Systems	sodB	0	0
	Stress Response Systems	sodC	0	0
	Signaling and Regulation Systems	lexA	1	2
	Protection and Maintenance Genes	dps	4	4
Tolerance to Alkaline pH	Proton ATPase Genes	atpA	1	1
	Proton ATPase Genes	atpB	1	1
	Proton ATPase Genes	atpC	1	1

	Proton ATPase Genes	atpD	1	1
	Proton ATPase Genes	atpG	1	1
	Proton ATPase Genes	atpH	1	1
	Cation Transport Systems	NhaC	3	3
	Cation Transport Systems	kdpFABC	0	0
	Outer Membrane Modification	phoE	4	4
	Amino Acid Decarboxylations	adiA	0	0
	Amino Acid Decarboxylations	adiC	0	0
	Proton Transport and pH Regulation	cadA	0	0
	Proton Transport and pH Regulation	cadB	0	0
	Bacillus-specific Alkaline Genes	alsSD	0	0
	Bacillus-specific Alkaline Genes	yhaTU	0	0
	Other Response Systems	csiD	0	0
	Membrane Adaptations	DesA	0	0
	Membrane Adaptations	DesB	0	0
Resistance to High Pressures	Protein Adaptations	dnaK	1	1
	Protein Adaptations	groEL	1	1
	Protein Chaperones	dnaK	1	1
	Protein Chaperones	dnaJ	1	1
	Protein Chaperones	grpE	1	1
Resistance to High Temperatures	Protein Chaperones	groEL	1	1
	Protein Chaperones	groES	1	1
	Protein Chaperones	hsp20	2	2
	Protein Chaperones	htpX	1	1
	DNA Repair Systems	recA	1	1

	DNA Repair Systems	uvrA	2	2
	DNA Repair Systems	uvrB	1	1
	DNA Repair Systems	uvrC	1	1
	Protection Against Free Radicals	sodA	2	2
	Protection Against Free Radicals	katG	1	1
	Heat Response Genes	rpoH	0	0
	RNA Stabilizing Proteins	ClpP	5	5
	RNA Stabilizing Proteins	ClpE	0	0
	RNA Stabilizing Proteins	GroS	0	0
	RNA Stabilizing Proteins	GroL	0	0
	Heat-inducible Transcriptional Repressor	hrcA	1	1
	Hyperthermophilic Proteins	TaqP	0	0
	Hyperthermophilic Proteins	HTa	0	0
Resistance to Low Temperatures	Cold-shock Protein	CspA	0	0
	Cold-shock Protein	CspB	0	0
	Cold-shock Protein	CspC	2	2
	Cold-shock Protein	CspD	0	0
	Cold-shock Protein	CspG	0	0
	Cold-shock Protein	CspI	0	0
	DEAD Box	CshB	0	0
	RNA Helicase	CshA	0	0
Alternative Metabolism	Carbon Fixation	cbbL	0	0
	Carbon Fixation	cbbS	0	0
	Carbon Fixation	cbbP	0	0
	Carbon Fixation	cbbF	0	0
	Carbon Fixation	cbbS	0	0

	Carbon Fixation	cbbA	0	0
	Sulfur Compound Oxidation	soxA	0	0
	Sulfur Compound Oxidation	soxB	0	0
	Sulfur Compound Oxidation	soxC	0	0
	Sulfur Compound Oxidation	soxS	0	0
	Sulfur Compound Oxidation	sqr	0	0
	Iron Oxidation	fox	0	0
	Hydrothermal Chemosynthesis Specific	aclA	0	0
	Hydrothermal Chemosynthesis Specific	aclB	0	0
	Hydrothermal Chemosynthesis Specific	frdA	0	0
	Hydrothermal Chemosynthesis Specific	frdB	1	1
	Hydrothermal Chemosynthesis Specific	idh	0	0
	Hydrothermal Chemosynthesis Specific	porA	1	1
	Hydrothermal Chemosynthesis Specific	porB	1	1
Nutrient Uptake Optimization	Phosphorus Uptake	pstA	1	1
	Phosphorus Uptake	pstB	1	1
	Phosphorus Uptake	pstC	1	1
	Nitrogen Uptake	amtB	1	1
	High Affinity Transport Systems	kdpA	0	0
	High Affinity Transport Systems	kdpB	0	0
	High Affinity Transport Systems	kdpC	0	0
	Siderophore Production and Uptake	dhbA	0	0
	Siderophore Production and Uptake	dhbB	0	0
	Siderophore Production and Uptake	dhbC	0	0

	Siderophore Production and Uptake dhbD	0	0
	Siderophore Production and Uptake dhbE	0	0
	Siderophore Production and Uptake feuA	0	0

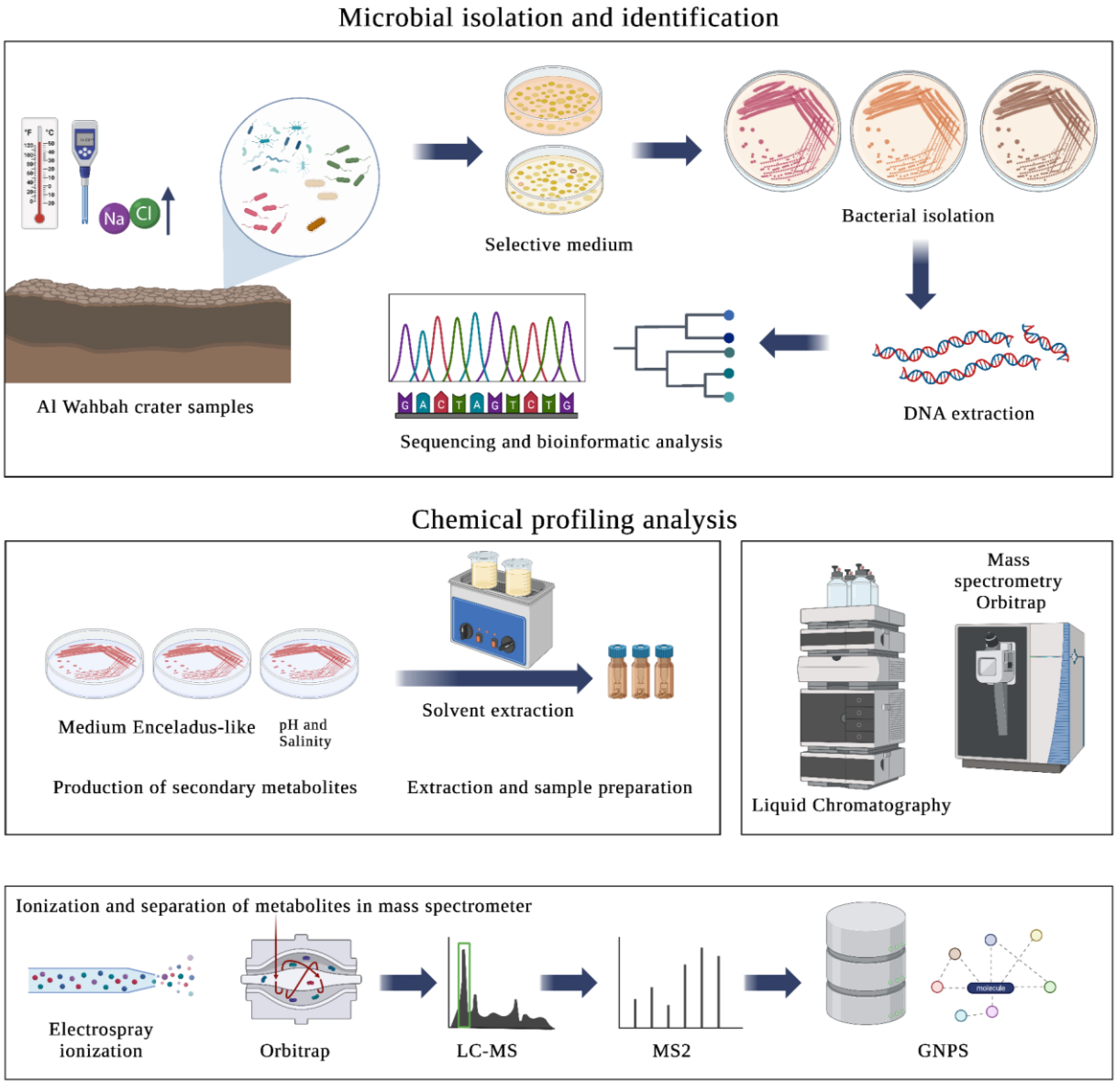

FIGURE S2.1 – Summary of the experimental design, involving the microbial isolation, culture, selection, and deeper analysis of genome characterization, as well as chemical profiling of targeted strains from the Al Wahbah crater, Saudi Arabia.

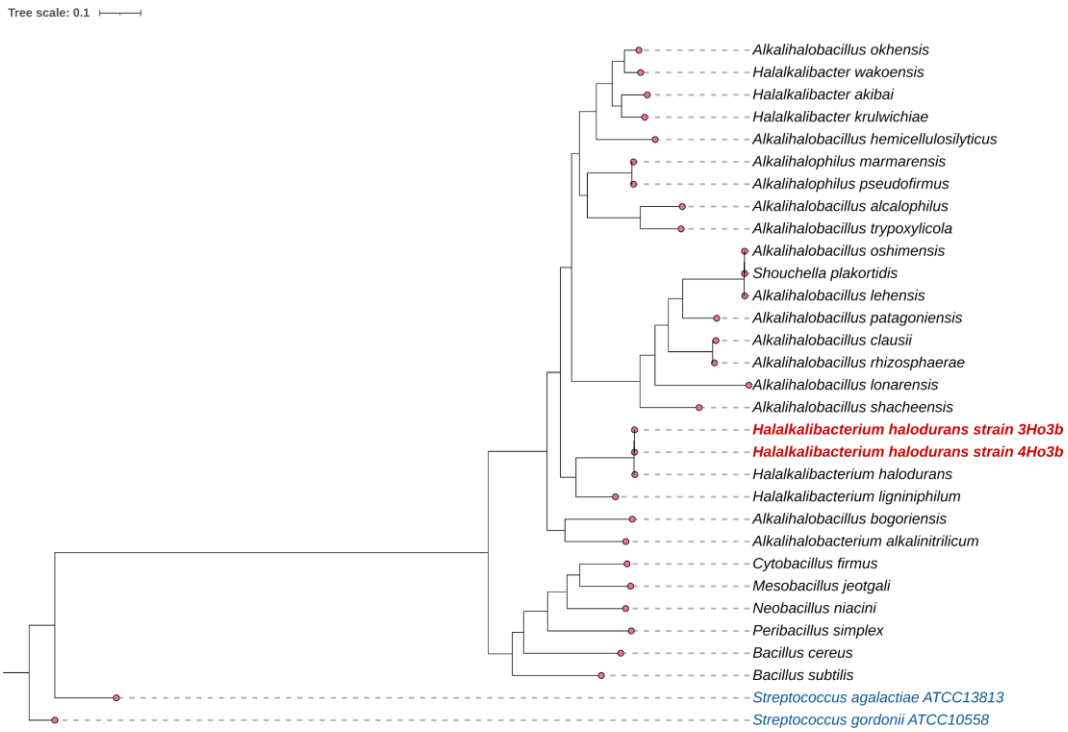

FIGURE S2.2 – Phylogenetic tree based on the core proteins of the 29 species of family *Bacillaceae*, including 27 species of members from Bacillaceae, available in NCBI genome database, and our studied genomes, strains 3Ho3b and 4Ho3b.

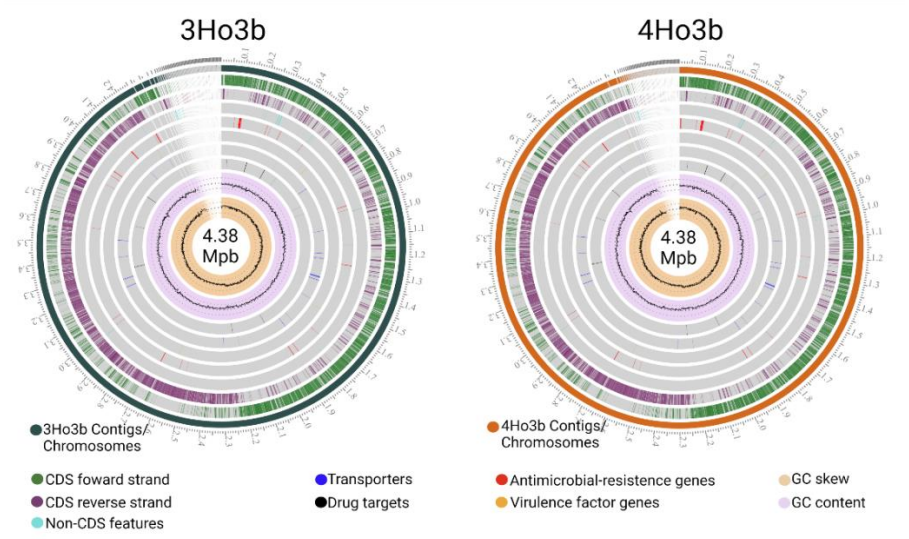

FIGURE S2.3 – Circular representation of the genomes of the 3Ho3b and 4Ho3b strains of *Halalkalibacterium halodurans* isolated from the Al Wahbah crater.

The genomes are approximately 4.4 Mb and are annotated with the following features: contigs, GC content, CDS on the forward and reverse strands, and genes related to antimicrobial resistance genes, drug targets, transporters and virulence factor genes.

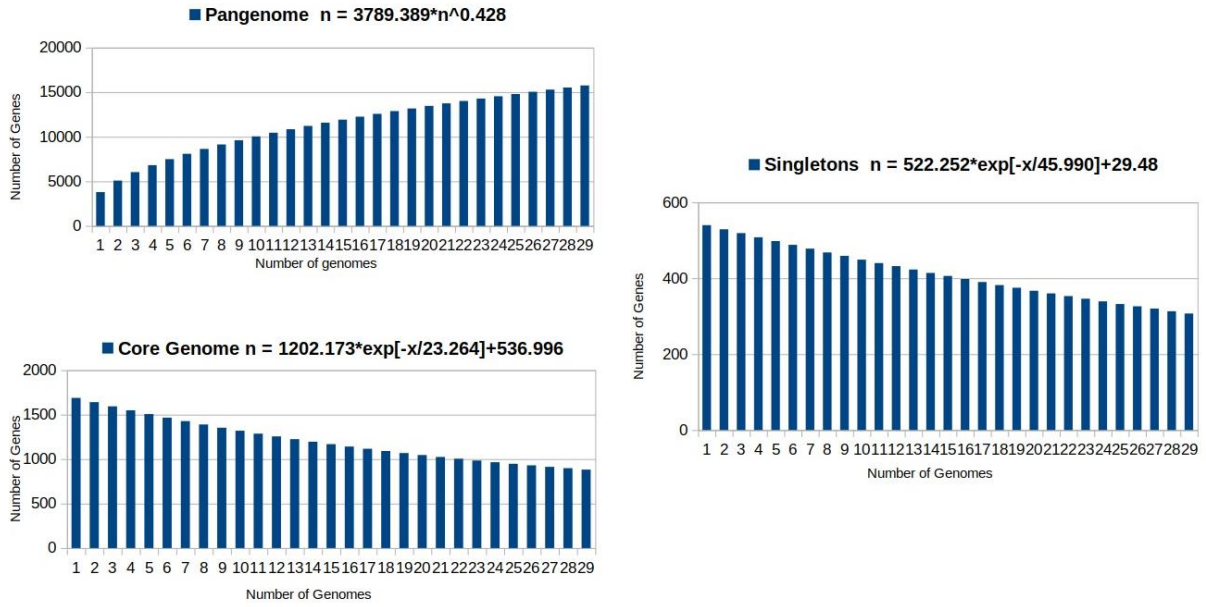

FIGURE S2.4 – Calculation of the pangenome, core genome, and singletons of 29 species from family *Bacillaceae* (27 genomes from NCBI genome database and 2 strains characterized in this study), keeping the newly sequenced genome 3Ho3b as the reference genome.

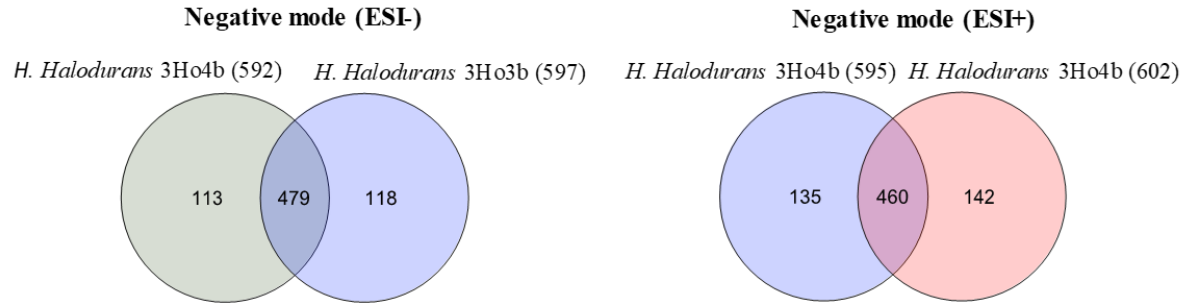

FIGURE S2.5 – Venn diagram illustrating the distribution of the chemical entities (nodes) when analyzed by ESI-MS in positive- and negative-acquisition modes of the two analyzed strains, 3Ho3b and 3Ho4b.